ENVELOPES OF BROAD BAND PROCESSES

by

Jozef Frans Maria Van Dyck

Ir.Bouwk., Katholieke Universiteit Leuven
(1978)

SUBMITTED TO THE DEPARTMENT OF
CIVIL ENGINEERING IN PARTIAL
FULFILLMENT OF THE
REQUIREMENTS FOR THE
DEGREE OF

MASTER OF SCIENCE

at the

MASSACHUSETTS INSTITUTE OF TECHNOLOGY

June 1981

Signature of Author _____
Department of Civil Engineering
April 24. 1981

Certified by _____
Daniele Veneziano
Thesis Supervisor

Accepted by _____
C. Allin Cornell
Chairman, Department Committee

ENVELOPES OF BROAD BAND PROCESSES

by

Jozef Frans Maria Van Dyck

Submitted to the Department of Civil Engineering
on April 24, 1981 in partial fulfillment of the
requirements for the Degree of Master of Science in
Civil Engineering

ABSTRACT

Envelopes of random processes X(t) are often used to obtain more accurate estimates of the probability distribution of the time when X(t) is first above a given level.
For narrow-band processes several envelope definitions have been proposed. Perhaps the most popular envelope definition is that by Cramer and Leadbetter. For broad-band processes, the same envelope is essentially useless because it does not follow the process closely enough.
An alternative envelope is proposed here, based on the seperation of the process X(t) into several components, followed by enveloping only some of the components (partial enveloping procedure).
It is found that this envelope is preferable to the Cramer-Leadbetter envelope in the case of wide-band processes and that, after correction for empty envelope excursions, it leads to a smaller upcrossing rate than the original process. Expressions are derived for seperation of X(t) into any number of components, but numerical results are restricted to 2, 3 and 4 components.
An attempt is made to generalize the concepts of envelope and partial envelope to random fields $X(\underline{t})$. The definition by Adler is shown to be equivalent to the Cramer-Leadbetter definition applied along a certain direction. As a result, the multidimensional envelope proposed by Adler depends on the choice of axis-system and is not isotropic when $X(\underline{t})$ is isotropic.
It is also found that the calculations needed for decomposition and partial enveloping of random fields are prohibitive; therefore no numerical results are given in this case.

Thesis supervisor: Daniele Veneziano

Title: Professor of Civil Engineering

Acknowledgements

I would like to express my sincere gratitude to my thesis supervisor, Prof. Daniele Veneziano, for his guidance, encouragement and inspiration.
I am also grateful to Prof. Erik Vanmarcke and Mr. Jean-Pierre Ramant, who introduced me to MIT and encouraged me to study here.
I am thankful to Mr. Michel Vandenbossche and my friends at the Belgian Institute of Management for their support and enthousiasm.
In addition, I would like to thank my friends and family. Especially, I want to acknowledge Brad and Nina, who made these two years in the USA into an exciting experience, and my wife, Bea, who patiently shared all the thesis-frustrations.
Finally, I want to dedicate this thesis to my father.

Table of contents

Introduction.

Although the general notion of envelope for a random process is clear, no unique definition exists. A variety of different definitions have been proposed by several authors (Rice, 1944; Crandall, 1963; Cramer and Leadbetter, 1967), all of which are reasonable and essentially equivalent for narrow-band processes. A first and simple requirement for $S(t)$ to be called an envelope of the scalar (random) function $X(t)$ is that $S(t) \geq X(t)$ at all times. A second, more vague but usually more restrictive requirement is that $S(t)$ be a "smoother" function than $X(t)$. Finally, $S(t)$ should be close to $X(t)$ at the points where the latter function is locally maximum.

Envelope processes have been often used in connection with "first passage problems", i.e., when the probability needs to be found that the maximum of $X(t)$ in the interval from t_o to t_o+T exceeds a given value r. Reliability analysis often requires solution of such extremal stochastic problems (random loads that exceed the maximum capacity of a system, spatially varying resistances that fall below a minimum acceptable level). Finding the exact distribution of the maximum of $X(t)$ in $[t_o, t_o+T]$ or the distribution of the time at which $X(t)$ first crosses a given level are still unresolved problems, except for very few special random processes (Siegert, 1951; Slepian, 1961).

Many approximations have been proposed (for a review, see Crandall, 1970), most of which complement Rice's (1944) result on the mean rate at which X(t) or S(t) upcross level r with an assumption about the random process of crossing events. The simplest assumption, that the points conform to a Poisson process, has been proven by Cramer (1966) to be asymptotically exact for very high crossing levels. The accuracy at lower levels depends, grossly speaking, on the amount of correlation in the process and thus on the bandwidth of the mean power spectral density function. For narrow-band processes, crossing events tend to cluster and the Poisson assumption leads to a conservative (too high) estimate of the exceedance probability. For processes of this class, it is convenient to replace X(t) with an envelope S(t), which acts almost like a smoothly varying amplitude-modulating function and by doing so groups crossing events that belong to the same crossing cluster (Fig. 1). The Poisson assumption may then be applied to upcrossings of S(t). Since the envelope process never falls below the original process, the exceedance probability is still overestimated, although typically by smaller amounts. In reliability application, the basic requirement on the envelope process S(t) is that it should lead to more accurate (less conservative) estimates of the exceedance probabilities.

For wide-band processes, none of the available envelope definitions performs satisfactorily : none follows the process closely and they all tend to produce results that are even more conservative than those based on the original process. One could argue that for wide-band processes the correlation between upcrossing events should be small and hence the Poisson assumption accurate. This may hold for some processes at high levels, but it is not true in general. It is certainly not true for processes that are locally very erratic, e.g., for nearly non-differentiable processes, and for processes the mean power of which is contributed by separate ranges of frequency. In both cases crossing events tend to occur in large clusters.
It is the purpose of this study to explore alternative envelope definitions that would be appropriate for broad-band and special type processes.
Generalization to random fields $X(\underline{t})$ ($\underline{t}$ is a vector-parameter) is not trivial. In the plane, crossings of $X(\underline{t})$ through a level r appear as disjoint contour lines. Counting the number of contour lines or of excursions (disjoint regions where $X(\underline{t}) \geqslant r$) is one way to generalize the concept of crossing on the line. However, no exact formula is known for the mean spatial density (a generalisation of the mean crossing rate) of these characteristics. Adler and Hasofer (1976) have proposed to characterise excursions through their "Euler

characteristic", which is a simpler parameter to study. The expected spatial density of this characteristic can be calculated; at high levels, it gives an accurate approximation of the expected number of disjoint excursions. Requirements for envelopes in several dimensions are similar to those for envelopes on the line. In the special case when the random field is isotropic, it would seem desirable that, in addition, also the envelope be isotropic. Adler (1978) has defined a multidimensional envelope as a direct generalization of the Cramer-Leadbetter envelope on the line and shown that such a generalization is useful for certain types of narrow-band random fields. We shall look at the adequacy of this envelope for other types of random fields including the case of isotropy.

The material is organised into three main sections. The first section reviews the Cramer-Leadbetter definition of envelope and introduces an extension of this definition for scalar processes. Specifically, a brief summary of results to be used later in this study is given in Section 1.1 . Section 1.2 illustrates the inadequacy of the Cramer-Leadbetter envelope for a special type of broad-band process. Section 1.3 introduces the concept of surface envelope, based on the representation of X(t) as the sum of several component processes and on enveloping only some of the components.

The second part of the thesis analyses in detail the properties of surface envelopes for scalar random processes. Section 2.1 considers X(t) as the sum of two independent components : for this case, the mean crossing rate of the envelope is derived and its performance illustrated for processes X(t) with different mean power density functions. Sections 2.2 and 2.3 extend the mean crossing rate results to the case of 3 and n ($n > 3$) components. Section 2.4 discusses the possible use of a time-averaging procedure to decompose X(t). Finally, in Section 2.5 a correction for empty envelope excursions is derived and its influence on the results obtained in Section 2.1 is studied.

The third part of the thesis deals with envelopes of random fields. Sections 3.1 and 3.2 review results by Adler and Hasofer for the envelope of a random field and its Euler characteristic. Section 3.3 shows that the Adler definition is equivalent with the one-dimensional Cramer-Leadbetter envelope along a certain direction. Section 3.4 demonstrates the dependency of the two-dimensional envelope on the orientation of the axes. Finally, Section 3.5 looks at the consequences of this dependence for isotropic fields.

Section 1 Envelopes of Random Processes on the Line

This section introduces several concepts and results that will be used extensively used in this study.
Section 1.1 reviews the definition of the Cramer-Leadbetter envelope and results on the mean upcrossing rate.
Its performance for a particular broad-band process is considered in Section 1.2.
Finally, Section 1.3 presents a class of envelopes that includes the Cramer-Leadbetter envelope as a special case and is more appropriate for broad-band processes.

1.1 The Cramer-Leadbetter envelope

A basic requirement for envelopes to be used in extremal problems is that they should lead to estimates of the exceedance probabilities which are more accurate than those from the original process. If estimates are based on the Poisson assumption, then S(t) should have a smaller upcrossing rate than X(t). Better estimates based on a correction for empty envelope excursions will be obtained in later sections.

Assuming that upcrossings of level r by the stationary process X(t) are independent events, the time T at which the first upcrossing occurs has exponential distribution with mean value $1/\nu_X(r)$, where $\nu_X(r)$ is the mean upcrossing rate for level r. In interpreting this as the distribution of the time at which function $X > r$, the exponential model may be corrected to account for the possibility that, at time 0, X is already above r. The correction is based on the fact that the mean value of the time between consecutive excursions above level r is $F_X(r)/\nu_X(r)$, where $F_X(r)$ is the cumulative distribution function of X. The probability density function of the time T at which first $X > r$ is then

$$f_T(t) = [1-F_X(r)]\,\delta(t) + \nu_X(r)\, e^{-\nu_X(r)t/F_X(r)} \qquad 0 \le t \le \infty \qquad (1)$$

For $F_X(r) \to 1$, this function approaches the exponential

density function with mean value $1/\nu_X(r)$.

Similarly, if one works with envelope upcrossings, one finds

$$f_T(t) = [1 - F_S(r)]\,\delta(t) + \nu_S(r)\, e^{-\nu_S(r)\, t / F_S(r)} \qquad 0 \le t \le \infty \qquad (2)$$

Some of the envelope excursions may be "empty" in the sense that they do not contain X(t) upcrossings. If one denotes by $\nu_S^q(r)$ the mean rate of qualified envelope upcrossings, i.e. of envelope upcrossings that are followed by at least one X(t) upcrossing, a better approximation to f_T is

$$f_T(t) = [1 - F_S(r)]\,\delta(t) + \nu_S^q(r)\, e^{-\nu_S^q(r)\, t / F_S(r)} \qquad 0 \le t \le \infty \qquad (3)$$

The need to calculate the mean crossing rate of a random process arises frequently in this study. Under mild conditions on the random process X(t), Rice (1944) derived the following formula

$$\nu_X(r) = f_X(r) \int_0^\infty y\, f_{\dot{X}|X}(y, r)\, dy \qquad (4)$$

where f_X is the PDF of X and $f_{\dot{X}|X}$ the conditional PDF of the derivative process $\dot{X}$ given that X equals r.

For any fixed t, the random variables X(t) and $\dot{X}(t)$ are uncorrelated if the process is stationary. If in addition

$X(t)$ and $\dot{X}(t)$ are independent, then Eq. 4 simplifies to

$$\nu_X(r) = f_X(r) \int_0^\infty y f_{\dot{X}}(y)\, dy \tag{5}$$

Stationary Gaussian processes satisfy this condition of independence. Their mean upcrossing rate is

$$\nu_X(r) = \frac{1}{2\pi} \sqrt{\frac{\lambda_2}{\lambda_0}}\ e^{-\frac{r^2}{2\lambda_0}} \tag{6}$$

where λ_0 and λ_2 are initial moments of order 0 and 2 of the one sided spectral density function $G(\omega)$,

$$\lambda_i = \int_0^\infty \omega^i\ G(\omega)\, d\omega \tag{7}$$

Cramer and Leadbetter (1967) have defined an envelope (the "C-L envelope") which is often used in connection with narrow-band processes. Extensions of their definition will be proposed later in this section, which seem preferable to the original envelope in the case of broad-band random functions. For easy reference, definition and basic properties of the C-L envelope are reviewed here.
The envelope is defined in terms of the original process $X(t)$ and its Hilbert transform $\hat{X}(t)$ as

$$S(t) = \left[X^2(t) + \hat{X}^2(t)\right]^{1/2} \tag{8}$$

If X(t) has a Fourier decomposition

$$X(t) = \int_0^\infty [U(\omega)\cos\omega t + V(\omega)\sin\omega t]\, d\omega \qquad (9)$$

then $\hat{X}(t)$ is defined as

$$\hat{X}(t) = \int_0^\infty [U(\omega)\sin\omega t - V(\omega)\cos\omega t]\, d\omega \qquad (10)$$

For a single frequency , $U(\omega)\cos\omega t$, $U(\omega)\sin\omega t$ and $V(\omega)\cos\omega t$, $V(\omega)\sin\omega t$ can be interpreted as projections of ortogonal vectors $\vec{U}(\omega)$ and $\vec{V}(\omega)$ that have amplitude $U(\omega)$ and $V(\omega)$ and turn around the origin with circular frequency ω (Fig. 2). The envelope is constant with value $\sqrt{V^2(\omega)+U^2(\omega)}$ equal to the length of the vector $\vec{V}(\omega)+\vec{U}(\omega)$. Alternatively, $\hat{X}(t)$ can be defined in the time domain as

$$\hat{X}(t) = \int_{-\infty}^{+\infty} \frac{X(t-\tau)}{\tau}\, d\tau \qquad (11)$$

which is a convolution of X(t) with the function $1/t$.
If X(t) is a stationary Gaussian process, then S(t) is also stationary with Rayleigh marginal distribution

$$f_S(s) = \frac{s}{\lambda_0}\, e^{-\frac{s^2}{2\lambda_0}} \qquad 0 \leq s \leq \infty \qquad (12)$$

where λ_0 is the quantity defined in Eq. 7 and equals the variance of X.

The Rayleigh form of f_S is a result of the fact that for given t X(t) and $\hat{X}(t)$ are independent variables with identical Gaussian distribution (Cramer and Leadbetter, Pgs. 141-142 , 1967). Under the same conditions, the derivative process $\dot{S}(t)$ has Gaussian marginal distribution with zero mean and variance

$$\sigma_{\dot{S}}^2 = \lambda_2 - \frac{\lambda_1^2}{\lambda_0} \tag{13}$$

Moreover, one can show that $\dot{S}(t)$ is independent of S(t) at fixed time t and calculate the mean rate at which S(t) upcrosses r; this mean rate is

$$\nu_S(r) = \frac{r}{\sqrt{2\pi}} e^{-\frac{r^2}{2\lambda_0}} \frac{1}{\lambda_0} \left(\lambda_2 - \frac{\lambda_1^2}{\lambda_0}\right)^{1/2} \tag{14}$$

Vanmarcke (1972) suggested that in the context of first-crossing problems, the dispersion of the spectral density function be measured in terms of a parameter q, which is defined

$$q = \left(1 - \frac{\lambda_1^2}{\lambda_2 \lambda_0}\right)^{1/2} \tag{15}$$

In terms of q, Eq. 14 can be written as

$$\nu_S(r) = \frac{q}{\sqrt{2\pi}} \sqrt{\frac{\lambda_2}{\lambda_0}} \frac{r}{\sqrt{\lambda_0}} e^{-\frac{r^2}{2\lambda_0}} \tag{16}$$

In the remainder of this study it will always be assumed that the original process is Gaussian and standardized to have zero mean and unit variance ($\lambda_o = 1$).

1.2 Introductory problem

We shall illustrate the deficiencies of the Cramer-Leadbetter envelope for broad-band processes through an example.

Consider a Gaussian random process X(t) with one sided spectral mass at frequencies ω_1 and ω_2, and spectral density function

$$G(\omega) = 0.5\,[\delta(\omega-\omega_1) + \delta(\omega-\omega_2)] \tag{17}$$

This function and a realisation of the process are schown in Fig. 3. One way to explicitly obtain the process is to express X(t) as

$$X(t) = A\cos(\omega_1 t + \phi_1) + B\cos(\omega_2 t + \phi_2) \tag{18}$$

in which A and B are iid Rayleigh random variables with variance 0.5 and ϕ_1 and ϕ_2 are iid variables with uniform distribution between 0 and 2π. In fact,

$$X(t) = A\cos\phi_1\cos\omega_1 t + B\cos\phi_2\cos\omega_2 t - A\sin\phi_1\sin\omega_1 t - B\sin\phi_2\sin\omega_2 t$$

and $A\cos\phi_1$ $A\sin\phi_1$ $B\cos\phi_2$ and $B\sin\phi_2$ are iid Gaussian variables with zero mean and variance 0.5.

One may consider the above process to be wide-banded if the difference $\Delta\omega = \omega_2 - \omega_1$ is large or if the ratio $v = \Delta\omega/(\omega_1+\omega_2)$ is large. From Eqs. 6 and 16 it follows that the ratio ν_S/ν_X is

$$\frac{\nu_S}{\nu_X} = \sqrt{2\pi}\, q r \tag{19}$$

with $q = [v^2/(1+v^2)]^{1/2}$ for the bichromatic process of Eq. 18. The regions of the (r,v)-plane in which the ratio ν_S/ν_q is smaller or larger than 1 are shown in Fig. 4. The larger the crossing level r, the smaller v (the more narrow-banded the process) must be in order that $\nu_S < \nu_X$. For v=0.75, a particular realisation of X(t) and the associated envelope S(t) are shown in Fig. 5. It is doubtfull whether in this case the random process S(t) should be considered as a valid "envelope" of X(t). For instance, the crossings of S(t) at level r (see Fig. 5) are totally unrelated to X(t) crossings.

1.3 Decomposition of X(t) and surface envelopes

The random process of Eq. 18, can be written as

$$X(t) = X_1(t) + X_2(t) \tag{20}$$

in which $X_1(t)$ and $X_2(t)$ are independent stationary Gaussian processes with spectral densities

$$G_i(\omega) = 0.5\,\delta(\omega-\omega_i) \qquad i=1,2 \tag{21}$$

As a consequence, the condition that $X \geq r$ can be reinterpreted in terms of the vector $\underline{X}= [X_1 \; X_2]^T$ as $X_1+X_2 \geq r$ (Fig. 6). Crossings by the process $\underline{X}(t)$ of the line $X_1+X_2= r$ are in one to one correspondance with crossings of level r by the process X(t). Decomposition of X(t) into the sum of several independent but not necessarily monochromatic processes $X_i(t)$, i=1,n , and treatment of the crossing problem in the n-dimensional space of the vector $\underline{X}= [X_1 \; \ldots \; X_n]^T$ leads to a variety of possible envelope definitions. We shall examine a few such definitions next.

Envelopes of vector processes X(t) can be conveniently defined as random sets S(t) in X-space, such that $X(t) \in S(t)$ at all times. Some set processes of this type can be generated using the ordinary notion of envelope for scalar processes.

For example, it is evident that if

$$X_{\underline{\alpha}}(t) = X_1(t)\cos\alpha + X_2(t)\sin\alpha \tag{22}$$

denotes the projection of X(t) along the direction of the unit vector $\underline{\alpha} = [\cos\alpha \ \sin\alpha]^T$, then the "bandprocess" $S_B(t)$, defined

$$S_B = \{ (X_1, X_2) : X_1\cos\alpha + X_2\sin\alpha \leq S_{\underline{\alpha}}(t) \} \qquad (23)$$

(shaded region in Fig. 6) is a possible choice for S(t), if $S_{\underline{\alpha}}(t)$ is the 1D envelope of $X_{\underline{\alpha}}(t)$.

Similarly, in terms of the (1-dimensional) envelopes S_1 and S_2 of X_1 and X_2, a possible choice of envelope in 2D is the "rectangular envelope" (Fig. 7)

$$S_R = \{ (X_1, X_2) : X_1 \leq S_1 \ , X_2 \leq S_2 \} \qquad (24)$$

This last envelope corresponds to the one-dimensional envelope $S(t) = S_1(t)+S_2(t)$ for X(t). In the case when $G(\omega) = 0.5\,\delta(\omega-\omega_i)$ the rectangular envelope is time invariant; hence there are no envelope upcrossings. The rectangular envelope is clearly not invariant with respect to rotation of the axes along which the enveloping is defined.

The circular envelope

$$S_C = \{ (X_1, X_2) : X_1^2 + X_2^2 \leq S_1^2 + S_2^2 \} \qquad (25)$$

is invariant to rotation. Fig. 8 shows that S_R is always contained in S_C, so that S_R follows X(t) and $\underline{X}(t)$ more closely.

One may finally mention the elliptical envelope S_E, obtained

as the common intersection of the bands S_θ for all directions . Explicitly S_E is defined as

$$S_E = \{ \underline{X} : |\underline{\alpha}^T \underline{X}| \leq S_{\underline{\alpha}} \text{ for all } \underline{\alpha} \} \tag{26}$$

in which $S_{\underline{\alpha}}$ is the 1-dimensional envelope of the projection of X along the direction of $\underline{\alpha}$; hence

$$S_{\underline{\alpha}} = Env[\underline{\alpha}^T \underline{X}] = [X_{\underline{\alpha}}^2 + \hat{X}_{\underline{\alpha}}^2]^{1/2} \tag{27}$$

In particular

$$\text{for } \begin{cases} \underline{\alpha} \perp \underline{X} \\ \underline{\alpha} \perp \hat{\underline{X}} \end{cases} , \quad S_{\underline{\alpha}} = 0 \tag{28a}$$

$$\text{for } \underline{\alpha} \perp \underline{X} , \quad S_{\underline{\alpha}} = \hat{X}_{\underline{\alpha}} \tag{28b}$$

$$\text{for } \underline{\alpha} \perp \hat{\underline{X}} , \quad S_{\underline{\alpha}} = X_{\underline{\alpha}} \tag{28c}$$

It follows from Eq. 28a that the ellipsoid S_E defined by Eq. 26 degenerates to an ellipse in the plane $(\underline{X}, \hat{\underline{X}})$. From Eqs. 28b and c it follows that $\underline{X}$ and $\hat{\underline{X}}$ lie on the boundary of this ellipse. Since $\underline{X}$ and $\hat{\underline{X}}$ define S uniquely, S_E is rotation invariant. Therefore, in the case of Eq. 17, the set that envelopes $\underline{X}(t)$ in R^n belongs to a surface of dimension not larger than 2. This is an example of what we shall call surface envelopes, $S_S(t)$, which are set envelopes defined by surfaces with dimension $m < n$.

Another example of surface envelope is

$$S_S = \{ \underline{X} : X_1 = X_1, \ldots, X_r = X_r, [X_{r+1}, \ldots, X_n] \in S_R[X_{r+1}, \ldots, X_n] \} \tag{29}$$

In this case, m= n-r.

For r=n, the surface envelope of Eq. 29 degenerates to a point and corresponds to the trajectory of $\underline{X}$.

For the random process defined by Eq. 18 and for r=1, Eq. 29 gives

$$S_S(t) = \left\{ (X_1, X_2) : X_1 = X_1(t) \; ; \; |X_2| \leq S_2 \right\} \qquad (30)$$

In this case S_S is a segment in the (X_1, X_2)-plane (a two-dimensional surface in (X_1, X_2, t)-space; see Fig. 9) and the process $\underline{X}(t)$ has sinusoidal trajectory on $S_S(t)$. Whereas $S_S(t)$ oscillates with frequency ω_1, $\underline{X}(t)$ oscillates on $S_S(t)$ with frequency ω_2. In a sense, $S_S(t)$ acts as a low-pass filter: the high frequencies are totally eliminated in the surface process which is defined to include all possible locations of $X_2(t)$ within the energy bounds provided by S_2 (see Eq. 30). In 1D, $S_S(t)$ corresponds to the envelope band S(t) in Fig. 10.

Section 2 Envelope of decomposed random processes

Section 2 discusses the practical application of the surface envelope to random processes.

In Section 2.1, the case of two independent components is studied and results for the ratio of upcrossing rates of X(t) and S(t) are obtained for several spectra.

Section 2.2 and 2.3 extend these results to 3 and more independent components.

Section 2.4 discusses the possibility of using a time averaging procedure to obtain the different components and shows the equivalence of this procedure with the previous results for a particular choice of the time averaging function.

Section 2.5 proposes two models to account for empty envelope upcrossings and, using these models, some of the results of Section 2.1 are recalculated.

2.1 Two independent components

Intersections of the surface envelope $S_S(t)$ in Eq. 30 with the line $X_1+X_2= r$ correspond to S(t) crossings of level r, if S(t) is defined as the 1-dimensional envelope

$$S(t) = X_1(t) + X_2(t) \tag{31}$$

and $S_2(t)$ is the C-L envelope of $X_2(t)$.

X_1 and X_2 are independent, stationary, Gaussian processes. If the initial absolute moment of order i of the mean power spectral density function of X is denoted by $\lambda_{i,j}$, then the variance of X(t) is $\lambda_o= \lambda_{o,1} + \lambda_{o,2}$. This quantity is set equal to 1. From the above assumptions it follows that the derivative process $\dot{S}(t)$ is the sum of the independent, Gaussian processes $\dot{X}_1$ and $\dot{S}_2$. Using Eq. 13, the variance of $\dot{S}$ is found to be

$$\sigma_{\dot{S}}^2 = \lambda_{2,1} + \lambda_{2,2} - \frac{\lambda_{1,2}^2}{\lambda_{o,2}} \tag{32}$$

and the partial expectation $E_o^\infty [\dot{S}(t)/S(t)=r] = E_o^\infty [\dot{S}(t)]$ is

$$\int_o^\infty y\, f_{\dot{S}}(y)\, dy = \frac{1}{\sqrt{2\pi}} \left(\lambda_{2,1} + \lambda_{2,2} - \frac{\lambda_{1,2}^2}{\lambda_{o,2}}\right)^{1/2} \tag{33}$$

The PDF of S is the convolution of a Rayleigh and a normal distribution

$$f_S(s) = \int_o^\infty \frac{s_2}{\lambda_{o,2}} e^{-\frac{s_2^2}{2\lambda_{o,2}}} \frac{1}{\sqrt{2\pi\lambda_{o,1}}} e^{-\frac{(s-s_2)^2}{2\lambda_{o,1}}} ds_2 \tag{34}$$

Using the condition that $\lambda_{o,1} + \lambda_{o,2} = 1$, the exponent can be written as

$$\frac{s_2^2}{2\lambda_{o,2}} + \frac{(s - s_2^2)^2}{2\lambda_{o,1}} = \frac{1}{2\lambda_{o,1}} \left[\frac{s_2^2}{\lambda_{o,2}} - 2ss_2 + s^2 \right] \tag{35}$$

and the integral of Eq. 34 can than be split into two terms :

$$f_S(s) = \int_o^\infty \frac{s_2 - s\lambda_{o,2}}{\lambda_{o,2}\sqrt{2\pi\lambda_{o,1}}} e^{-\frac{1}{2\lambda_{o,1}}\left[\frac{s_2^2}{\lambda_{o,2}} - 2ss_2 + s^2\right]} + \int_o^\infty \frac{s\lambda_{o,2}}{\lambda_{o,2}\sqrt{2\pi\lambda_{o,1}}} e^{-\frac{1}{2\lambda_{o,1}}\left[\frac{s_2^2}{\lambda_{o,2}} - 2ss_2 + s^2\right]} \tag{36}$$

The first term equals

$$\sqrt{\frac{\lambda_{o,1}}{2\pi}}\, e^{-\frac{s^2}{2\lambda_{o,1}}} \tag{37}$$

and the second term can be written as

$$\frac{s}{\sqrt{2\pi\lambda_{o,1}}} e^{-\frac{s^2}{2}} \int_o^\infty e^{-\frac{1}{2\lambda_{o,1}\lambda_{o,2}}(s_2 - s\lambda_{o,2})^2} ds_2 \tag{38}$$

$$= \sqrt{\lambda_{o,2}}\; s\, e^{-\frac{s^2}{2}} \left\{ 1 - \Phi\left[-s\sqrt{\frac{\lambda_{o,2}}{\lambda_{o,1}}} \right] \right\}$$

in which Φ is the cumulative Gaussian density function. Combining Eqs. 37 and 38 one finds that the PDF of S has the form

$$f_S(s) = \sqrt{\frac{\lambda_{o,1}}{2\pi}}\, e^{-\frac{s^2}{2\lambda_{o,1}}} + \sqrt{\lambda_{o,2}}\, s\, e^{-\frac{s^2}{2}} \left[1 - \Phi\left(-s\sqrt{\frac{\lambda_{o,2}}{\lambda_{o,1}}} \right) \right] \tag{39}$$

The mean crossing rate of S(t) above a level r can now be found, using Rice's formula (Eq. 5) and results in Eqs. 32 and 39 :

$$\nu_S = \left(\lambda_{2,1} + \lambda_{2,2} - \frac{\lambda_{1,2}^2}{\lambda_{0,2}}\right)^{1/2} \left\{ \frac{\sqrt{\lambda_{0,1}}}{2\pi} e^{-\frac{r^2}{2\lambda_{0,1}}} + \sqrt{\frac{\lambda_{0,2}}{2\pi}}\, r e^{-\frac{r^2}{2}} \left[1 - \Phi\left(-r\sqrt{\frac{\lambda_{0,2}}{\lambda_{0,1}}}\right)\right] \right\} \tag{40}$$

The mean crossing rate of $X(t) = X_1(t) + X_2(t)$ above level r is given in Eq. 6. Since $\lambda_{2,1} + \lambda_{2,2} = \lambda_2$, the ratio ν_S/ν_X is

$$\frac{\nu_S}{\nu_X} = \left(1 - \frac{\lambda_{1,2}^2}{\lambda_2 \lambda_{0,2}}\right)^{1/2} \left\{ \sqrt{\lambda_{0,1}}\, e^{-\frac{r^2 \lambda_{0,2}}{2\lambda_{0,1}}} + \sqrt{2\pi\lambda_{0,2}}\, r \left[1 - \Phi\left(-r\sqrt{\frac{\lambda_{0,2}}{\lambda_{0,1}}}\right)\right] \right\} \tag{41}$$

The second factor in Eq. 41 is only a function of the crossing level r and of the variance of the process X_2, $\lambda_{0,2}$. We shall call this factor J and rewrite Eq. 41 as

$$\frac{\nu_S}{\nu_X} = \left(1 - \frac{\lambda_{1,2}^2}{\lambda_2 \lambda_{0,2}}\right)^{1/2} J(\lambda_{0,2}, r) \tag{42}$$

As was said in Sec. 1.1, it is desirable to have small ν_S/ν_X ratios. Eq. 42 shows that for a given spectral shape and for a given crossing level and variance of X_2, it is better to associate X_2 with the higher frequencies. In this respect, the partition of the spectral density function into

two non overlapping frequency bands (Fig. 12) and associating component processes X_1 and X_2 to each band is optimal. Clearly X_1 and X_2 are independent processes. The factor J does not depend on the shape of the spectral density function and is given numerically in Table 1. Fig. 11 shows that for crossing levels above 1, which are those of greater engineering interest, the factor J is an increasing function of $\lambda_{0,2}$. It follows that the 2D envelope has a smaller upcrossing rate than the original process only if the first factor in Eq. 42 is sufficiently small.

In order to evaluate the effect of the spectral width on the ratio ν_s/ν_x in Eq. 42, this quantity is plotted (Figs. 13-29) as a function of the variance of the enveloped component, $\lambda_{0,2}$. Different curves correspond to different crossing levels r or to different spectra. Three basic spectral shapes are used : rectangular, discrete and a mixture of exponential functions (Fig. 12) For given $\lambda_{0,2}$ the spectrum is divided into two components and the process associated with the higher frequency range is enveloped. Enveloping the lower frequency component would lead to higher values of ν_s/ν_x.

The rectangular spectrum from ω_1 to ω_2 with unit area (Fig. 12.a) is used in 5 cases (Figs. 13-17). These cases range from the extreme narrow-bandness when $\omega_2/\omega_1=1$ (Fig. 13) to almost white noise ($\omega_2/\omega_1=10^{+4}$; see Fig.17). For relatively narrow-band processes ($\omega_2/\omega_1 = 2$) the value of $\lambda_{0,2}$ that minimizes the mean crossing rate is found to be 1. This value corresponds to the conventional envelope of X(t). For larger ratios ω_2/ω_1 the value of $\lambda_{0,2}$ that (locally) minimizes the mean crossing rate decreases to about 0.78 for $\omega_2/\omega_1 = 5$, to about 0.7 for $\omega_2/\omega_1 = 10$, and to 0.65 for $\omega_2/\omega_1 = 10^4$. Sensitivity of this parameter to the crossing level is very small.

At crossing levels r higher than 1, the value of ν_s/ν_x at the (local) minimum point is larger than 1 for all the above cases. This indicates that a large fraction of envelope excursions above r are "empty" (they do not contain any process crossing event). A correction to ν_s is therefore needed if the envelope is to be used in place of the original process in approximating the first crossing probability from the mean crossing rate. One can say, however, that relative to the C-L envelope, the present envelope is significantly smoother, has a smaller number of empty upcrossings and follows the original process more closely.

The spectrum to be considered next consist of two rectangular blocks from ω_1 to ω_2 and from ω_3 to ω_4. Each

block has area 0.5 (Fig. 12.b). Fig. 18 shows the results for the extreme case of two peaks ($\omega_2/\omega_1 = 1$ and $\omega_4/\omega_3 = 1$) and frequency ratio $\omega_3/\omega_2 = 5$. The upcrossing rate is clearly minimal when only the high frequency peak is enveloped ($\lambda_{0,2} = 0.5$); the ratio is smaller than 1 for crossing levels up to 2.5. If the peaks are replaced with rectangular blocks with $\omega_4/\omega_3 = 5/3$ and $\omega_2/\omega_1 = 3$, while the frequency ratio ω_3/ω_2 is kept equal to 5, the ratios ν_s/ν_x for $\lambda_{0,2} = 0.5$ are lower than 1 for crossing levels up to 3 (Fig. 19). This is probably due to the larger ratio between the central frequencies of the two blocks, compared to the previous case. When the two blocks are closer, as they are in Fig. 20 ($\omega_3/\omega_2 = 2$), the crossing rate ratio increases by about 70 % for $\lambda_{0,2} = 0.5$, while the optimum remains very pronounced. A further increase of bandwidth of the two blocks (Fig. 21) does not change the results substantially. If the variance of the high frequency component is modified, the optimal value of $\lambda_{0,2}$ changes accordingly (Figs. 22 and 23). The ratio ν_s/ν_x is slightly smaller when that variance decreases. This means that partial enveloping is more effective when a small high-frequency component is superimposed on a low-frequency component with larger variance.

All previous results indicate that the existence of a spectral gap determines the optimal value of $\lambda_{o,2}$, while the detailed shape of the spectrum has only secondary importance. To more quantitatively assess the effect of such a spectral gap, a discrete spectrum (Fig. 12.c) composed of two equal peaks is considered as the frequency ratio is changed (Figs. 24-26). For extremely large frequency ratios, as in Fig. 26, the ratio ν_s/ν_x is nearby zero for all crossing levels. This is a consequence of the fact that ν_x tends to infinity, while ν_s remains finite. For a frequency ratio of 2 (fig. 24), the minimum is not very pronounced.

Results for a frequency ratio of 2 have also been obtained after replacing spectral peaks with exponentially decaying functions (Fig. 12.d) centered at frequencies 5 and 10. In a first case (Fig. 27) the peaks are very narrow and thus well seperated. As expected, results are not very different from those of Fig. 24, although now the crossing rate is less sensitive to variations of $\lambda_{o,2}$ above the value 0.5. This means that enveloping also part of the low-frequency component does not appreciably alter the mean crossing rate. When the lower frequency component is less pronounced (Fig. 28) a minimum occurs around $\lambda_{o,2}= 3/4$, i.e. for the case when the high frequency part and about half of the lower frequency part are enveloped. Finally, when both

peaks are less accentuated and partially overlap (Fig. 29) no local minimum is found, although the upcrossing rate is relatively insensitive to $\lambda_{0,2}$ around $\lambda_{0,2} = 0.5$.

In summary, for narrow-band processes ($\omega_2/\omega_1 \leq 2$) the Cramer-Leadbetter envelope has the smallest upcrossing rate within the class of envelopes considered here. If a narrow-band process is composed of two slightly pronounced peaks, then a partial envelope can have a smaller upcrossing rate, but there is no general valid result on the optimal amount of spectral density that one should associate with the enveloped component. For broad-band processes or processes with clearly seperated spectral masses, the upcrossing rate becomes minimal for less than complete enveloping, with a value significantly smaller than for the Cramer-Leadbetter envelope.

Section 2.2 Three components

A random process may have more than two components with distinctively different frequency content. An extreme case with three such components would be a process X(t) with one-sided spectral density

$$G(\omega) = \frac{1}{3}\delta(\omega-\omega_1) + \frac{1}{3}\delta(\omega-\omega_2) + \frac{1}{3}\delta(\omega-\omega_3) \qquad (43)$$

in which ω_1, ω_2 and ω_3 are widely seperated frequencies. Figs. 30 and 31 show some results when this process is viewed as the sum of only two component processes and the component process with higher frequency content is envelóped. In this case and for frequency ratios $\omega_2/\omega_1 = 2$ and $\omega_3/\omega_2 = 2$, ν_s/ν_x is locally minimum for $\lambda_{0,2} = 1/3$ and $\lambda_{0,2} = 2/3$ (Fig. 30). The first minimum corresponds to enveloping only the highest-frequency peak, the second to enveloping both the intermediate and high frequency components. When the fequency ratio of the last peak is increased to $\omega_3/\omega_2 = 4$, the first minimum becomes more pronounced and the second minimum vanishes (Fig. 31). Clearly, enveloping only the higher-frequency peak results in a relatively small upcrossing rate.

Another possibility is to consider three instead of two components and seperately envelope the intermediate and high fequency components. One might expect that doing so would further reduce the upcrossing rate.

The definition of the surface envelope S_S in Eq. 29 holds for any number of components. In particular, for 3 components, S_S becomes

$$S_S = \left\{ (X_1, X_2, X_3) \;:\; X_1 = X_1 \;;\; |X_2| \le S_2 \;;\; |X_3| \le S_3 \right\} \qquad (44)$$

in which S_2 and S_3 are the envelopes of X_2 and X_3 in the Cramer-Leadbetter sense.

Times at which the surface envelope is tangent to the plane $X_1+X_2+X_3 = r$ correspond to times when the associated 1D envelope S(t) upcrosses or downcrosses level r (Fig. 32). S(t) is given by

$$S(t) = X_1(t) + S_2(t) + S_3(t) \qquad (45)$$

In order to evaluate the mean upcrossing rate of S(t) using Rice's formula (Eq. 5) one needs to calculate the PDF of S and the partial expectation of the derivative process $\dot{S}$. If the component processes X_1, X_2 and X_3 are independent stationary, Gaussian processes, then at any given time, $\dot{S}$ is the sum of the independent Gaussian variables $\dot{X}_1$, $\dot{S}_2$ and $\dot{S}_3$; the variance of the latter two variables is given by Eq. 13 and since $\dot{S}$ is Gaussian and independent of S the partial expectation can be expressed in terms of the variance of S. The final expression of the mean crossing rate is

$$\nu_S = \frac{1}{\sqrt{2\pi}} \left(\lambda_2 - \frac{\lambda_{1,2}^2}{\lambda_{0,2}} - \frac{\lambda_{1,3}^2}{\lambda_{0,3}} \right)^{1/2} \qquad (46)$$

$$\frac{1}{\sqrt{2\pi\,\lambda_{0,1}}\,\lambda_{0,2}\,\lambda_{0,3}} \int_0^\infty \int_0^\infty x_2 x_3 \, e^{-\frac{(r-x_2-x_3)^2}{2\lambda_{0,1}}} \, e^{-\frac{x_2^2}{2\lambda_{0,2}}} \, e^{-\frac{x_3^2}{2\lambda_{0,3}}} \, dx_2\, dx_3$$

where the second factor corresponds to the PDF of S, obtained as a convolution of the normal density function of X_1 with the two Rayleigh density functions of S_2 and S_3. As before, the ratio ν_s/ν_x can be written as the product of a factor which depends on the shape of the spectral density function and a factor J, which depends on the crossing level r and on the variances $\lambda_{0,2}$ and $\lambda_{0,3}$ of the components X_2 and X_3. The parameters $\lambda_{0,2}$ and $\lambda_{0,3}$ can be conveniently replaced by two parameters, ϵ and γ, such that

$$\gamma = \lambda_{0,2} + \lambda_{0,3} \quad , \quad \epsilon = \frac{\lambda_{0,3}}{\lambda_{0,2} + \lambda_{0,3}} \tag{47}$$

Hence, γ is the total amount of variance of X(t) associated with the envelopes S_2 and S_3 and ϵ is the fraction of that variance associated with S_3. In terms of these quantities the ratio ν_s/ν_x can be written

$$\frac{\nu_s}{\nu_x} = \left(1 - \frac{\lambda_{1,2}^2}{\lambda_{0,2}\lambda_2} - \frac{\lambda_{1,3}^2}{\lambda_{0,3}\lambda_2}\right)^{1/2} J(\gamma, r, \epsilon) \tag{48}$$

It follows from Eq. 47 that for $\epsilon = 0$, the present factor J coincides with the factor J used for the two-component envelope, i.e.,

$$J(\gamma, r, 0) = J(\lambda_{0,2}, r) \tag{49}$$

From considerations of symmetry it also follows that

$$J(\gamma, r, \epsilon) = J(\gamma, r, 1-\epsilon) \tag{50}$$

Unlike for the case of two components, the integral in Eq. 46 cannot be simplified and calculations were performed using a straightforward double integration over a finite region of the plane. Because for $\epsilon = 0$ ($\lambda_{0,3} = 0$) or $\gamma = 0$ ($\lambda_{0,2} = \lambda_{0,3} = 0$) this integration method fails, γ has been varied from 0.01 to 1 and ϵ from 0.01 to 0.5 . Table 2 gives the results for crossing levels r= 0, 1, 2 and 3. Figs. 33 to 36 show J as a function of γ and ϵ for the same crossing levels. The J factor is proportional to the PDF of $(X_1 + S_2 + S_3)$ at the crossing level r. The shapes of the Gaussian PDF of X_1 and of the Rayleigh PDF of S_2 and S_3 are shown in Fig. 37. It is clear that at low levels (r= 0), the PDF of the sum decreases as the envelopes S_2 and S_3 become more important; thus J decreases when γ or ϵ increases (see Fig. 33). At high levels (r=3), the PDF increases when the components S_2 or S_3 become more important, since they are more likely to assume high values than the corresponding Gaussian variables X_2 or X_3 (see Figs. 35 and 36). The level r=1 (Fig. 34) represents an intermediate case.

Since for levels $r > 1$ the factor J increases when a third component is used, the spectral factor in Eq. 48 should decrease sufficiently to obtain lower ν_s/ν_x ratios. Whether this is the case when the spectral density is the sum of three exponentially decaying functions (Fig. 38) is

investigated next. For given γ and ϵ, the spectrum is divided into three frequency ranges. Contrary to the case when only two components are used, this does not necessarily lead to the smallest possible ratio ν_S/ν_X for those values of γ and ϵ. When the peaks are centered at frequencies 1, 3 and 9, results show that use of a 3 component envelope ($\gamma = 2/3, \epsilon = 0.5$), that seperately envelopes the second and third peaks, leads to the minimal upcrossing rate. When a 2 component envelope is used, the minimum ratio ν_S/ν_X is obtained by enveloping the third peak only. For the crossing level r=2, the latter minimum value is slightly smaller than for the 3 component envelope. At level r= 3, the reverse is true (Figs. 39 and 40).

The value of γ at which ν_S/ν_X is minimum is very sensitive to changes in ϵ, although the value of ν_S/ν_X itself changes very little. Figs. 39 and 40 show that at the minimum point the product $\gamma\epsilon$ is nearly constant. This minimum corresponds to $\lambda_{a3} = 1/3$, i.e. to the case where the third component coincides with the third exponential spectral density function.

When the peaks are closer together at frequencies 1, 2 and 4, the above statements remain valid. However, the ratio ν_S/ν_X for the 3 component envelope is smallest when γ is about 0.84 and ϵ about 0.4 (figs. 41 and 42). In this case the second component contains not only the second peak but also about half of the first peak; the third component still corresponds to the third peak.

Section 2.3 Arbitrary number of components

Previous results have shown that X(t) decomposition by partitioning of the spectral density function and use of the rectangular envelope is useful when the spectrum has two or three well seperated peaks. A similar conclusion can be expected for more than three peaks. In the general case when X(t) is the sum of n components $X(t)=\sum_{i=1}^{n} X_i(t)$, and each of the $X_i(t)$ is associated with seperate intervals of frequency contributions, the 1D envelope that corresponds to the surface envelope of Eq. 29 is

$$S(t) = X_1(t) + \sum_{i=2}^{n} S_i(t) \quad . \tag{51}$$

The ratio between the mean upcrossing rates of S(t) and X(t) can be written as

$$\frac{\nu_S}{\nu_X} = \left(1 - \sum_{i=2}^{n} \frac{\lambda_{1,i}^2}{\lambda_{0,i}\lambda_2}\right)^{1/2} J(\delta, r, \epsilon_3, \ldots, \epsilon_n) \tag{52}$$

where ϵ_i is the fraction of the variance of $\sum_{j=2}^{n} X_j(t)$ due to $X_i(t)$,

$$\epsilon_i = \frac{\lambda_{0,i}}{\sum_{j=2}^{n} \lambda_{0,j}} = \frac{\lambda_{0,i}}{1-\lambda_{0,1}} \tag{53}$$

and J is related to the PDF of S as

$$J = \sqrt{2\pi}\, f_S(r)\, e^{r^2/2} \tag{54}$$

The PDF of S results from a convolution of order n-1. However, as n increases and under mild conditions on the component envelopes $S_i(t)$, the process S(t) approaches a normal process

For small n, a better approximation to the distribution of S is obtained by using a series expansion of the Edgeworth type. Towards this end, consider a standardized random variable Q, defined

$$Q = \frac{\sum_{i=1}^{n} (Y_i - m_i)}{\left(\sum_{i=1}^{n} \sigma_i^2\right)^{1/2}} \tag{55}$$

where the Y_i are independent random variables with mean m_i, variance σ_i^2 but otherwise arbitrary distribution.

The PDF of Q can be approximated by the Edgeworth's expansion

$$f_Q(q) = Z(q) - \frac{\gamma_1}{6} Z^{(3)}(q) - \frac{\gamma_2}{24} Z^{(4)}(q) + \frac{\gamma_1^2}{72} Z^{(6)}(q) \tag{56}$$

where

$$\gamma_1 = \frac{\sum_i \chi_{3,i}}{\left(\sum_i \sigma_i^2\right)^{3/2}} \quad , \quad \gamma_2 = \frac{\sum_i \chi_{4,i}}{\left(\sum_i \sigma_i^2\right)^2} \tag{57a}$$

and in which $Z^{(i)}(q)$ is the i th derivative of the normal PDF Z(q) or also

$$Z^{(i)}(q) = (-1)^i \, Z(q) \, He_i(q) \tag{57b}$$

in terms of $He_i(q)$, the Hermite polynomial of order i, and $\varkappa_{j,i}$ the j th cumulant of the random variable Y . Going back to the definition of S(t) in Eq. 51, the variable $X_1(t)$ (the non-enveloped component of X(t)) is normal with zero mean, variance $\lambda_{o,1}$ and zero cumulants, whereas the generic envelope term $S_i(t)$ has Rayleigh ditribution with r th initial moment

$$\mu'_r = 2^{r/2} \Gamma\left(1+\frac{1}{2}r\right) \tag{58}$$

In particular, the first four moments are

$$\mu'_{1,i} = \sqrt{\frac{\pi}{2}} \sqrt{\lambda_{o,i}} \tag{59a}$$

$$\mu'_{2,i} = 2\,\lambda_{o,i} \tag{59b}$$

$$\mu'_{3,i} = 3\sqrt{\frac{\pi}{2}}\,\lambda_{o,i}^{3/2} \tag{59c}$$

$$\mu'_{4,i} = 8\,\lambda_{o,i}^2 \tag{59d}$$

So that

$$E[S_i] = \sqrt{\frac{\pi}{2}}\sqrt{\lambda_{0,i}} = 1.2533\ \lambda_{0,i} \tag{60a}$$

$$\sigma^2_{S_i} = \left(2 - \frac{\pi}{2}\right)\lambda_{0,i} = 0.4292\ \lambda_{0,i} \tag{60b}$$

$$\kappa_{3,i} = \mu_{3,i} = \left(\mu'_{3,i} - 3\mu'_{2,i}\mu'_{1,i} + 2\mu'^{3}_{1,i}\right) \tag{60c}$$

$$= \sqrt{\frac{\pi}{2}}\,(\pi - 2)\,\lambda^{3/2}_{0,i} = 0.17746\ \lambda^{3/2}_{0,i}$$

$$\kappa_{4,i} = \mu_{4,i} - 3\mu_{2,i} = \left(\mu'_{4,i} - 4\mu'_{3,i}\mu'_{1,i} + 12\mu'_{2,i}\mu'^{2}_{1,i} - 6\mu'^{4}_{1,i} - 3\mu'^{2}_{2}\right)$$

$$= \left(-4 + 6\pi - 15\pi^2\right)\lambda^2_{0,i} = 0.04515\,\lambda^2_{0,i} \tag{60d}$$

Combining previous results, one obtains

$$E[S] = 1.2533\ \sum_{i=2}^{n}\sqrt{\lambda_{0,i}} \tag{61a}$$

$$\sigma^2_S = \lambda_{0,1} + 0.4292\ \sum_{i=2}^{n}\lambda_{0,i} \tag{61b}$$

and using Eqs. 57 and 60

$$\gamma_1 = \frac{0.1774\ \sum_{i=2}^{n}\left(\lambda_{0,i}\right)^{3/2}}{\left(\lambda_{0,1} + 0.4292\ \sum_{i=2}^{n}\lambda_{0,i}\right)^{3/2}} \tag{62a}$$

$$\gamma_2 = \frac{0.04515\ \sum_{i=2}^{n}\lambda_{0,i}}{\left(\lambda_{0,1} + 0.4292\ \sum_{i=2}^{n}\lambda_{0,i}\right)^{2}} \tag{62b}$$

If the sum $X_1 + \sum_{i=2}^{n} S_i$ is interpreted as the sum $\Sigma_i Y_i$ in Eq. 55 then the random variable Q corresponds to the standardized envelope S. The distribution of Q can be appoximated by using Eqs. 56 and 62; the associated approximation for the PDF of S is found from

$$f_S(r) = \frac{1}{\sigma_S} f_Q\left[\frac{r - E[S]}{\sigma_S}\right] \tag{63}$$

Finally the factor J is calculated from Eq. 54.

Table 3 contains results for n= 4 (for $S(t)=X_1(t)+S_2(t)+S_3(t)+S_4(t)$) and for the crossing level r= 2.

The fraction of total variance that is enveloped (first column) varies from 0 to 100 %. ϵ_3 and ϵ_4 give the fractions of total enveloped variance that are assigned to S_3

$$\epsilon_3 = \frac{\lambda_{0,3}}{\lambda_{0,2} + \lambda_{0,3} + \lambda_{0,4}}$$

and to S

$$\epsilon_4 = \frac{\lambda_{0,4}}{\lambda_{0,2} + \lambda_{0,3} + \lambda_{0,4}}$$

Because of symmetry, only the combinations of ϵ_3 and ϵ_4 inside the shaded region of Fig. 43 must be examined.

(Notice that Table 3 contains also some redundant combinations for $\epsilon_4 > 1/3$.)

For $\epsilon_4 = 0$, one is back into a case with 3 components. Comparison of the results from this special case with results in Table 2 shows that the present approximation of the PDF of S is very accurate. As one should expect, accuracy decreases as γ increases and ϵ_3 and ϵ_4 are small, because in this case $S(t) \simeq S(t)$, with nearly Rayleigh distribution and the Rayleigh density is not accurately approximated by the formula of Eq. 56. The results of Table 3 again confirm that adding one more envelope component produces an increase of J.

To illustrate the use of Table 3, a very special case will be examined. Consider the spectrum of Fig. 44, composed of 4 peaks at the frequencies 1, 5, 10 and 20. A Gaussian process with that spectrum upcrosses the level r= 2 at a mean rate 0.247 (Eq. 6), whereas the C-L envelope has mean upcrossing rate 0.767 (Eq. 14). In the extreme case when each peak is enveloped seperately, the mean crossing rate becomes zero. One may envelope only and seperately the 3 highest peaks so that $\gamma = 3/4$, $\epsilon_3 = 1/3$ and $\epsilon_4 = 1/3$. From Table 3 one finds

$\gamma = 0.75$	$\epsilon_3 = 0.3$	$\epsilon_3 = 0.4$
$\epsilon_4 = 0.3$	9.503	9.503
$\epsilon_4 = 0.4$	9.503 (symmetry)	9.446

and, by interpolation, J has value 9.497 . Using Eq. 49 the ratio ν_s/ν_x is then

$$\frac{\nu_s}{\nu_x} = \left(1 - \frac{0.25\,5^2 + 0.25\,10^2 + 0.25\,20^2}{131.5}\right)^{1/2} J = 0.414$$

and the upcrossing rate of the envelope is 0.102 . If on the other hand one envelopes the two highest peaks seperately and leaves the remainder of X(t) unenveloped, one finds for $\gamma = 0.5$, $\epsilon_3 = 0.5$ and $\epsilon_4 = 0.0$, that J= 5.778 and $\nu_s/\nu_x = 1.285$. In this case the upcrossing rate of S(t) is higher than that of the original process.

Finally one might envelope the component of X(t) with spectrum at frequencies 5, 10 and 20. Then, for $\gamma = 3/4$, $\epsilon_3 = 0.0$ and $\epsilon_4 = 0.0$, one finds J= 5.03 and $\nu_s/\nu_x = 2.38$. From comparison of the above cases one might conclude that it is better to seperately envelope the higher peaks. In this case

$$\nu_s = 0.0436\,\nu_x \quad J\left(r, \gamma = 0.75, \epsilon_3 = \frac{1}{3}, \epsilon_4 = \frac{1}{3}\right)$$

Other relevant statistics of S(t) are from Eqs. 61 and 62,

$$E[S] = 1.88 \quad , \quad \sigma_s^2 = 0.5719 \quad , \quad \gamma_1 = 0.1539 \quad , \quad \gamma_2 = 0.0259$$

from which it is easy to approximate the factor J using Eqs. 54, 57 and 63. Fig. 45 shows the mean upcrossing rates ν_s and ν_x as functions of r. Above level 2.6, the envelope

has a higher upcrossing rate than the original process.

Section 2.4 Time averaging

In previous sections the process X(t) has been split into mutually independent components $X_i(t)$, each associated with a seperate frequency range of the mean power spectral density function.

In some cases it may be desirable that the component processes have a time domain interpretation (a time-domain relationship with the original process). Next, we consider a decomposition of the process X(t) based on the concept of local averaging, which lends itself to this interpretation.

As before, X(t) is assumed to be a Gaussian and stationary process with zero mean and unit variance. We shall define the first component $X_1(t)$ as a weighted average transformation of X(t) of the type

$$X_1(t) = \int_{-\infty}^{+\infty} k(z)\, X(t-z)\, dz \tag{64}$$

in which k(z) is a given weight or kernel function, chosen to be even and to integrate to 1 (i.e. Fig. 46),

$$k(z) = k(-z) \quad , \quad \int_{-\infty}^{+\infty} k(z)\, dz = 1 \tag{65}$$

The second component $X_2(t)$ is the difference between X(t) and $X_1(t)$; hence

$$X_2(t) = X(t) - X_1(t) \tag{66}$$

One may view $X_1(t)$ as the low-frequency component of X(t)

and $X_2(t)$ as the high-frequency component. Undesirable crossing events are typically due to $X_2(t)$ and this is why a reasonable definition of envelope S(t) is obtained by summing the average process to the C-L envelope of X_2,

$$S(t) = X_1(t) + S_2(t) \tag{67}$$

or more explicitly,

$$S(t) = X_1(t) + \left[X_2^2(t) + \hat{X}_2^2(t) \right]^{1/2} \tag{68}$$

where $\hat{X}_2$ is the Hilbert transform of X_2. Thus the derivative process $\dot{S}(t)$ is

$$\dot{S}(t) = \dot{X}_1(t) + \left(X_2^2 + \hat{X}_2^2 \right)^{-1/2} \left(X_2 \dot{X}_2 + \hat{X}_2 \dot{\hat{X}}_2 \right) \tag{69}$$

The two components X_1 and X_2 are in general not independent, and, as will be seen next, this dependence significantly complicates the calculation of the mean crossing rate of S.

Since the six processes X_1, X_2, $\hat{X}_2$, $\dot{X}_1$, $\dot{X}_2$, $\dot{\hat{X}}_2$ are defined through linear operations on X(t) (Fig. 47), they are all Gaussian with zero mean; it follows that their joint distribution at any given time is completely defined by their covariance matrix. Due to normality and stationarity the derivatives $\dot{X}_1$, $\dot{X}_2$ and $\dot{\hat{X}}_2$ are pairwise independent of the corresponding processes X_1, X_2 and $\hat{X}_2$. The other

elements of the covariance matrix can be calculated as weighted integrals of the spectral density function of X. The weighting functions are the transfer functions of the associated linear operators. For instance, the transfer function associated with the weighted average in Eq. 64 is

$$K(\omega) = \int_{-\infty}^{+\infty} k(\tau)\, e^{-i\omega\tau}\, d\tau \tag{70}$$

Since $k(\tau)$ is even and real, $K(\omega)$ is also even and real. Similarly, the Hilbert transform has associated transfer function (see the convolution integral of Eq. 11)

$$H(\omega) = \begin{cases} -j & , \omega > 0 \\ +j & , \omega < 0 \end{cases} \tag{71}$$

In this case $h(\tau)$ is odd and real; hence $H(\omega)$ is an odd and imaginary function.

Finally, differentation corresponds to the transfer function $D(\omega)$, where

$$D(\omega) = j\omega \tag{72}$$

Using the theory of linear, time-invariant transformation of random processes, the mean power and cross spectral density functions of the processes X_1, X_2, $\hat{X}_2$, $\dot{X}_1$, $\dot{X}_2$, $\dot{\hat{X}}_2$ can be

evaluated. For example, in the case of X_1 and X_2,

$$S_{11}(\omega) = K^2(\omega)\, S_{xx}(\omega) \tag{73a}$$

$$S_{22}(\omega) = [1 - K(\omega)]^2\, S_{xx}(\omega) \tag{73b}$$

$$S_{12}(\omega) = K(\omega)\,[1 - K(\omega)]\, S_{xx}(\omega) \tag{73c}$$

where the fact was used that the complex conjugate of $K(\omega)$ is identical to $K(\omega)$ itself, since $K(\omega)$ is a real function. The variances and covariances can now be evaluated by integrating the spectral density functions over all frequencies. For example, the covariance between X_1 and X_2, σ^2_{12}, is

$$\sigma^2_{12} = \int_{-\infty}^{+\infty} K(\omega)\,[1 - K(\omega)]\, S_{xx}(\omega)\, d\omega \tag{74}$$

Similarly, the covariance between X_1 and $\hat{X}_2$ is

$$\sigma^2_{1\hat{2}} = \int_{-\infty}^{+\infty} K(\omega)\,[1 - K(\omega)]\, H^*(\omega)\, S_{xx}(\omega)\, d\omega \tag{75}$$

but since $H(\omega)$ is an odd function, $\sigma^2_{1\hat{2}}$ equals zero and X_1 and X_2 are uncorrelated (in this case independent) variables. Note that this correlation being zero is a direct consequence of the fact that the kernel function $K(\omega)$ is real and even.

The complete covariance matrix has the form :

$$
\begin{array}{c}
\begin{array}{cccccc} X_1 & X_2 & \dot{\hat{X}}_2 & \dot{X}_1 & \hat{X}_2 & \dot{X}_2 \end{array} \\
\begin{bmatrix}
\lambda_{0,11} & \lambda_{0,12} & \lambda_{1,12} & & & \\
\lambda_{0,12} & \lambda_{0,22} & \lambda_{1,22} & & 0 & \\
\lambda_{1,1\hat{2}} & \lambda_{1,22} & \lambda_{2,22} & & & \\
 & & & \lambda_{2,11} & \lambda_{1,12} & \lambda_{2,12} \\
 & 0 & & \lambda_{1,12} & \lambda_{0,22} & \lambda_{1,22} \\
 & & & \lambda_{2,12} & \lambda_{1,22} & \lambda_{2,22}
\end{bmatrix}
\end{array}
\tag{76}
$$

The notation $\lambda_{i,\bullet}$ for terms that are not necessarily zero stands for the i th initial moment of the mean power or cross spectrum $S_\bullet$. As one can see, there are two independent groups of variables, $(X_1, X_2, \dot{\hat{X}}_2)$ and $(\dot{X}_1, \hat{X}_2, \dot{X}_2)$.

We now have all the elements to theoretically calculate the mean crossing rate of the envelope proces S(t) in Eq. 68, using Rice's formula. Unfortunately,this is not a trivial task in practice.

The PDF of S(t) can be found as a weighted integral of the conditional PDF of S given X_2 and $\hat{X}_2$, the weight being given by the joint distribution of X_2 and $\hat{X}_2$

$$
f_S(s) = \iint f_{S|X_2,\hat{X}_2}(s, x_2, \hat{x}_2)\, f_{X_2,\hat{X}_2}(x_2, \hat{x}_2)\, dx_2\, d\hat{x}_2 \tag{77}
$$

For given X_2 and $\hat{X}_2$, S equals X_1 plus a constant; therefore, the conditional distribution of S given X_2 and $\hat{X}_2$ is Gaussian. Its mean and variance can be evaluated using elements of the covariance matrix in Eq. 76 with the following result

$$E[S|X_2,\hat{X}_2] = (X_2^2 + \hat{X}_2^2)^{1/2} + E[X_1|X_2,\hat{X}_2] \tag{78a}$$
$$= (X_2^2 + \hat{X}_2^2)^{1/2} + X_2 \frac{\lambda_{0,12}}{\lambda_{0,22}}$$

$$\sigma^2[S|X_2,\hat{X}_2] = \lambda_{0,11} - \frac{\lambda^2_{0,12}}{\lambda_{0,22}} \tag{78b}$$

Since X_2 and $\hat{X}_2$ are independent Gaussian variables, their joint density function is

$$f_{X_2,\hat{X}_2}(x_2,\hat{x}_2) = \frac{1}{2\pi\lambda_{0,22}} e^{-\frac{x_2^2}{2\lambda_{0,22}}} e^{-\frac{\hat{x}_2^2}{2\lambda_{0,22}}} \tag{79}$$

In the case when X_1 and X_2 are independent variables(it is not so here), the term $X_2 \frac{\lambda_{0,12}}{\lambda_{0,22}}$ in Eq. 78a vanishes and a transformation of coordinates from cartesian $(X_2,\hat{X}_2)$ to polar (R,ϕ) simplifies the double integral of Eq. 77, reducing it to a single integral. Unfortunately, dependence of X_1 on X_2 makes the above procedure impossible (or valid only in approximation) and forces one to use numerical integration.

Calculation of the partial expectation of $\dot{S}$ given S= r, which is needed to calculate the mean crossing rate, is even

more complicated. Only the general procedure to calculate this quantity is outlined here.

The conditional mean values and covariance matrix of the variables $(X_1, \dot{X}_1)$ given the four quantities $(X_2, \dot{\hat{X}}_2, \hat{X}_2, \dot{X}_2)$ can be found from the covariance matrix in Eq. 76. One can immediately see that X_1 and $\dot{X}_1$ remain uncorrelated. Because for given $(X_2, \dot{\hat{X}}_2, \hat{X}_2, \dot{X}_2)$ the envelope S(t) depends only on X_1 and the envelope derivative $\dot{S}$ depends only on $\dot{X}_1$, it also follows that S and $\dot{S}$ are independent and their conditional bivariate distribution is the product of two Gaussian distributions,

$$f_{S,\dot{S}|X_2,\dot{\hat{X}}_2,\hat{X}_2,\dot{X}_2} = f_{S|X_2,\hat{X}_2}\, f_{\dot{S}|X_2,\dot{\hat{X}}_2,\hat{X}_2,\dot{X}_2} \tag{80}$$

Integration of this conditional density multiplied by the density of $(X_2, \dot{\hat{X}}_2, \hat{X}_2, \dot{X}_2)$ leads to the unconditional bivariate density function $f_{S,\dot{S}}$. And since the vector $(X_2, \dot{\hat{X}}_2)$ is independent of the vector $(\hat{X}_2, \dot{X}_2)$,

$$f_{S,\dot{S}} = \iiiint f_{S|X_2,\hat{X}_2}\, f_{\dot{S}|X_2,\dot{\hat{X}}_2,\hat{X}_2,\dot{X}_2}\, f_{X_2\dot{\hat{X}}_2}\, f_{\hat{X}_2\dot{X}_2}\, dx_2\, d\dot{\hat{x}}_2\, d\hat{x}_2\, d\dot{x}_2 \tag{81}$$

The integral can be simplified further, since it is symmetrical in the pairs $(X_2, \dot{\hat{X}}_2)$ and $(\hat{X}_2, \dot{X}_2)$ - e.g. it is not necessary to integrate over the complete 4D space - however, it still remains a four dimensional integral. Using the joint distribution of $(S, \dot{S})$ and the marginal

distribution of S, the conditional partial expected value of $\dot{S}$,

$$E_o^\infty [\dot{S} | S=r] = \int_o^\infty \dot{s} f_{\dot{S}|S}(\dot{s},r)\, d\dot{s} \tag{82}$$

can be found as

$$E_o^\infty [\dot{S} | S=r] = \int_o^\infty \dot{s} \frac{f_{S,\dot{S}}(r,s)}{f_S(r)} d\dot{s} \tag{83}$$

As shown above, calculation of the mean upcrossing rate of the present envelope is prohibitively complicated. Simplification is possible if the components $(X_1, \dot{X}_1)$ are independent of the remaining components $(X_2, \dot{X}_2, \hat{X}_2, \dot{\hat{X}}_2)$, a case which leads to the solution of previous sections. In terms of the elements of the covariance matrix in Eq. 76, this requires that

$$\lambda_{0,12} = \lambda_{1,12} = \lambda_{2,12} = 0 \tag{84}$$

where

$$\lambda_{0,12} = 2\int_o^\infty K(\omega)[1-K(\omega)] S_{xx}(\omega)\, d\omega \tag{85a}$$

$$\lambda_{1,12} = 2\int_o^\infty \omega K(\omega)[1-K(\omega)] S_{xx}(\omega)\, d\omega \tag{85b}$$

$$\lambda_{2,12} = 2\int_o^\infty \omega^2 K(\omega)[1-K(\omega)] S_{xx}(\omega)\, d\omega \tag{85c}$$

These conditions are satisfied, irrespective of the spectrum $S_{XX'}$ when $K(\omega)$ is a function with values 0 and 1 only. For

example, for the two independent components in Section 2.2, $K(\omega)$ corresponds to a low frequency filter (Fig.48), with

$$K(\omega) = \begin{cases} 1 & , \ \omega \leq \omega_c \\ 0 & , \ \omega > \omega_c \end{cases} \tag{86}$$

and associated kernel function (Fig. 49)

$$k(z) = \frac{\sin \omega_c z}{\omega_c z} \tag{87}$$

Unfortunately, the conditions of Eq. 85 are typically not satisfied, except for very special cases. The correlation between X_1 and X_2 has been calculated in the case of exponential kernel function and rectangular block spectrum (Fig. 50), i.e., for

$$k(z) = \frac{1}{2T} e^{-\frac{|z|}{T}} \tag{88a}$$

$$S_{xx}(\omega) = \frac{1}{2\Delta\omega} \qquad \omega_1 \leq |\omega| \leq \omega_2 \tag{88b}$$

The associated transferfunction $K(\omega)$ is

$$K(\omega) = \frac{1}{1 + (T\omega)^2} \tag{89}$$

Therefore

$$\sigma_{11}^2 = \frac{1}{2\Delta\omega T}\left[\arctan T\omega_2 - \arctan T\omega_1 + \frac{\omega_2 T}{(\omega_2 T)^2+1} - \frac{\omega_1 T}{(\omega_1 T)^2+1}\right] \quad (90a)$$

$$\sigma_{12}^2 = \frac{1}{2\Delta\omega T}\left[\arctan T\omega_2 - \arctan T\omega_1 - \frac{\omega_2 T}{(\omega_2 T)^2+1} + \frac{\omega_1 T}{(\omega_1 T)^2+1}\right] \quad (90b)$$

and the variance of X_2 can be found from the relation

$$\sigma_{11}^2 + \sigma_{22}^2 + 2\sigma_{12}^2 = 1 \quad (91)$$

Fig. 51 shows these variance and covariance terms as functions of $T\omega_2$ for different values of $T\omega_1$. The covariance is half the complement to 1 of $\sigma_{11}^2 + \sigma_{22}^2$.

Near the origin ($T\omega_1 \simeq T\omega_2 \simeq 0$) either T is very small (the kernel function is very steep) or ω_1 and ω_2 are very small (the process varies slowly). These two conditions are clearly equivalent. In both cases the first component X_1 is practically identical to the process X(t) and no enveloping results.

When $T\omega_1$ and $T\omega_2$ are large, the weighted-average tends to coincide with the mean of the process and hence is eventually zero. In this case, the present envelope coincides with the C-L envelope.

For intermediate values of the parameters, Fig. 51 shows that the covariance is not negligible relative to the variances (that correlation is high); hence the assumption

that X_1 and X_2 are independent is likely to produce rather erroneous results.

It is possible, by linear transformation, to define two new components, say Y_1 and Y_2, in terms of X_1 and X_2 that are independent. However, the conditions in Eq.85 b and c are not necessarily satisfied by the new processes. For instance, the processes Y_1 and Y_2 may be made independent at any given time and their derivatives $\dot{Y}_1$ and $\dot{Y}_2$ still be dependent.

One may conclude that the time averaging procedure proposed in this section is difficult to use in practice. However, it is interesting to note that our previous results correspond to a very special case of the time averaging procedure and might be interpreted in that perspective.

Section 2.5 Empty envelope excursions

At high levels crossing events are more frequent for the C-L envelope (and also for the modified C-L envelope proposed here) than for the original process. Hence, some of the envelope excursions are "empty", in the sense that they do not contain any level crossing by the process X(t). If ν_S denotes the mean rate of envelope excursions and P_E is the probability (or fraction) of empty excursions, then qualified (non-empty) excursions occur with mean rate $\nu_S P_E$. Clearly, we are interested here in this last quantity, which is necessarily not larger than the mean rate of process upcrossings ν_X.

An approximation to P_E, derived by Vanmarcke (1970) for the case of narrow-band processes and the Cramer-Leadbetter envelope is reviewed first. This approximation is found inadequate in the case of broad-band processes and alternative approximations are proposed in this section. A first model, model A, approximates the average number of X(t) crossings during a qualified envelope upcrossing, while the second model, model B, approximates the probability of having no X(t) crossing during any envelope upcrossing (similar to Vanmarcke's approximation). Model A differs from model B in its assumptions about the occurrence of X(t) crossings during S(t) excursions. Model A describes a certain pattern of these occurrences during qualified

envelope excursions only, while model B makes assumptions about the pattern during any envelope excursions.

The results of Vanmarcke for non-empty envelope excursions are based on the following model.
In a narrow-band process X(t), peaks tend to occur with regularity at distance approximately equal to $1/\nu_{X,0}$, where $\nu_{X,0}$ is the zero upcrossing rate of the process (Fig. 52). The same process is nearly equal to its C-L envelope S(t) at the points of local maximum. Hence, excursions of S(t) during which X(t) attains at least one local maximum can be considered as not empty.
It is assumed that the sequence of times at which X(t) is maximum is perfectly regular with frequency $\nu_{X,0}$ and that it is independent of the envelope process S(t). Suppose that S(t) upcrosses level r at time 0 and denote by $P_X(t)$ the probability of having no peak of X within the time interval 0 to t. The latter probability varies linearly with t from the value 1 at t=0 to the value 0 at $t=1/\nu_{X,0}$ (Fig. 53). The probability P_E that the generic envelope excursion above a given level r is empty is then

$$P_E = \int_0^\infty P_X(t)\, f_T(t) \tag{92}$$

where f_T is the PDF of the duration T of envelope excursions above level r, and is approximated as follows.

Let T_u be the time between upcrossing events of S(t) relative to level r. In terms of the mean upcrossing rate of r by S and under the condition that S(t) is ergodic in $E[T_u]$, the expected value of T_u is

$$E[T_u] = \frac{1}{\nu_S} \tag{93}$$

The ratio between the expected values of T= duration of excursions of S <u>above</u> level r and T^*= duration of excursion of S <u>below</u> level r is

$$\frac{E[T]}{E[T^*]} = \frac{P[S \geq r]}{P[S < r]} \tag{94}$$

and since

$$E[T] + E[T^*] = E[T_u] \tag{95}$$

it follows that

$$m_T = E[T] = \frac{P[S \geq r]}{\nu_S} \tag{96}$$

A convenient, although approximate distribution for T is the exponential distribution : it only requires one parameter and is asymptotically exact for large values of T. According to the present approximation for $P_X(t)$ and $f_T(t)$, the fraction of qualified envelopes, $1-P_E$, is from Eq. 92

$$1 - P_E = \nu_{X,0}\, m_T \left(1 - e^{-\frac{1}{\nu_{X,0}\, m_T}}\right) \tag{97}$$

The associated ratio Q between the rate of qualified envelope exursions and the rate of upcrossings by the process X(t) is equal to $\nu_s(1-P_E)/\nu_x$ and using Eqs. 96 and 97 one finds

$$Q = \frac{\nu_{x,o}\, P[S \geq r]}{\nu_x} \left(1 - e^{-\frac{1}{\nu_{x,o} m_T}}\right) \tag{98}$$

For the case when S(t) is the C-L envelope, the first factor in Eq. 98 reduces to 1 and the above ratio Q becomes

$$Q = 1 - e^{-\frac{1}{\nu_{x,o} m_T}} = 1 - e^{-\frac{\nu_s}{\nu_x}} \tag{99}$$

and is always smaller than 1.

For broad-band processes, the approximations of the previous model become inaccurate, as one can easily see from the example of Fig. 5, in which realizations of X(t) and S(t) are shown for the case of a bichromatic process with well-seperated frequencies. In this case it is not necessarily true that if S(t) is above level r at the time when X(t) has a local maximum then the process X(t) is also above level r. The fact that Eq. 99 still gives values of Q less than 1 should be seen as coincidental.
We shall next present two models, A and B, which are more appropriate for broad-band processes.

Model A explicitly considers that qualified envelope excursions are only a fraction of the process upcrossings. By definition, every upcrossing of X(t) must occur during a qualified envelope upcrossing. Therefore, the total number of X(t) upcrossings during a period of length T equals the sum of the number of X(t) upcrossings during each qualified envelope excursion in that period (except for boundary effects that become negligible for large T), and

$$N_X = \frac{N_{X|S_1} + N_{X|S_2} + \ldots}{N_{S,q}} N_{S,q} \tag{100}$$

in which $N_{S,q}$ is the number of qualified envelope excursions in T. In the limit as $T \to \infty$ and under the condition that the process is ergodic, the fraction in the right hand side is the mean clump size, i.e., the average number of X(t) upcrossings during each qualified envelope upcrossing. Ergodicity is required to replace the ensamble mean with a time average. Then, Eq. 100 can be written also as

$$\frac{\nu_S}{\nu_X}(1 - P_E) = \frac{1}{E[clumpsize]} \tag{101}$$

Model A approximates the mean clumpsize by assuming that during a qualified envelope excursion the local maxima of X(t) occur at constant distance, which corresponds to the rate of zero upcrossings by the derivative process $\dot{X}(t)$ (this is the mean rate of local maxima). It is also assumed

that during qualified envelope excursions, each point of local maximum is also a point of tangency with the envelope. The first local maximum is assumed to occur at the time of envelope upcrossing. The expected number of upcrossings is then equal to

$$E\,[\,clumpsize\,] = 1 + \int_0^\infty Int\,(\nu_{\dot{x},0}\,t)\,f_T(t)\,dt \tag{102}$$

If the excursion length of the envelope, T, has exponential density

$$f_T(t) = \frac{1}{m_T}\,e^{-\frac{t}{m_T}} \tag{103}$$

then Eq. 102 becomes

$$E\,[clumpsize] = 1 + \int_0^\infty \frac{Int\,(\nu_{\dot{x},0}t)}{m_T}\,e^{-\frac{t}{m_T}}\,dt \tag{104}$$

or also

$$E[clumpsize] = 1 + \Sigma_i \int_{\frac{i}{\nu_{\dot{x},0}}}^{\frac{i+1}{\nu_{\dot{x},0}}} \frac{i}{m_T}\,e^{-\frac{t}{m_T}}\,dt \tag{105}$$

$$= 1 + \Sigma_i\; i\,e^{-\frac{i}{\nu_{\dot{x},0}\,m_T}}$$

The summation term in Eq. 105 corresponds to the expected value of a geometric distribution with probability masses $p(1-p)^i$, and

$$p = 1 - e^{-\frac{1}{\nu_{\dot{x},0}\,m_T}}$$

Hence

$$E[\text{clumpsize}] = 1 + \frac{e^{-\frac{1}{\nu_{\dot{x},0} m_T}}}{1 - e^{-\frac{1}{\nu_{\dot{x},0} m_T}}} \tag{106}$$

$$= \frac{1}{1 - e^{-\frac{1}{\nu_{\dot{x},0} m_T}}}$$

The associated ratio Q is

$$Q = 1 - e^{-\frac{1}{\nu_{\dot{x},0} m_T}} \tag{107}$$

For a narrow-band process, $\nu_{\dot{x},0} \approx \nu_{x,0}$ and Eq. 107 is equivalent to Eq. 99 (which is valid for the Cramer-Leadbetter envelope). However, since in general $\nu_{\dot{x},0} \geq \nu_{x,0}$, Eq. 107 leads to smaller Q ratios for broad-band processes.

Model B is similar to Vanmarcke's model for narrow-band processes; it differs in the assumption that peaks of X occur regularly with frequency $\nu_{\dot{x},0}$ instead of $\nu_{x,0}$. This is a more accurate assumption for broad-band processes (Fig. 54). Since all the calculations remain the same, one can directly modify Eq. 97 which becomes

$$1 - P_E = \nu_{\dot{x},0} m_T \left(1 - e^{-\frac{1}{\nu_{\dot{x},0} m_T}}\right) \tag{108}$$

and Q is given by

$$Q = \frac{\nu_{\dot{x},0}}{\nu_x(r)} P[S \geq r] \left(1 - e^{-\frac{1}{\nu_{\dot{x},0} m_T}}\right) \tag{109}$$

When the C-L envelope is used, Eq. 109 can be written

$$Q = \frac{\sqrt{\lambda_4}}{\lambda_2}\left(1 - e^{-\frac{1}{\nu_{\dot{x},0} m_T}}\right) \tag{110}$$

At high levels, m_T becomes very small and the above expressions simplify to

$$Q = \frac{\sqrt{\lambda_4}}{\lambda_2} \geq 1 \tag{111}$$

The fact that that for broad-band processes and C-L envelopes, Q is larger than 1 shows that the reduction based on this model is too small and that part of the envelope upcrossings considered as qualified are actually empty. The main reason for this error is the assumption that the envelope coincides with the process at the points where the latter is locally maximum. Comparison of Eqs. 107 and 109 shows that the results obtained by the two models only differ by the factor $\frac{\nu_{\dot{x},0}}{\nu_x} P[S \geq r]$. Since the models are essentially equivalent when all points of local maxima of X(t) are points of tangency to S(t), this factor is a measure of how closely S(t) is to X(t). Eqs. 107 and 109 are valid for an arbitrary envelope. However, in order to evaluate the expected duration of envelope excursions above level r, m_T in Eq. 96, one needs to know the mean upcrossing rate of S and the distribution of S, or at least the exceedance probability

$$P[S \geq r] = \int_r^\infty f_S(s)\, ds \tag{112}$$

In the case of partial enveloping $f_S(s)$ is given in Eq. 39. The integral of the first term in Eq. 39 is

$$\lambda_{o,1}\left[1 - \Phi\left(\frac{+r}{\sqrt{\lambda_{o,1}}}\right)\right] \tag{113}$$

The integral of the second term can be written

$$\lambda_{o,2}\int_r^\infty \left[1 - \Phi\left(-s\sqrt{\frac{\lambda_{o,2}}{\lambda_{o,1}}}\right)\right] d\left(-e^{-\frac{s^2}{2}}\right) \tag{114}$$

and after integration by parts the same term becomes

$$\sqrt{\lambda_{o,2}}\, e^{-\frac{r^2}{2}}\left[1 - \Phi\left(-r\sqrt{\frac{\lambda_{o,2}}{\lambda_{o,1}}}\right)\right] \tag{115}$$

$$+\sqrt{\lambda_{o,2}}\int_r^\infty \sqrt{\frac{\lambda_{o,2}}{\lambda_{o,1}}}\,\frac{1}{\sqrt{2\pi}}\, e^{-\frac{s^2\lambda_{o,2}}{2\lambda_{o,1}}}\, e^{-\frac{s^2}{2}}\, ds$$

By using the fact that $\lambda_{o,1} + \lambda_{o,2} = 1$, the integral of the last equation can be simplified to

$$\lambda_{o,2}\left[1 - \Phi\left(\frac{r}{\sqrt{\lambda_{o,1}}}\right)\right] \tag{116}$$

Substitution of these results into Eq. 110 gives

$$P[S \geq r] = 1 - \Phi\left(\frac{r}{\sqrt{\lambda_{o,1}}}\right) + \sqrt{\lambda_{o,1}}\, e^{-\frac{r^2}{2}}\left[1 - \Phi\left(-r\sqrt{\frac{\lambda_{o,2}}{\lambda_{o,1}}}\right)\right] \tag{117}$$

Table 4 gives values of $P(S \geq r)$ for selected values of r and of the fraction $\lambda_{o,2}$ of total variance associated with the enveloped component.

Use of this table to calculate the ratio Q for model A is illustrated next for a spectrum composed of two rectangular blocks, the same as considered earlier in Sec. 2.1 (Fig. 19). In this case one finds, for example, that $\nu_s/\nu_x = 1.56$ for r=3 and $\lambda_{0,2} = 0.5$ (i.e. the spectral density function is split into two parts with equal area and the part with higher frequency is enveloped). A correction for empty envelope excursions is necessary because $\nu_s/\nu_x > 1$. From Table 4, one finds that for $\lambda_{0,2} = 0.5$ the probability that S is larger than 3 is 0.0056 . The second and fourth initial moments of the spectrum are $34.83\,\omega_1^2$ and $2317.7\,\omega_1^4$ respectively (Fig. 55). Therefore the mean upcrossing rate of the envelope is

$$\nu_s = 1.53\,\nu_x = 1.53\,\frac{1}{2\pi}\sqrt{\lambda_2}\;e^{-\frac{r^2}{2}} = 0.016\,\omega_1$$

and the zero upcrossing rate of the derivative process X(t) is

$$\nu_{\dot{x},0} = \frac{1}{2\pi}\sqrt{\frac{\lambda_4}{\lambda_2}} = 1.30\,\omega_1$$

It follows from Eq. 96 that $m_T = 0.35/\omega_1$ and from Eq. 107 that Q, the rate of qualified envelope upcrossings and process upcrossings, is 0.89 (at level 3 and for enveloping only the higher frequency component), which is a number significantly smaller than 1.

Before obtaining some results for the model B, we shall slightly modify Eq. 111. We mentioned already that the assumption of exponential distribution for the duration T of envelope excursions is asymptotically exact for large T. However, at high levels and in all cases for small values of T, Rice (1958) showed that the distribution of T is of the Rayleigh type. We shall develop next a more flexible distribution, which meets both requirements, i.e., that starts as a Rayleigh and has exponential right tail.
The probability that the time T is larger than t can be expressed in terms of the conditional downcrossing rate for the envelope, given that the envelope is upcrossing at time 0 and has remained above level r from 0 to the present time. If $\nu_{s|c}(t)$ denotes this conditional downcrossing rate at time t (the hazard function at t associated with downcrossing events) then

$$\frac{d}{dt} P[T \geq t] = -\nu_{s|c}(t) P[T \geq t] \tag{118}$$

so that

$$P[T \geq t] = e^{-\int_0^t \nu_{s|c}(t)\, dt} \tag{119}$$

Next we assume that $\nu_{s|c}$ is proportional to t for small t (this assumption corresponds to the Rayleigh distribution) and is constant for large t (so that the tail of F_T is

exponential); see Fig. 56.

The fact that ν_{SIC} is small soon after the upcrossing event reflects the idea that at small times t, the condition that $\dot{S}(t) > 0$ at time 0 makes downcrossings less likely. Specifically, it is assumed that

$$\nu_{SIC} = \begin{cases} \frac{a}{m_T}\,\frac{t}{m_T} & \frac{t}{m_T} \le f \\ \frac{a}{m_T}\,f & \frac{t}{m_T} \ge f \end{cases} \tag{120}$$

where a and f are parameters.

The associated complementary CDF of T is

$$P[T \ge t] = \begin{cases} e^{-a\frac{t^2}{2m_T^2}} & \frac{t}{m_T} \le f \\ e^{-af\left(\frac{t}{m_T} - \frac{f}{2}\right)} & \frac{t}{m_T} \ge f \end{cases} \tag{121}$$

Since the expected value m_T can be calculated, the following relation must hold between a and f

$$m_T \left\{ \frac{e^{-\frac{af^2}{2}}}{af} + \sqrt{\frac{2\pi}{a}}\left[\Phi\left(f\sqrt{a}\right) - 0.5\right] \right\} = m_T \tag{122}$$

Fig. 57 shows a, the product af and the coefficient of variation of T as a function of f. For $f \to 0$, the distribution becomes exponential (in this case af goes to 1

and a goes to infinity). As f goes to infinity, the distribution becomes Rayleigh; in this case a equals $\pi/2$ and the product af diverges. The coefficient of variation of T decreases monotonically as f increases.

The parameter f cannot be determined, unless some other characteristic of the distribution of T is known. A simple assumption is that the initial condition, that S(t) upcrosses the level r at time 0, influences the shape of the distribution over a time fm_T, the derivation of which depends only on the correlation of the envelope process.

Following Vanmarcke's mean clump size model (except for the distribution of T), the ratio Q can be calculated from Eq. 92, which, for $fm_T \leq \frac{1}{\nu_{x,0}}$, gives

$$1 - P_E = \nu_{x,0} m_T \left(1 - e^{\frac{af^2}{2}} e^{-\frac{af}{\nu_{x,0} m_T}/af}\right) \qquad (123a)$$

For $fm_T \geq \frac{1}{\nu_{x,0}}$, Eq. 92 integrates only the Rayleigh part of the distribution of T from 0 to $1/\nu_{x,0}$ and gives

$$1 - P_E = \nu_{x,0} m_T \left(1 - \frac{\nu_{x,0} m_T}{a} e^{-\frac{a}{2(\nu_{x,0} m_T)^2}}\right) \qquad (123b)$$

For the C-L envelope, $\nu_{x,0} m_T$ equals ν_x/ν_s.

Fig. 58 shows the fraction of qualified envelopes, $1-P_E$, as a function of ν_s/ν_x, for different values of f.

When f=0, the distribution of T is exponential and results coincide with those of Vanmarcke.

When $fm_T \geq \frac{1}{\nu_{x,0}}$ (i.e, $f \geq \nu_s/\nu_x$), T has a Rayleigh

distribution over the integration interval $(0, 1/\nu_{x,o})$ and Eq. 123b holds. The latter case leads to a larger fraction of qualified envelope upcrossings because the Rayleigh distribution has more envelope excursions with large duration than the exponential distribution. However, the fraction of qualified envelope upcrossings is only moderately sensitive to the parameter f.

We will next present a revision of some of the results in Section 2.1 comparing models A and B.
First, however we shall summarize shortly the characteristics of the two models and present some numerical results.
Model A uses Eq. 107 and explicitly approximates the number of X(t) crossings during a qualified envelope excursion. Fig. 59 shows Q as a function of the enveloped variance and different crossing levels r for a rectangular block spectrum with $\omega_2/\omega_1 = 5$ (Fig. 11.a). At $\lambda_{o,2} = 0$ (no enveloping) the envelope coincides with the process and Q should be 1. The source of the error is that in deriving Eq. 107, independence was assumed between X(t) and S(t) crossings. For nearly complete enveloping ($\lambda_{o,2}$ close to 1) the results must be evaluated in consideration of earlier observations on the uncorrected ν_s/ν_x ratio (Fig. 14). For instance, we know that for $\lambda_{o,2}$ about 0.7 the envelope has less upcrossings than for $\lambda_{o,2} = 1$. On the other hand,

Fig. 59 shows that after correction for empty upcrossings, the upcrossing rate is practically the same. However, the envelope for $\lambda_{0,2} = 0.7$ is smoother and follows the original process more closely than the Cramer-Leadbetter envelope. Model B, on the other hand, uses Eqs. 123a and 123b but replaces $\nu_{x,0}$ with $\nu_{\dot{x},0}$. Thus :

$$Q = \begin{cases} \frac{\nu_s}{\nu_x} \nu_{\dot{x},0} m_T \left[1 - \frac{e^{\frac{af^2}{2}} e^{\frac{-af}{\nu_{\dot{x},0} m_T}}}{af}\right] & \text{if } f m_T \leq \frac{1}{\nu_{\dot{x},0}} \quad (124a) \\ \frac{\nu_s}{\nu_x} \nu_{\dot{x},0} m_T \left[1 - \frac{\nu_{\dot{x},0} m_T}{a} e^{-\frac{a}{2(\nu_{\dot{x},0} m_T)^2}}\right] & \text{if } f m_T \geq \frac{1}{\nu_{\dot{x},0}} \quad (124b) \end{cases}$$

In contrast to model A, model B uses an approximation to the probability of having no upcrossing during <u>any</u> envelope excursion. Since the assumption is made that $S(t) \doteq X(t)$ at the points of local maximum of the process, it follows that the accuracy depends on how closely the envelope follows the process. An example is given in Fig. 60, where the spectral density function has the same rectangular form as previously considered. The parameter f is set equal to 0.1, hence it is assumed that the distribution of the excursion length for the envelope is exponential above $0.1 m_T$. For nearly complete enveloping and high levels r, the crossing rate ratio Q tends to $\sqrt{\lambda_4}/\lambda_2$ as was mentioned before. Q decreases rapidly for smaller values of $\lambda_{0,2}$. For smaller than 0.5, the model seems to be extremely sensitive

to the assumption that X(t) crossings are independent of S(t) crossings and the results are unreliable. For instance, when S(t) coincides with X(t) ($\lambda_{0,2} = 0$), the probability that the time of the first X(t) crossing during the excursion exceeds t is zero everywhere, except at time 0. Model B, however, assumes that this probability varies linearly (Fig. 53).

Fig. 61 shows similar results for f= 10. In that case, only the upper tail of the distribution of the excursion length of the envelope, above $10m_T$, is exponential; the lower part has a Rayleigh distribution. Comparison of Figs. 61 and 60 shows that in the region of interest ($\lambda_{0,2} > 0.5$) and for high crossing levels, Q is slightly higher for f=10 than for f=0.1. However, the difference is small and further results will all be based on f= 1.

The first spectrum, that has been reconsidered is the rectangular blockshape (Fig. 11.a, Figs. 62-66). In the extreme case of a single spectral mass concentrated at one frequency, the Cramer-Leadbetter envelope has clearly the smallest Q ratio (Fig. 62). As the bandwidth of the spectrum increases (Figs. 63 and 64), one can see that the minimum in model B at $\lambda_{0,2} = 1$ vanishes and the best agreement between model A and B is reached values of around 0.7. This is true also for extremely wide spectra as in the case of Figs. 65 and 66. In all cases, agreement

between models A and B is poor for small $\lambda_{o,2}$, mainly due to the inadequacy of model B.

The second spectrum consists of two seperate rectangular blocks (Fig. 11.b, Figs. 67-72). In the special case of two density peaks at ω_1 and ω_2 with frequency ratio $\omega_2/\omega_1 = 5$, both models lead to a pronounced minimum of Q at $\lambda_{o,2} = 0.5$ (each part is enveloped seperately) and results from the two models agree "reasonably" well at this point (Fig. 67). When the peaks are replaced with rectangular blocks, the agreement at the minimum point, $\lambda_{o,2} = 0.5$, is slightly better (Fig. 68). This may be due to the fact that crossings of the envelope and the generic process are less correlated. Bringing the blocks closer together (Fig. 69) has a negative effect on the agreement of the two models. Again increasing the bandwidth of the individual blocks (Fig. 70) improves the results. In all cases, however, the point at which Q is minimal for model A remains unchanged. Figs. 71 and 72 show results when the variance of the high frequency component is increased and decreased. Again, the minimal ratio corresponds to partial high-frequency enveloping of components. When the variance of the enveloped part is increased (Fig. 71), model A and B agree very well. In contrast, when the variance of the enveloped part is decreased (Fig. 72), model B becomes inaccurate and the results differ considerably.

Finally, Figs. 73 and 74 give some additional results for a

discrete spectrum. Note that for $\omega_2/\omega_1 = 2$, it is not very clear whether partial enveloping is useful. For $\omega_2/\omega_1 = 10$, the results clearly indicate that partial enveloping of the peaks reduces the ratio Q. In this case, results from the two models are in relatively good agreement.

The results of this section confirm previous conclusions in Section 2.1. In particular, they emphasize the importance of a spectral gap in finding a minimum crossing rate ratio Q. They also show that when a spectral gap exists, the results at the minimum point are very robust to changes in the individual bandwidth of the components. In general,however , models A and B lead to quite different results. Model A appears to be more accurate than model B, especially at low $\lambda_{o,2}$ values.

In all cases the correction for empty envelope upcrossings is found to be very important. In several case, the ratio of qualified envelope upcrossings to process upcrossings for the partial envelope is considerably lower than that of the Cramer-Leadbetter envelope, and, in these cases, the partial enveloping procedure is a better alternative.

Section 3 Envelopes of random fields

Extension of the definition of envelope from random functions on the line to random functions in higher dimensional spaces is not a trivial operation. Some work in this direction has been done by Adler and Hasofer and is reviewed in the first two subsections.

Specifically, Section 3.1 introduces a definition of envelope for random fields and gives some examples, whereas Section 3.2 presents some results on the so-called Euler characteristic of excursion sets.

In Section 3.3 we shall demonstrate the equivalence of the definition of the envelope by Adler and Hasofer with the Cramer-Leadbetter envelope along a certain direction.

Section 3.4 looks at the dependence of the envelope properties on the reference system. Section 3.5 focuses on the consequences of this dependence for isotropic fields and points out the difficulties of developing alternative definitions.

3.1 A definition of envelope for random fields

The critical point in generalizing the Cramer-Leadbetter definition of envelope to more than one dimension is to find a suitable definition of one-sided spectral density function in the latter case. In this section we shall review the definition by Adler for the case of a random function on the plane (1978) and illustrate its properties in some particular cases.

Consider a 2D homogeneous random field $X(t_1, t_2)$ with zero mean and mean power spectral density function $S_X(\omega_1, \omega_2)$.

$X(t_1, t_2)$ can be associated with a random field $F(\omega_1, \omega_2)$ in a frequency plane such that

$$X(t_1, t_2) = \int_{R_2} e^{i(\omega_1 t_1 + \omega_2 t_2)} \, dF(\omega_1, \omega_2) \tag{125}$$

where R_2 is the plane (ω_1, ω_2) and $F(\omega_1, \omega_2)$ is a field with ortogonal increments that satisfies

$$E\left[\int_{\Delta_1} dF(\omega_1, \omega_2) \int_{\Delta_2} dF(\omega_1, \omega_2) \right] = 0 \tag{126}$$

for any disjoint regions Δ_1, Δ_2 in R_2.

The incremental field $dF(\omega_1, \omega_2)$ has zero mean and its

variance is directly related to the spectral density function of $X(t_1, t_2)$:

$$E\left[dF(\omega_1, \omega_2) \right] = 0 \tag{127}$$

$$E\left[d^2F(\omega_1, \omega_2) \right] = S_X(\omega_1, \omega_2)\, d\omega_1 d\omega_2$$

When $X(t_1, t_2)$ is real, $dF(\omega_1, \omega_2)$, as defined in Eq. 125, is symmetrical around the origin in the sense that

$$dF(-\omega_1, -\omega_2) = dF^*(\omega_1, \omega_2) \tag{128}$$

where $dF^*(\omega_1, \omega_2)$ is the complex conjugate of $dF(\omega_1, \omega_2)$. In this case, it is possible to reduce the 2D Fourier transform in Eq. 125 to an integral over the halfplane

$$R_2^+ = \left\{ (\omega_1, \omega_2) : -\infty \leq \omega_1 \leq +\infty \;\; ; \omega_2 \geq 0 \right\} \tag{129}$$

by defining two real-valued incremental random fields as

$$dU(\omega_1, \omega_2) = dF(\omega_1, \omega_2) + dF(-\omega_1, -\omega_2) \tag{130a}$$

and

$$dV(\omega_1, \omega_2) = i\, dF(\omega_1, \omega_2) - i\, dF(-\omega_1, -\omega_2) \tag{130b}$$

Eq. 125 can be rewritten then

$$X(t_1, t_2) = \int_{R_2^+} \cos(\omega_1 t_1 + \omega_2 t_2)\, dU(\omega_1, \omega_2) + \sin(\omega_1 t_1 + \omega_2 t_2)\, dV(\omega_1, \omega_2) \tag{131}$$

One can show from Eqs. 130a and 130b that $U(\omega_1, \omega_2)$ and $V(\omega_1, \omega_2)$, associated with $dU(\omega_1, \omega_2)$ and $dV(\omega_1, \omega_2)$ and defined up to an integration constant, are real and independent random fields with ortogonal increments, and that

$$E[dU(\omega_1,\omega_2)] = E[dV(\omega_1,\omega_2)] = 0 \tag{132}$$

$$E[d^2U(\omega_1,\omega_2)] = E[d^2V(\omega_1,\omega_2)] = 2 S_X(\omega_1,\omega_2)\, d\omega_1\, d\omega_2$$

Using Eq. 131, the multidimensional Hilbert transform $X(t_1, t_2)$ can be defined in a way similar to the 1D Hilbert transform :

$$\hat{X}(t_1,t_2) = \int_{R_2^+} \cos(\omega_1 t_1 + \omega_2 t_2)\, dU(\omega_1,\omega_2) - \sin(\omega_1 t_1 + \omega_2 t_2)\, dV(\omega_1,\omega_2) \tag{133}$$

It follows from Eqs. 131 and 132 that $\hat{X}(t_1, t_2)$ is independent of $X(t_1, t_2)$ at a fixed position (t_1, t_2) and that $\hat{X}(t_1, t_2)$ has the same spectral density function $S_X(\omega_1, \omega_2)$ as $X(t_1, t_2)$.

Finally, the multidimensional envelope $S(t_1, t_2)$ is defined as

$$S(t_1,t_2) = [X^2(t_1,t_2) + \hat{X}^2(t_1,t_2)]^{1/2} \tag{134}$$

Next we analyze this envelope definition for a few specific spectral density functions.

Consider first a spectrum composed of a single mass at the frequency point (λ_1, λ_2) (Fig. 75). The associated random fields dU and dV are clearly zero everywhere, except at (λ_1, λ_2).

If we define

$$A = \int_{\Delta(\lambda_1,\lambda_2)} d\,U(\omega_1,\omega_2) \tag{135a}$$

$$B = \int_{\Delta(\lambda_1,\lambda_2)} d\,V(\omega_1,\omega_2) \tag{135b}$$

where $\Delta(\lambda_1, \lambda_2)$ is any region of the plane (ω_1, ω_2) that contains the point (λ_1, λ_2), then using Eq. 131, $X(t_1, t_2)$ can be expressed as

$$X(t_1, t_2) = A \cos \lambda_1 t_1 + \lambda_2 t_2 + B \sin(\lambda_1 t_1 + \lambda_2 t_2) \tag{136}$$

and using Eq. 133, $\hat{X}(t_1, t_2)$ is

$$\hat{X}(t_1, t_2) = A \sin(\lambda_1 t_1 + \lambda_2 t_2) - B \cos(\lambda_1 t_1 + \lambda_2 t_2) \tag{137}$$

A and B are iid normal random variables.

X(t) is constant along the family of lines that satisfy $\lambda_1 t_1 + \lambda_2 t_2 =$ const. and therefore is a cylindrical surface.

Using Eqs. 136 and 137 one finds that

$$S(t_1, t_2) = (A^2 + B^2)^{1/2} \tag{138}$$

In this particular case the 2D envelope along an arbitrary direction corresponds to the 1D envelope along that direction (except for the direction along which X(t) is constant).

Consider next a random field with two spectral masses located at (λ_1, λ_2) and (ϵ_1, ϵ_2) (Fig. 76).
Similar to the previous example, one can now write

$$X(t_1, t_2) = A\cos(\lambda_1 t_1 + \lambda_2 t_2) + B\sin(\lambda_1 t_1 + \lambda_2 t_2) + C\cos(\epsilon_1 t_1 + \epsilon_2 t_2) + D\sin(\epsilon_1 t_1 + \epsilon_2 t_2) \tag{139}$$

where A, B, C and D are mutually independent random variables.
The corresponding Hilbert transform is

$$\hat{X}(t_1, t_2) = A\sin(\lambda_1 t_1 + \lambda_2 t_2) - B\cos(\lambda_1 t_1 + \lambda_2 t_2) + C\sin(\epsilon_1 t_1 + \epsilon_2 t_2) - D\cos(\epsilon_1 t_1 + \epsilon_2 t_2) \tag{140}$$

and the envelope can be expressed as

$$S(t_1, t_2) = \{ A^2 + B^2 + C^2 + D^2 + 2(AC+BD)\cos[(\lambda_1-\epsilon_1)t_1 + (\lambda_2-\epsilon_2)t_2] + 2(BC-AD)\sin[(\lambda_1-\epsilon_1)t_1 + (\lambda_2-\epsilon_2)t_2] \} \tag{141}$$

Along the line

$$t_1(\lambda_1 - \epsilon_1) + t_2(\lambda_2 - \epsilon_2) = c \tag{142}$$

(see Fig. 76) and with $t = \sqrt{t_1^2 + t_2^2}$, $X(t_1, t_2)$ is equal to

$$X(t) = (A\cos c + B\sin c + C)\cos\omega_1 t + (-A\sin c + B\cos c + D)\sin\omega_1 t \tag{143}$$

where

$$\omega_1 = \frac{\lambda_1\epsilon_2 - \lambda_2\epsilon_1}{\left[(\lambda_2 - \epsilon_2)^2 + (\lambda_1 - \epsilon_1)^2\right]^{1/2}} \tag{144}$$

Along this line (and in fact along any line parallel to it) the random field varies as a monochromatic signal. The 2D envelope along the same line is, from Eq. 141,

$$S(t) = \left\{A^2 + B^2 + C^2 + D^2 + 2(AC + BD)\cos c + 2(BC - AD)\sin c\right\}^{1/2} \tag{145}$$

or also

$$S(t) = \left[(A\cos c + B\sin c + C)^2 + (-A\sin c + B\cos c + D)^2\right]^{1/2} \tag{146}$$

which corresponds to the C-L envelope of X(t) along that direction.

Along the ortogonal direction

$$t_1(\lambda_2 - \epsilon_2) - (\lambda_1 - \epsilon_1)t_1 = c \tag{147}$$

the random field is composed of two monocromatic signals

with frequency seperation that is the largest among all directions. The 2D envelope along this line fluctuates with a frequency equal to the distance between the two central frequencies :

$$S(t) = \left\{ A^2 + B^2 + C^2 + D^2 + K_1 \cos \omega_2 t_2 + K_2 \sin \omega_2 t_2 \right\}^{1/2} \qquad (148)$$

where

$$K_1 = 2(AC + BD) \cos \frac{\lambda_1 - \epsilon_1}{\lambda_2 - \epsilon_2} c + 2(BC - AD) \sin \frac{\lambda_1 - \epsilon_1}{\lambda_2 - \epsilon_2} c \qquad (149)$$

$$K_2 = -2(AC + BD) \sin \frac{\lambda_1 - \epsilon_1}{\lambda_2 - \epsilon_2} c + 2(BC - AD) \cos \frac{\lambda_1 - \epsilon_1}{\lambda_2 - \epsilon_2} c$$

and

$$\omega_2 = \sqrt{(\lambda_1 - \epsilon_1)^2 + (\lambda_2 - \epsilon_2)^2} \qquad (150)$$

Hence, when the distance between the two central frequencies becomes large, the 2D envelope will show the same deficiencies as the 1D envelope of a broad-band process, at least along the directions close to that defined by Eq. 147. One can conclude that similar to the C-L envelope, the 2D envelope is useful for narrow-band random fields, which are defined here to be fields the spectral density function of which is concentrated around a single point.

3.2 Excursions of random fields

As for 1D processes, properties of excursions of a random field above a given level r are of considerable interest. For a 2D field $X(t_1,t_2)$, an excursion is a connected set of points (t_1,t_2) such that $X(t_1,t_2) \geq r$. Crossings with the plane X= r appear as contour lines, but the distinction between up- and down-crossings is now lost. One way to characterise excursions is to count the number of contour lines, but unfortenately, there is in this case no analytical relationship between the number of contour lines and the number of excursions, and results about the former properties are themselves very limited. As a consequence several other methods of counting excursions have been proposed (for a review ,see Adler, 1976).
Adler and Hasofer (1976) have studied the number of excursions in terms of their Euler characteristic, which is a quantity more amenable to treatment (e.g., one can calculate its expected value at any level r). We will briefly illustrate their properties for a two-dimensional field.

First we have to introduce the concept of critical point.
A critical point is a point (t_1,t_2) of a contour line, where the partial derivative of X with respect to t_1 is zero and the partial derivative with respect to t_2 is positive.

Thus, the point (t_1, t_2+dt) belongs to the excursion set and the point (t_1, t_2-dt) does not (Fig. 77).
Furthermore we say that a critical point is positive, if the second partial derivative of X with respect to t_1 is negative. This means that neither (t_1-dt, t_2), nor (t_1+dt, t_2) belong to the excursion set (Fig. 78).
Conversely, at a negative critical point, the second partial derivative is positive. One can see (Fig. 79) that at negative critical points two disjoint excursion intervals along the line t = const join into one excursion interval.
Mathematically, the conditions for a point (t_1, t_2) to be a critical point are

$$X(t_1, t_2) = r \tag{151a}$$

$$\frac{\partial X}{\partial t_1}(t_1, t_2) = 0 \tag{151b}$$

$$\frac{\partial X}{\partial t_2}(t_1, t_2) > 0 \tag{151c}$$

$$\frac{\partial^2 X}{\partial t_1^2}(t_1, t_2) \begin{cases} < 0 & \text{positive critical point} \\ > 0 & \text{negative critical point} \end{cases} \tag{151d}$$

To assure the proper existence of these points, certain regularity conditions must be imposed on the random field (see Adler and Hasofer, 1976).

The Euler characteristic χ is defined as the difference of the number of positive and negative critical points, say N_P and N_N; hence

$$\chi = N_P - N_N \tag{152}$$

For an excursion set without holes $\chi = 1$; for an excursion set with one hole $\chi = 0$ (Fig. 80).
More in general, χ equals the number of disjoint excursion sets minus the number of disjoint holes in the excursion sets. Since holes will be very rare at high levels, approaches the number of excursions at high levels.
The Euler characteristic has other desirable properties. For instance, it can be defined for fields of higher dimensions; for a random process it corresponds to the number of upcrossings of the process. The Euler characteristic is also invariant with respect to rotation of the axes.

Adler and Hasofer (1976) have derived a formula for the expected value of the Euler characteristic at any level r for a generic random field $X(t_1, t_2)$. The only constraints are that the random field should have zero mean, be homogeneous, and satisfy the regularity conditions and that the spectrum should be continuous an have finite moments up to and including order 6.
The mean value of the Euler characteristic per unit area is

then given by

$$E[\dot{X}] = -\int_{\dot{X}_2>0} \int_{\dot{X}_{11}=-\infty}^{+\infty} \dot{x}_2 \, \dot{x}_{11} \, \varphi(r,0,\dot{x}_2,\dot{x}_{11}) \, d\dot{x}_2 \, d\dot{x}_{11} \quad (153)$$

where $\varphi(x,\dot{x}_1,\dot{x}_2,\dot{x}_{11})$ is the joint probability density function of $(X,\dot{X}_1,\dot{X}_2,\dot{X}_{11})$ and where

$$\dot{X}_i \text{ stands for } \frac{\partial X_i}{\partial t_i} \quad (154)$$

$$\dot{X}_{ij} \text{ stands for } \frac{\partial^2 X_i}{\partial t_i \, \partial t_j}$$

For a Gaussian random field in two dimensions, Adler and Hasofer (1976) arrived at the following formula

$$E[\dot{X}] = \frac{r}{(2\pi\sigma^2)^{-3/2}} |A|^{1/2} e^{-\frac{r^2}{2\sigma^2}} \quad (155)$$

where r is the crossing level, σ^2 is the variance of the random field and $|A|$ is the determinant value of the covariance matrix of the first order derivatives of X. Similar calculations for the envelope of a random field with arbitrary spectral density function are very difficult, even in the isotropic case. For the special case, when the one sided spectral density function has polar symmetry around a central frequency (λ_1, λ_2), Adler (1978) arrived at the following formula

$$E[\dot{X}] = \frac{(\mu_{20}^2 - \mu_{11}^2)^{1/2}}{2\pi} \frac{r^2}{\mu_{00}^{3/2}} \left(1 - \frac{\mu_{00}}{r^2}\right) e^{-\frac{r^2}{2\mu_{00}^2}} \quad (156)$$

where

$$\mu_{ij} = 2 \int_{R_2^+} (\omega_1 - \lambda_1)^i \, (\omega_2 - \lambda_2)^j \, S_X(\omega_1, \omega_2) \, d\omega_1 \, d\omega_2$$

Consider for instance a one-sided spectral density function, that is constant with value $1/a^2$ inside a square of side a, centered at (λ_1, λ_2), and is zero elsewhere. The variance of the random field is 1. In this case, Eq. 156 gives

$$E[X] = \frac{a^2}{24\pi} \, r^2 \left(1 - \frac{1}{r^2}\right) \, e^{-\frac{r^2}{2}} \qquad (157)$$

The covariance matrix of the first order derivatives of X is

$$\begin{bmatrix} \lambda_1^2 + \frac{a^2}{12} & \lambda_1 \lambda_2 \\ \lambda_1 \lambda_2 & \lambda_2^2 + \frac{a^2}{12} \end{bmatrix}$$

and the ratio Q between the expected Euler characteristic of the envelope and that of the field is

$$Q = \sqrt{2\pi} \, \frac{a^2}{12} \, r \left(1 - r^2\right) \, \frac{1}{\sqrt{\frac{a^2}{12}(\lambda_1^2 + \lambda_2^2) + \frac{a^4}{144}}} \qquad (158)$$

This ratio exceeds 1 (Fig. 81) when

$$a \geq \sqrt{\frac{6}{\pi}} \, \frac{1}{\sqrt{r^2 - 2}} \sqrt{\lambda_1^2 + \lambda_2^2}$$

Notice that for $r \geq \sqrt{\mu_{00}}$, Eq. 156 gives a negative mean value of the Euler characteristic. This indicates that below this level there are more holes than excursions. As for 1D processes, when the random field is broad-banded (a is large) or at high levels of r, the envelope experiences more excursions than the random field.

3.3 Equivalence between the 2D and the C-L envelope

In this section, we shall show that the 2D envelope, as defined by Eq. 134, is equivalent to a series of one-dimensional C-L envelopes along the direction of the t_2 axis.

The random field $X(t_1, t_2)$ along a line $t_1 = a$ has frequency representation

$$X(a,t_2) = \int_{R_2^+} \cos(a\omega_1 + \omega_2 t)\, dU(\omega_1,\omega_2) + \sin(\omega_1 a + \omega_2 t)\, dV(\omega_1,\omega_2) \tag{159}$$

Expanding the trigonometric function into parts, leads to

$$X(a,t_2) = \int_{R_2^+} \cos\omega_2 t_2 \left[\cos\omega_1 a\, dU(\omega_1,\omega_2) + \sin\omega_1 a\, dV(\omega_1,\omega_2)\right] + \int_{R_2^+} \sin\omega_2 t_2 \left[-\sin\omega_1 a\, dU(\omega_1,\omega_2) + \cos\omega_1 a\, dV(\omega_1,\omega_2)\right] \tag{160}$$

Similarly, for the corresponding 1D Hilbert transform,

$$\hat{X}(a,t_2) = \int_{R_2^+} \sin\omega_2 t_2 \left[\cos\omega_1 a\, dU(\omega_1,\omega_2) + \sin\omega_1 a\, dV(\omega_1,\omega_2)\right] - \int_{R_2^+} \cos\omega_2 t_2 \left[-\sin\omega_1 a\, dU(\omega_1,\omega_2) + \cos\omega_1 a\, dV(\omega_1,\omega_2)\right] \tag{161}$$

One can easily check that this is also the 2D Hilbert transform along the line $t_1 = a$

$$\hat{X}(a,t_2) = \int_{R_2^+} \sin(\omega_1 a + \omega_2 t_2)\, dU(\omega_1,\omega_2) - \cos(\omega_1 a + \omega_2 t_2)\, dV(\omega_1,\omega_2) \tag{162}$$

Since the 1D and 2D Hilbert transform along the line $t_1 = a$ coincide, the 1D and 2D envelopes along this line are also identical.

Using Eq. 11, the 2D Hilbert transform can be written as a convolution of the random field $X(t_1, t_2)$

$$\hat{X}(t_1, t_2) = \int_{\tau=-\infty}^{+\infty} \frac{X(t_1, t_2+\tau)}{\tau} d\tau \tag{163}$$

It is clear that the 2D envelope of a particular realization depends on the orientation of the axes, since in general the 1D Hilbert transforms at a point along two different directions do not coincide. In the next section we shall investigate the dependence of the 2D envelope on the orientation of the coordinate axes.

3.4 Directionality of the envelope

The 2D envelope is defined in terms of the original random field $X(t_1, t_2)$ and its Hilbert transform $\hat{X}(t_1, t_2)$. For any choice of axis-system, $X(t_1, t_2)$ and $\hat{X}(t_1, t_2)$ are independent random variables at a fixed point (t_1, t_2) and the random fields X and $\hat{X}$ have the same spectral density function $S_X(\omega_1, \omega_2)$. It follows from the first property that the marginal distribution of $S(t_1, t_2)$ is independent of the choice of the axis-system. This independence is to be understood in the sense of probability distribution. The numerical value of $S(t_1, t_2)$ typically varies with the orientation of the axes.

In the calculation of the expected Euler characteristic for S, the PDF of the first and second partial derivatives of the random field are also used and in general these functions depend on the crosscorrelation between $X(t_1, t_2)$ and $\hat{X}(t_1, t_2)$.
We shall show next that this crosscorrelation typically varies with the choice of the axis-system.

In the original reference, the cross-correlation between $X(t_1, t_2)$ and $\hat{X}(t_1 + \tau_1, t_2 + \tau_2)$ is

$$R_{X\hat{X}}(\tau_1, \tau_2) = 2 \int_{R_2^+} \sin(\omega_1 \tau_1 + \omega_2 \tau_2)\, S_X(\omega_1, \omega_2)\, d\omega_1 d\omega_2 \tag{164}$$

Consider next a rotated reference (t_1', t_2') and the associated

reference (ω_1', ω_2') in the frequency domain. By definition,

$$X(t_1, t_2) = X'(t_1', t_2') \tag{165}$$

where X' is the random field defined in the new coordinate system and (t_1, t_2) corresponds to (t_1', t_2'). It was shown in Section 3.3 that in general $\hat{X}(t_1, t_2)$ and $\hat{X}'(t_1', t_2')$ are random fields with different characteristics. This should be no surprise because $\hat{X}(t_1, t_2)$ is generated as a convolution along the t_2 direction whereas $\hat{X}'(t_1', t_2')$ is generated as a convolution along the t_2' direction. The cross-correlation between $X'(t_1', t_2')$ and $\hat{X}'(t_1', t_2')$ is

$$R'_{X'\hat{X}'}(\tau_1', \tau_2') = 2 \int_{R_2^{+}} \sin(\omega_1' \tau_1' + \omega_2' \tau_2') \, S'_X(\omega_1', \omega_2') \, d\omega_1' \, d\omega_2' \tag{166}$$

or equivalently

$$R'_{X'\hat{X}'}(\tau_1', \tau_2') = 2 \int_{D_I'} \sin(\omega_1' \tau_1' + \omega_2' \tau_2') \, S'_X(\omega_1', \omega_2') \, d\omega_1' \, d\omega_2' \tag{167}$$

$$+ \; 2 \int_{D_{II}} \sin(\omega_1' \tau_1' + \omega_2' \tau_2') \, S'_X(\omega_1', \omega_2') \, d\omega_1' \, d\omega_2'$$

where D_{II} is the common region of $R_2^{+'}$ and R_2^{+}, see also Fig. 82,

$$D_{II} = \left\{ (\omega_1', \omega_2') : \omega_2 \geq 0, \; \omega_2' \geq 0 \right\} \tag{168}$$

$$D_I' = \left\{ (\omega_1', \omega_2') : \omega_2 \leq 0, \; \omega_2' \geq 0 \right\} \tag{169}$$

It follows that

$$R'_{x,\hat{x}}(\tau'_1,\tau'_2) = 2\int_{D_I} \sin(-\omega'_1\tau'_1-\omega'_2\tau'_2)\, S'_x(\omega'_1,\omega'_2)\, d\omega'_1\, d\omega'_2 + 2\int_{D_{II}} \sin(\omega'_1\tau'_1+\omega'_2\tau'_2)\, S'_x(\omega'_1,\omega'_2)\, d\omega'_1\, d\omega'_2 \tag{170}$$

where

$$D_I = \{(\omega'_1,\omega'_2) : \omega'_2 \le 0,\ \omega_2 \ge 0\} \tag{171}$$

Since $\omega'_1\tau'_1 + \omega'_2\tau'_2 = \omega_1\tau_1 + \omega_2\tau_2$

and $S_x(\omega_1,\omega_2) = S'_x(\omega'_1,\omega'_2)$

Eq. 170 can be rewritten as

$$R'_{x,\hat{x}}(\tau'_1,\tau'_2) = -\int_{D_I} \sin(\omega_1\tau_1+\omega_2\tau_2)\, S_x(\omega_1,\omega_2)\, d\omega_1\, d\omega_2 + \int_{D_{II}} \sin(\omega_1\tau_1+\omega_2\tau_2)\, S_x(\omega_1,\omega_2)\, d\omega_1\, d\omega_2 \tag{172}$$

Comparison of Eqs. 161 and 172 shows that

$$R_{x\hat{x}}(\tau_1,\tau_2) \neq R'_{x,\hat{x}}(\tau'_1,\tau'_2) \tag{173}$$

unless

$$\int_{D_I} \sin(\omega_1\tau_1+\omega_2\tau_2)\, S_x(\omega_1,\omega_2)\, d\omega_1\, d\omega_2 = 0$$

3.5 Isotropic random fields

In part because of their simple representation, isotropic random fields are frequently encountered in practical applications. For such fields, it would seem logical to search for an isotropic envelope definition. One should first recognize that isotropic fields are in general not narrow-banded along a line, since their spectral density function has spherical symmetry about the origin. If the normalized spectral density function is regarded as a joint density function in frequency space, then the normalized spectral density function of the process along any line is the associated marginal density along ω_1, and the latter is typically distributed over a broad range of frequencies (Fig. 83).

Secondly, because of its directional dependence the envelope as previously defined is not isotropic and this is an undesirable feature. Lack of isotropy of the envelope is difficult to directly check, e.g. through calculation of the correlation function of the envelope. Instead, we shall show this property by considering the crosscorrelation between X and $\hat{X}$.

Isotropy of X(t) implies that the mean spectral density function $S_x(\omega_1,\omega_2)$ is only a function of ω, the distance from the origin, so that the correlation function of X can

be written as

$$R_X(\tau_1,\tau_2) = 2\int_{R_2^+} \cos(\omega_1\tau_1+\omega_2\tau_2)\, S_X(\omega_1,\omega_2)\, d\omega_1 d\omega_2 \qquad (174)$$

$$= 2\int_{\omega=0}^{\infty}\int_{\psi=0}^{\pi} \cos\left[\omega\tau\cos(\theta-\psi)\right]\omega\, S_X(\omega)\, d\psi\, d\omega$$

where (ω,ψ) are polar coordinates in the frequency plane (ω_1,ω_2) and (τ,θ) are polar coordinates in the time plane (t_1,t_2). The trigonometric function inside the integral can be expanded into a series of Bessel functions as

$$\cos\left[\omega\tau\cos(\theta-\psi)\right] = J_0(\omega\tau) + 2\sum_{k=1}^{\infty}(-1)^k J_{2k}(\omega\tau)\cos\left[2k(\psi-\theta)\right] \qquad (175)$$

This allows one to seperate the integration over and and since

$$\int_0^{\pi} \cos 2k(\psi-\theta)\, d\psi = 0 \qquad (176)$$

it follows that

$$R_X(\tau_1,\tau_2) = \int_0^{\infty} 2\pi\, J_0(\omega\tau)\,\omega\, S_X(\omega)\, d\omega \qquad (177)$$

Thus the correlation function of X is only a function of τ, as required by isotropy.

Similarly, one can write the crosscorrelation function between X and $\hat{X}$ as

$$R_{X\hat{X}}(\tau_1,\tau_2) = 2\int_{\omega=0}^{\infty}\int_{\psi=0}^{\pi} \sin\left[\omega\tau\cos(\psi-\theta)\right]\omega S_X(\omega)\,d\psi\,d\omega \qquad (178)$$

The series expansion of the trigonometric function inside the integral is

$$\sin[\omega\tau\cos(\psi-\theta)] = 2\sum_{k=0}^{\infty}(-1)^k J_{2k+1}(\omega\tau)\cos\left[(2k+1)(\psi-\theta)\right] \qquad (179)$$

Since

$$\int_0^{\pi}\cos(2k+1)(\psi-\theta)\,d\psi = \frac{2\sin(2k+1)\theta}{2k+1} \qquad (180)$$

the crosscorrelation is

$$R_{X\hat{X}}(\tau_1,\tau_2) = 8\sum_{k=1}^{\infty}\frac{(-1)^k\sin(2k+1)\theta}{2k+1}\int_0^{\infty}\omega J_{2k+1}(\omega\tau)\,S_X(\omega)\,d\omega \qquad (181)$$

and depends on the angle θ as well as on τ. One can conclude that $S(\underline{t})$ is not isotropic.
Notice that for $\theta = 0$, X and $\hat{X}$ are uncorrelated and thus independent in the case of Gaussian random fields.

In summary, it is found that enveloping of random fields poses more challenging problems than enveloping on the line.

As mentioned in Section 3.1, for random fields with spectral density function centered around several widely seperated frequencies, the 2D envelope that normally generalizes the Cramer-Leadbetter definition along the line exhibits deficiencies similar to those of the 1D envelope for broad-band processes. Theorethically, it is again possible to decompose the random field into several narrow-band random fields and to envelope only the 'higher-frequency' components. For instance, for two components X_1 and X_2 one could define an envelope S as

$$S(t_1,t_2) = X_1(t_1,t_2) + S_2(t_1,t_2) \tag{182}$$

However, calculation of the crossing properties of S (e.g., the expected Euler characteristic) requires the knowledge of the joint distribution of S, S_1, S_2 and S_{11}. For two components, this requires the calculation of a multiple convolution integral and the method becomes impractical.

A second problem is the directionality of the 2D envelope, especially in reference to isotropic fields. A theorethical elegant solution would be to redefine a new envelope as the maximum or the average of the directional envelope over all directions. (Notice that the minimum of the directional envelopes is the field $X(\underline{t})$ itself). But again, calculations become very complicated.

References

Adler, R.J. (1976), "On Generalizing the Notion of Upcrossings to Random Fields," Adv. Appl. Prob., 8, pp. 789-805.

Adler, R.J. (1978), "On the envelope of a Gaussian random field," J. Appl. Prob., 15, no.3, pp. 502-513.

Adler, R.J. and Hasofer, A.M. (1976), "Level Crossings for Random Fields," Ann. Prob., 4, pp. 1-12.

Cramer, H. (1966), "On the Intersections Between the Trajectory of a Normal Stationary Stochastic Process and a High Level," Arkiv. Mat., 6, p.337.

Cramer, H. and Leadbetter, M.R. (1967), Stationary and Related Stochastic Processes, John Wiley&Sons, New York.

Crandall, S.H. (1963), "Zero Crossings, Peaks and Other Statistical Measures of Random Responses," J. Acoust. Soc. Am., Vol. 35, No. 11, pp. 1693-1699.

Crandall, S.H. (1970), "First-Crossing Probabilities of the Lineair Oscillator," J. Sound and Vibration, 12, No.3, pp.285-299.

Rice, S.O. (1944), "Mathematical Analysis of Random Noise," Bell System Tech. J., 23, pp. 282-332, (1945) 24, pp. 46-156.

Rice, S.O. (1958), "Distribution of the Duration of Fades in Radio Transmission: Gaussian Noise Model," Bell System Tech. J., 37, pp. 581-635.

Siegert, A.J.F. (1951), "On the First Passage Time Probability Problem," Phys. Rev., Vol. 81, pp. 617-623.

Slepian, D. (1961), "First Passage Time for a Particular Gaussian Process," Ann. Math. Stat., 32, pp. 610-612.

Vanmarcke, E.H. (1970), "First Passage and Other Failure Criteria in Narrow-Band Random Vibration: A Discrete State Approach," Research Report R69-68, Dep. of Civil Eng., MIT, Cambridge, Mass.

Vanmarcke, E.H. (1972), "Properties of Spectral Moments with Applications to Random Vibration," J. Eng. Mech. Div., ASCE, Vol. 98, pp. 425-446.

$\tau / \lambda_{0,2}$	0.000	0.500	1.000	1.500	2.000	2.500	3.000
0.000	1.000	1.000	1.000	1.000	1.000	1.000	1.000
0.020	0.990	1.081	1.177	1.278	1.385	1.496	1.611
0.040	0.980	1.110	1.251	1.401	1.562	1.731	1.910
0.060	0.970	1.131	1.307	1.499	1.705	1.924	2.156
0.080	0.959	1.147	1.355	1.583	1.830	2.095	2.375
0.100	0.949	1.160	1.397	1.659	1.945	2.251	2.576
0.120	0.938	1.171	1.435	1.730	2.051	2.397	2.764
0.140	0.927	1.181	1.471	1.796	2.152	2.535	2.941
0.160	0.917	1.189	1.504	1.858	2.248	2.667	3.110
0.180	0.906	1.196	1.535	1.918	2.340	2.794	3.273
0.200	0.894	1.202	1.564	1.976	2.429	2.916	3.429
0.220	0.883	1.208	1.593	2.031	2.515	3.034	3.579
0.240	0.872	1.213	1.620	2.085	2.599	3.149	3.725
0.260	0.860	1.217	1.646	2.138	2.681	3.261	3.867
0.280	0.849	1.221	1.672	2.190	2.761	3.370	4.004
0.300	0.837	1.224	1.696	2.240	2.839	3.477	4.138
0.320	0.825	1.227	1.720	2.290	2.917	3.581	4.269
0.340	0.812	1.230	1.744	2.339	2.992	3.683	4.396
0.360	0.800	1.232	1.767	2.387	3.067	3.784	4.520
0.380	0.787	1.233	1.790	2.434	3.140	3.882	4.642
0.400	0.775	1.235	1.812	2.482	3.212	3.978	4.761
0.420	0.762	1.236	1.834	2.528	3.284	4.073	4.877
0.440	0.748	1.236	1.856	2.574	3.354	4.165	4.990
0.460	0.735	1.237	1.877	2.620	3.424	4.257	5.102
0.480	0.721	1.237	1.899	2.665	3.492	4.346	5.211
0.500	0.707	1.237	1.920	2.711	3.560	4.435	5.318
0.520	0.693	1.236	1.941	2.756	3.627	4.521	5.423
0.540	0.678	1.236	1.963	2.800	3.693	4.607	5.526
0.560	0.663	1.235	1.984	2.845	3.758	4.691	5.627
0.580	0.648	1.234	2.005	2.889	3.823	4.773	5.727
0.600	0.632	1.233	2.026	2.933	3.887	4.855	5.825
0.620	0.616	1.231	2.048	2.977	3.950	4.935	5.921
0.640	0.600	1.230	2.069	3.021	4.012	5.013	6.016
0.660	0.583	1.228	2.091	3.064	4.074	5.091	6.109
0.680	0.566	1.226	2.113	3.108	4.135	5.167	6.201

Table 1 - continued on next page

0.700	0.548	1.224	2.135	3.151	4.195	5.243	6.291
0.720	0.529	1.222	2.158	3.194	4.254	5.317	6.381
0.740	0.510	1.220	2.180	3.237	4.313	5.391	6.469
0.760	0.490	1.218	2.204	3.279	4.370	5.463	6.556
0.780	0.469	1.216	2.227	3.321	4.428	5.534	6.641
0.800	0.447	1.214	2.251	3.363	4.484	5.605	6.726
0.820	0.424	1.213	2.276	3.405	4.540	5.674	6.809
0.840	0.400	1.211	2.301	3.446	4.595	5.743	6.892
0.860	0.374	1.211	2.327	3.487	4.649	5.811	6.973
0.880	0.346	1.211	2.352	3.527	4.703	5.878	7.054
0.900	0.316	1.212	2.378	3.567	4.756	5.945	7.134
0.920	0.283	1.215	2.404	3.606	4.808	6.010	7.213
0.940	0.245	1.221	2.430	3.645	4.860	6.075	7.291
0.960	0.200	1.229	2.456	3.684	4.912	6.140	7.368
0.980	0.141	1.241	2.481	3.722	4.963	6.204	7.444
1.000	0.000	1.253	2.507	3.760	5.013	6.267	7.520

Table 1 - J factor in Eq. 42 as a function of the variance of the enveloped component $\lambda_{0,2}$ and of the crossing level r.

R=0.

δ \ ϵ	0.01	.100	.200	.300	.400	.500
0.010	.992	.988	.987	.986	.985	.984
0.050	.965	.950	.942	.937	.934	.933
0.100	.932	.901	.886	.877	.872	.870
0.150	.897	.852	.830	.817	.810	.808
0.200	.862	.803	.774	.758	.749	.746
0.250	.826	.753	.719	.699	.689	.685
0.300	.790	.704	.664	.641	.629	.625
0.350	.752	.654	.609	.584	.571	.566
0.400	.713	.603	.554	.528	.513	.508
0.450	.673	.553	.500	.472	.457	.452
0.500	.631	.502	.447	.417	.402	.397
0.550	.588	.450	.394	.364	.349	.343
0.600	.543	.399	.341	.312	.297	.292
0.650	.496	.346	.290	.261	.247	.242
0.700	.446	.294	.239	.212	.199	.195
0.750	.393	.241	.190	.166	.154	.150
0.800	.336	.188	.142	.122	.112	.109
0.850	.272	.134	.097	.081	.074	.072
0.900	.200	.082	.055	.045	.041	.040
0.950	.113	.034	.021	.017	.015	.014
0.990	.022	.004	.002	.002	.001	.001

R=1.

δ \ ϵ	0.01	0.10	0.20	0.30	0.40	0.50
0.010	1.14	1.16	1.17	1.17	1.17	1.17
0.050	1.30	1.35	1.37	1.38	1.38	1.38
0.100	1.43	1.48	1.51	1.52	1.53	1.53
0.150	1.52	1.58	1.61	1.62	1.63	1.63
0.200	1.60	1.66	1.69	1.70	1.70	1.70
0.250	1.67	1.73	1.75	1.76	1.76	1.76
0.300	1.73	1.79	1.80	1.80	1.81	1.81
0.350	1.79	1.83	1.84	1.84	1.84	1.84
0.400	1.84	1.88	1.87	1.87	1.86	1.86
0.450	1.90	1.91	1.90	1.89	1.88	1.88
0.500	1.94	1.94	1.92	1.90	1.89	1.88
0.550	1.99	1.97	1.93	1.90	1.89	1.88
0.600	2.04	1.99	1.94	1.90	1.88	1.87
0.650	2.08	2.01	1.94	1.89	1.86	1.85
0.700	2.13	2.03	1.94	1.88	1.84	1.83
0.750	2.18	2.04	1.93	1.85	1.81	1.80
0.800	2.23	2.06	1.92	1.82	1.77	1.76
0.850	2.28	2.07	1.90	1.79	1.73	1.71
0.900	2.34	2.08	1.88	1.75	1.68	1.65
0.950	2.40	2.10	1.86	1.70	1.62	1.59
0.990	2.45	2.13	1.84	1.66	1.57	1.54

Table 2 - continued on next page

R=2.

δ \ ϵ	0.01	0.10	0.20	0.30	0.40	0.50
0.010	1.29	1.34	1.37	1.38	1.39	1.39
0.050	1.71	1.86	1.92	1.96	1.98	1.99
0.100	2.07	2.31	2.42	2.48	2.52	2.53
0.150	2.37	2.69	2.85	2.93	2.98	2.99
0.200	2.64	3.04	3.24	3.35	3.41	3.43
0.250	2.89	3.38	3.61	3.74	3.82	3.84
0.300	3.13	3.70	3.97	4.13	4.21	4.24
0.350	3.36	4.01	4.32	4.50	4.60	4.63
0.400	3.59	4.32	4.67	4.87	4.98	5.01
0.450	3.81	4.62	5.01	5.24	5.35	5.39
0.500	4.02	4.92	5.35	5.60	5.73	5.77
0.550	4.23	5.22	5.69	5.96	6.10	6.14
0.600	4.44	5.52	6.03	6.32	6.47	6.52
0.650	4.64	5.81	6.37	6.68	6.85	6.90
0.700	4.84	6.11	6.71	7.05	7.23	7.28
0.750	5.03	6.40	7.05	7.42	7.61	7.67
0.800	5.22	6.69	7.39	7.79	7.99	8.06
0.850	5.41	6.98	7.74	8.16	8.38	8.45
0.900	5.59	7.27	8.08	8.54	8.78	8.85
0.950	5.77	7.55	8.43	8.92	9.18	9.26
0.990	5.91	7.78	8.71	9.23	9.51	9.59

R=3.

δ \ ϵ	0.01	0.10	0.20	0.30	0.40	0.50
0.010	1.46	1.55	1.60	1.62	1.63	1.64
0.050	2.19	2.49	2.64	2.73	2.77	2.79
0.100	2.85	3.41	3.69	3.85	3.94	3.97
0.150	3.42	4.24	4.66	4.91	5.04	5.08
0.200	3.94	5.04	5.60	5.94	6.13	6.19
0.250	4.43	5.81	6.54	6.97	7.21	7.29
0.300	4.90	6.58	7.47	8.01	8.30	8.40
0.350	5.35	7.33	8.40	9.05	9.41	9.52
0.400	5.79	8.08	9.33	10.1	10.5	10.7
0.450	6.20	8.83	10.3	11.2	11.6	11.8
0.500	6.61	9.56	11.2	12.2	12.8	13.0
0.550	7.00	10.3	12.1	13.3	13.9	14.1
0.600	7.39	11.0	13.1	14.4	15.1	15.3
0.650	7.76	11.8	14.0	15.5	16.3	16.5
0.700	8.13	12.5	15.0	16.6	17.4	17.7
0.750	8.49	13.2	15.9	17.7	18.6	19.0
0.800	8.84	13.9	16.9	18.8	19.8	20.2
0.850	9.18	14.6	17.8	19.9	21.0	21.4
0.900	9.52	15.4	18.8	21.0	22.2	22.7
0.950	9.86	16.1	19.8	22.1	23.5	23.9
0.990	10.1	16.6	20.5	23.0	24.4	24.9

Table 2 - Factor J in Eq. 48 as a function of the crossing level r, the variance of the enveloped components δ and the variance of the third component ϵ .

δ	$\epsilon_4 \backslash \epsilon_3$	0.000	0.100	0.200	0.300	0.400	0.500
0.00	0.0	1.000	1.000	1.000	1.000	1.000	1.000
	0.1		1.000	1.000	1.000	1.000	1.000
	0.2			1.000	1.000	1.000	1.000
	0.3				1.000	1.000	1.000
	0.4					1.000	1.000
	0.5						1.000
0.05	0.0	1.636	1.860	1.929	1.968	1.988	1.995
	0.1		2.101	2.171	2.209	2.226	2.226
	0.2			2.239	2.271	2.282	2.271
	0.3				2.297	2.297	2.271
	0.4					2.282	2.226
	0.5						1.995
0.10	0.0	1.945	2.310	2.424	2.488	2.523	2.534
	0.1		2.709	2.827	2.889	2.918	2.918
	0.2			2.940	2.995	3.012	2.995
	0.3				3.038	3.038	2.995
	0.4					3.012	2.918
	0.5						2.534
0.15	0.0	2.200	2.696	2.851	2.939	2.986	3.001
	0.1		3.240	3.401	3.486	3.525	3.525
	0.2			3.555	3.629	3.652	3.629
	0.3				3.688	3.688	3.629
	0.4					3.652	3.525
	0.5						3.001
0.20	0.0	2.429	3.050	3.245	3.356	3.415	3.434
	0.1		3.732	3.933	4.040	4.088	4.088
	0.2			4.124	4.217	4.246	4.217
	0.3				4.290	4.290	4.217
	0.4					4.246	4.088
	0.5						3.434
0.25	0.0	2.640	3.385	3.619	3.752	3.824	3.846
	0.1		4.200	4.438	4.565	4.622	4.622
	0.2			4.664	4.774	4.807	4.774
	0.3				4.859	4.859	4.774
	0.4					4.807	4.622
	0.5						3.846

Table 3 - continued on next page

0.30	0.0	2.839	3.708	3.980	4.135	4.219	4.245
	0.1		4.651	4.925	5.069	5.134	5.134
	0.2			5.183	5.306	5.344	5.306
	0.3				5.403	5.403	5.306
	0.4					5.344	5.134
	0.5						4.245
0.35	0.0	3.030	4.022	4.333	4.510	4.605	4.635
	0.1		5.090	5.397	5.558	5.630	5.630
	0.2			5.683	5.819	5.861	5.819
	0.3				5.925	5.925	5.819
	0.4					5.861	5.630
	0.5						4.635
0.40	0.0	3.213	4.330	4.680	4.879	4.985	5.019
	0.1		5.521	5.858	6.033	6.112	6.112
	0.2			6.168	6.315	6.360	6.315
	0.3				6.428	6.428	6.315
	0.4					6.360	6.112
	0.5						5.019
0.45	0.0	3.390	4.634	5.024	5.244	5.362	5.399
	0.1		5.944	6.309	6.497	6.581	6.581
	0.2			6.641	6.796	6.843	6.796
	0.3				6.915	6.915	6.796
	0.4					6.843	6.581
	0.5						5.399
0.50	0.0	3.561	4.936	5.365	5.608	5.737	5.778
	0.1		6.363	6.753	6.952	7.040	7.040
	0.2			7.102	7.263	7.311	7.263
	0.3				7.385	7.385	7.263
	0.4					7.311	7.040
	0.5						5.778
0.55	0.0	3.729	5.237	5.707	5.971	6.111	6.156
	0.1		6.779	7.190	7.398	7.489	7.489
	0.2			7.552	7.717	7.765	7.717
	0.3				7.839	7.839	7.717
	0.4					7.765	7.489
	0.5						6.156

Table 3 - continued on next page

0.60	0.0	3.892	5.537	6.049	6.335	6.487	6.535
	0.1		7.192	7.623	7.837	7.929	7.929
	0.2			7.993	8.157	8.206	8.157
	0.3				8.278	8.278	8.157
	0.4					8.206	7.929
	0.5						6.535
0.65	0.0	4.051	5.838	6.392	6.702	6.865	6.916
	0.1		7.605	8.051	8.269	8.361	8.361
	0.2			8.424	8.586	8.632	8.586
	0.3				8.702	8.702	8.586
	0.4					8.632	8.361
	0.5						6.916
0.70	0.0	4.207	6.140	6.738	7.071	7.246	7.301
	0.1		8.018	8.477	8.695	8.786	8.786
	0.2			8.847	9.002	9.046	9.002
	0.3				9.110	9.110	9.002
	0.4					9.046	8.786
	0.5						7.301
0.75	0.0	4.360	6.443	7.087	7.444	7.631	7.689
	0.1		8.431	8.899	9.115	9.204	9.204
	0.2			9.262	9.406	9.446	9.406
	0.3				9.503	9.503	9.406
	0.4					9.446	9.204
	0.5						7.689
0.80	0.0	4.511	6.746	7.438	7.820	8.020	8.082
	0.1		8.846	9.321	9.531	9.616	9.616
	0.2			9.669	9.799	9.833	9.799
	0.3				9.881	9.881	9.799
	0.4					9.833	9.616
	0.5						8.082
0.85	0.0	4.663	7.049	7.791	8.200	8.412	8.479
	0.1		9.262	9.742	9.944	10.02	10.02
	0.2			10.07	10.18	10.20	10.18
	0.3				10.24	10.24	10.18
	0.4					10.21	10.02
	0.5						8.479

Table 3 - continued on next page

0.90	0.0	4.817	7.347	8.142	8.580	8.807	8.878
	0.1		9.679	10.16	10.36	10.42	10.42
	0.2			10.47	10.56	10.57	10.56
	0.3				10.59	10.59	10.56
	0.4					10.57	10.43
	0.5						8.878
0.95	0.0	4.981	7.636	8.485	8.956	9.200	9.276
	0.1		10.09	10.59	10.77	10.83	10.83
	0.2			10.86	10.92	10.93	10.92
	0.3				10.93	10.93	10.92
	0.4					10.93	10.83
	0.5						9.276
1.00	0.0	5.165	7.903	8.809	9.319	9.583	9.665
	0.1		10.50	11.01	11.19	11.24	11.24
	0.2			11.23	11.29	11.29	11.29
	0.3				11.27	11.27	11.29
	0.4					11.29	11.24
	0.5						9.665

Table 3 - Factor J in Eq. 52 for 4 components and crossing level r = 2.
γ = variance of enveloped component.
ϵ_3 = fraction of γ associated with variance of third component.
ϵ_4 = fraction of γ associated with variance of fourth component.

$r/\lambda_{0,2}$	0.0000	0.5000	1.0000	1.5000	2.0000	2.5000	3.0000
0.0000	1.0000	1.0000	1.0000	1.0000	1.0000	1.0000	1.0000
0.0200	0.9800	0.9891	0.9949	0.9980	0.9994	0.9999	1.0000
0.0400	0.9600	0.9776	0.9891	0.9956	0.9985	0.9996	0.9999
0.0600	0.9400	0.9658	0.9830	0.9928	0.9975	0.9993	0.9998
0.0800	0.9200	0.9537	0.9765	0.9898	0.9963	0.9989	0.9997
0.1000	0.9000	0.9414	0.9697	0.9865	0.9950	0.9985	0.9996
0.1200	0.8800	0.9289	0.9626	0.9831	0.9936	0.9980	0.9995
0.1400	0.8600	0.9161	0.9554	0.9795	0.9921	0.9975	0.9994
0.1600	0.8400	0.9032	0.9479	0.9757	0.9905	0.9969	0.9992
0.1800	0.8200	0.8901	0.9402	0.9718	0.9888	0.9964	0.9990
0.2000	0.8000	0.8768	0.9323	0.9677	0.9870	0.9957	0.9989
0.2200	0.7800	0.8633	0.9241	0.9634	0.9852	0.9951	0.9987
0.2400	0.7600	0.8497	0.9159	0.9590	0.9832	0.9944	0.9985
0.2600	0.7400	0.8359	0.9074	0.9545	0.9812	0.9937	0.9983
0.2800	0.7200	0.8220	0.8987	0.9499	0.9792	0.9930	0.9981
0.3000	0.7000	0.8079	0.8899	0.9451	0.9771	0.9922	0.9979
0.3200	0.6800	0.7936	0.8809	0.9402	0.9749	0.9915	0.9977
0.3400	0.6600	0.7792	0.8717	0.9352	0.9727	0.9907	0.9975
0.3600	0.6400	0.7647	0.8623	0.9301	0.9704	0.9899	0.9973
0.3800	0.6200	0.7499	0.8527	0.9248	0.9681	0.9891	0.9971
0.4000	0.6000	0.7351	0.8430	0.9195	0.9657	0.9883	0.9969
0.4200	0.5800	0.7200	0.8331	0.9140	0.9633	0.9875	0.9967
0.4400	0.5600	0.7048	0.8231	0.9085	0.9608	0.9866	0.9964
0.4600	0.5400	0.6895	0.8128	0.9028	0.9583	0.9858	0.9962
0.4800	0.5200	0.6739	0.8024	0.8970	0.9558	0.9849	0.9960
0.5000	0.5000	0.6582	0.7918	0.8911	0.9532	0.9841	0.9958
0.5200	0.4800	0.6424	0.7811	0.8851	0.9506	0.9832	0.9956
0.5400	0.4600	0.6263	0.7701	0.8790	0.9480	0.9823	0.9953
0.5600	0.4400	0.6100	0.7589	0.8729	0.9453	0.9815	0.9951
0.5800	0.4200	0.5936	0.7476	0.8666	0.9427	0.9806	0.9949
0.6000	0.4000	0.5770	0.7361	0.8603	0.9400	0.9797	0.9947
0.6200	0.3800	0.5601	0.7244	0.8539	0.9373	0.9788	0.9945
0.6400	0.3600	0.5430	0.7125	0.8473	0.9345	0.9779	0.9942
0.6600	0.3400	0.5257	0.7004	0.8408	0.9318	0.9771	0.9940
0.6800	0.3200	0.5082	0.6881	0.8341	0.9291	0.9762	0.9938

Table 4 - continued on next page

0.7000	0.3000	0.4903	0.6755	0.8274	0.9263	0.9753	0.9936
0.7200	0.2800	0.4722	0.6628	0.8207	0.9236	0.9744	0.9933
0.7400	0.2600	0.4538	0.6499	0.8139	0.9208	0.9735	0.9931
0.7600	0.2400	0.4351	0.6368	0.8070	0.9180	0.9726	0.9929
0.7800	0.2200	0.4161	0.6234	0.8001	0.9153	0.9718	0.9927
0.8000	0.2000	0.3966	0.6099	0.7932	0.9125	0.9709	0.9925
0.8200	0.1800	0.3767	0.5962	0.7863	0.9097	0.9700	0.9922
0.8400	0.1600	0.3564	0.5823	0.7793	0.9070	0.9691	0.9920
0.8600	0.1400	0.3355	0.5682	0.7724	0.9042	0.9682	0.9918
0.8800	0.1200	0.3141	0.5540	0.7654	0.9014	0.9673	0.9916
0.9000	0.1000	0.2920	0.5397	0.7585	0.8986	0.9665	0.9913
0.9200	0.0800	0.2691	0.5253	0.7515	0.8959	0.9656	0.9911
0.9400	0.0600	0.2454	0.5109	0.7446	0.8931	0.9647	0.9909
0.9600	0.0400	0.2208	0.4965	0.7376	0.8903	0.9638	0.9907
0.9800	0.0200	0.1955	0.4821	0.7307	0.8876	0.9629	0.9905
1.0000	0.0000	0.1699	0.4677	0.7237	0.8848	0.9620	0.9902

Table 4 - $P[S \geq r]$ as a function of the crossing level r and the variance of the enveloped components $\lambda_{o,2}$.

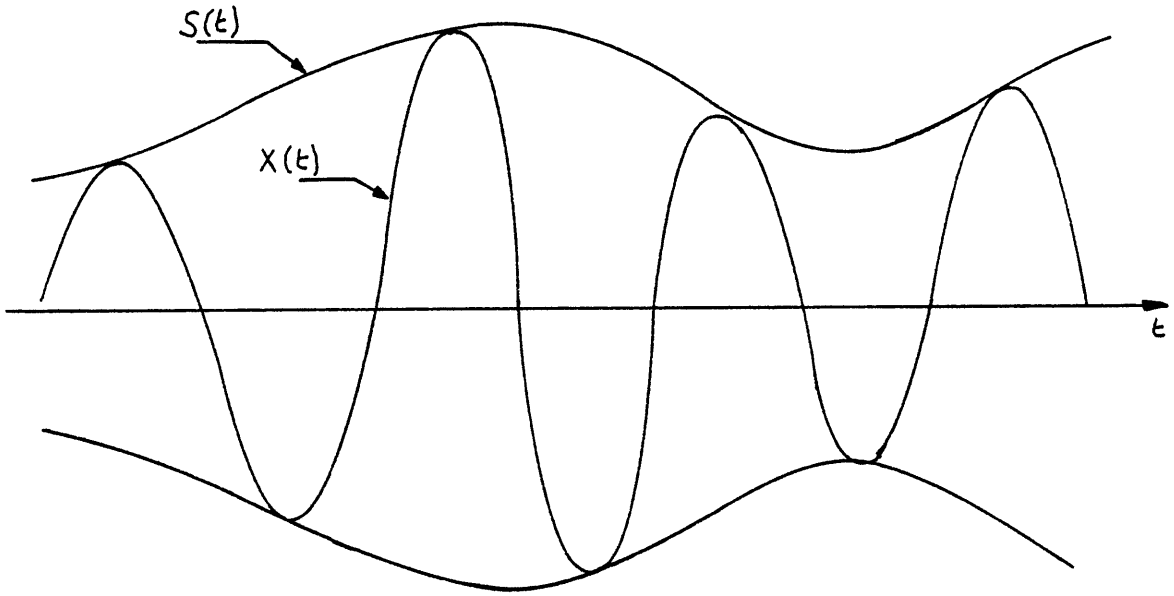

Fig. 1 - Illustration of envelope for a narrow-band process

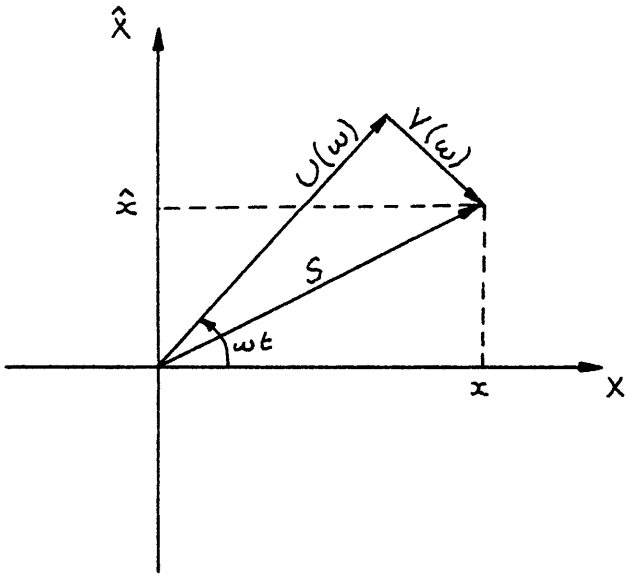

Fig. 2 - Interpretation of the C-L envelope in the $(X,\hat{X})$-plane

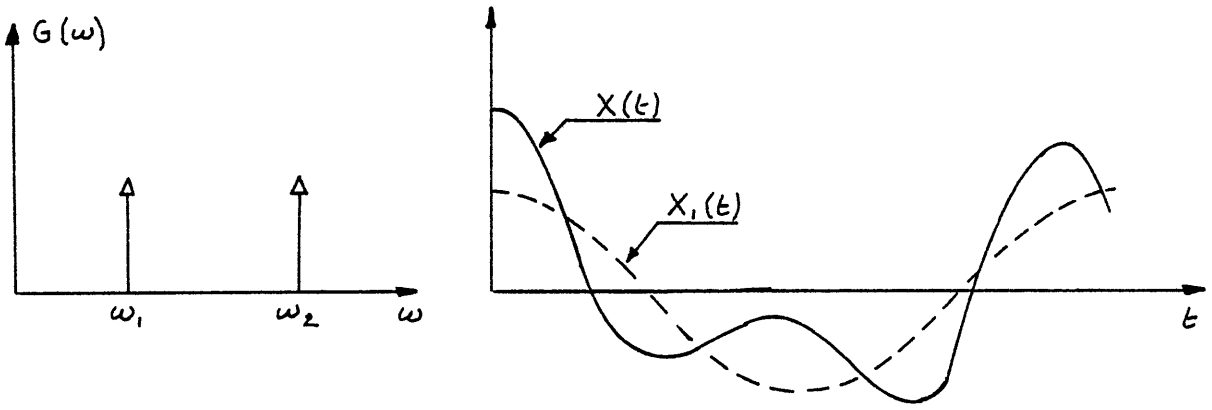

Fig. 3 - Discrete spectral density and associated typical realisation of X(t)

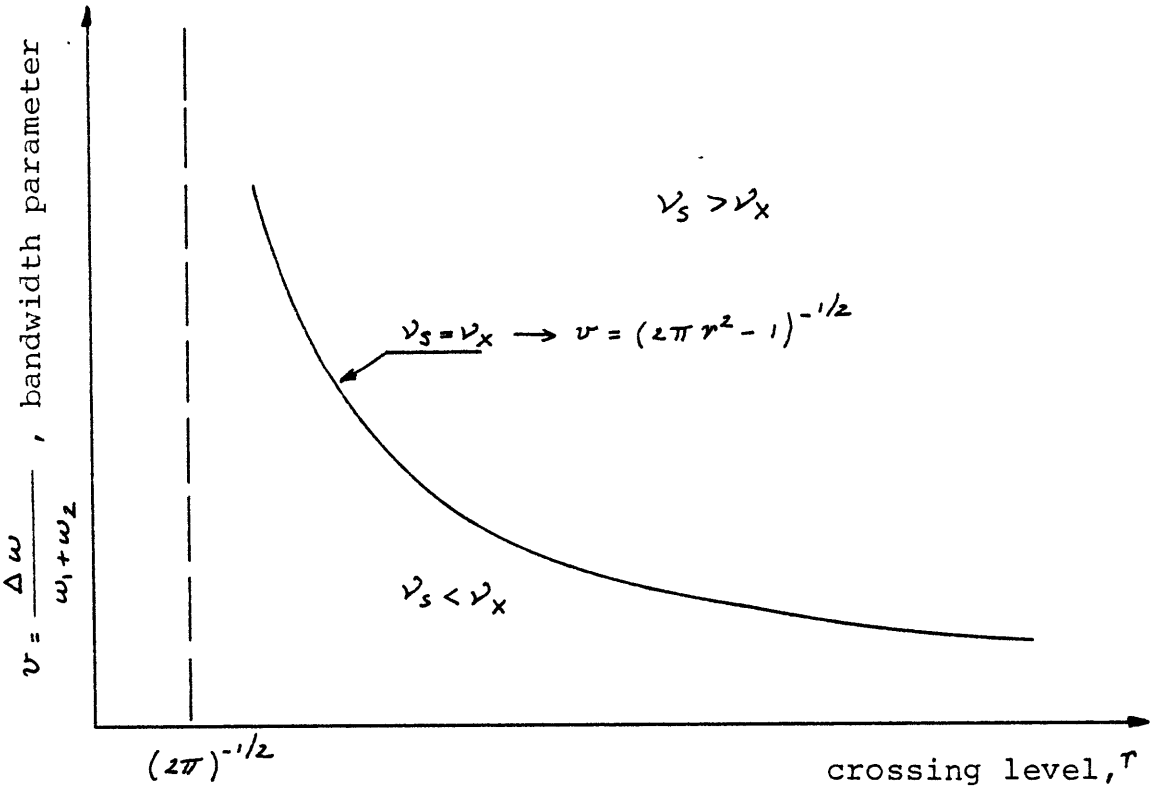

Fig. 4 - Comparison between ν_s and ν_x in the (r,v)-plane

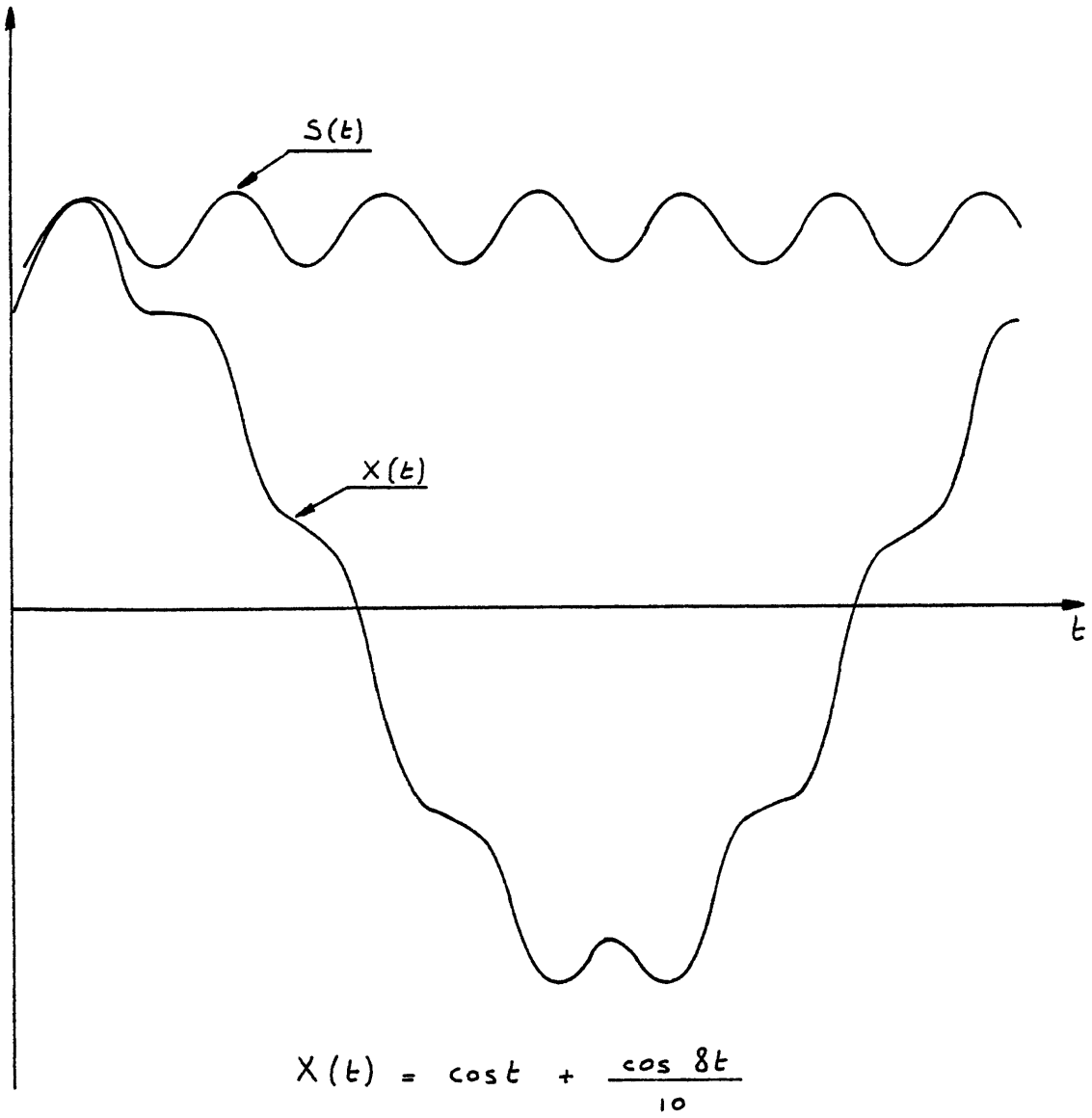

Fig. 5 - Realisation of a bichromatic wide-band process and associated C-L envelope S(t)

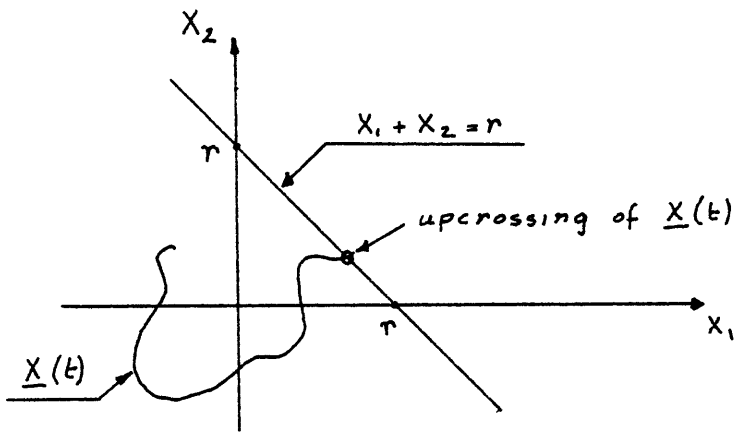

Fig. 6 - Decomposition of the process X(t) into two components X_1 and X_2

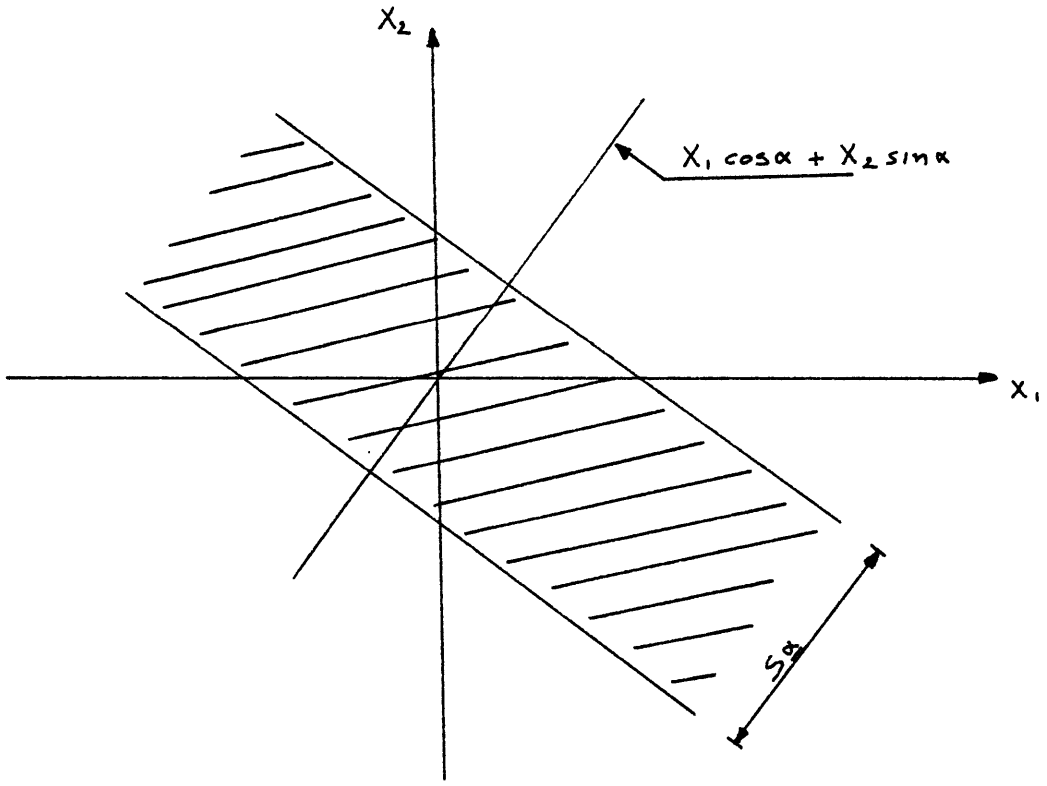

Fig. 7 - Bandenvelope S_B

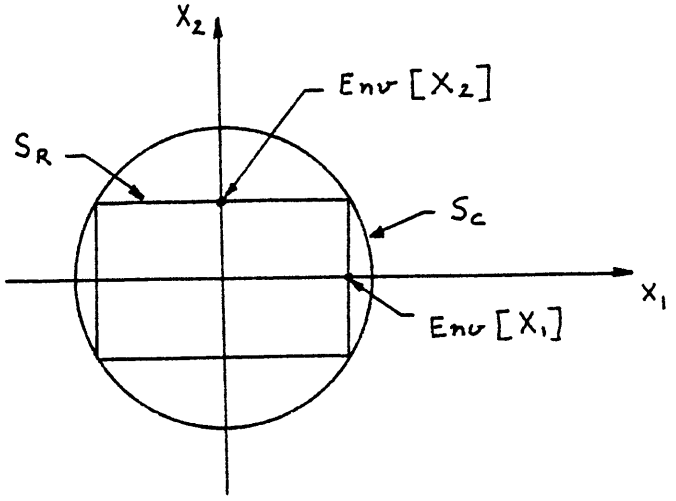

Fig. 8 - Rectangular envelope S_R and circular envelope S_C

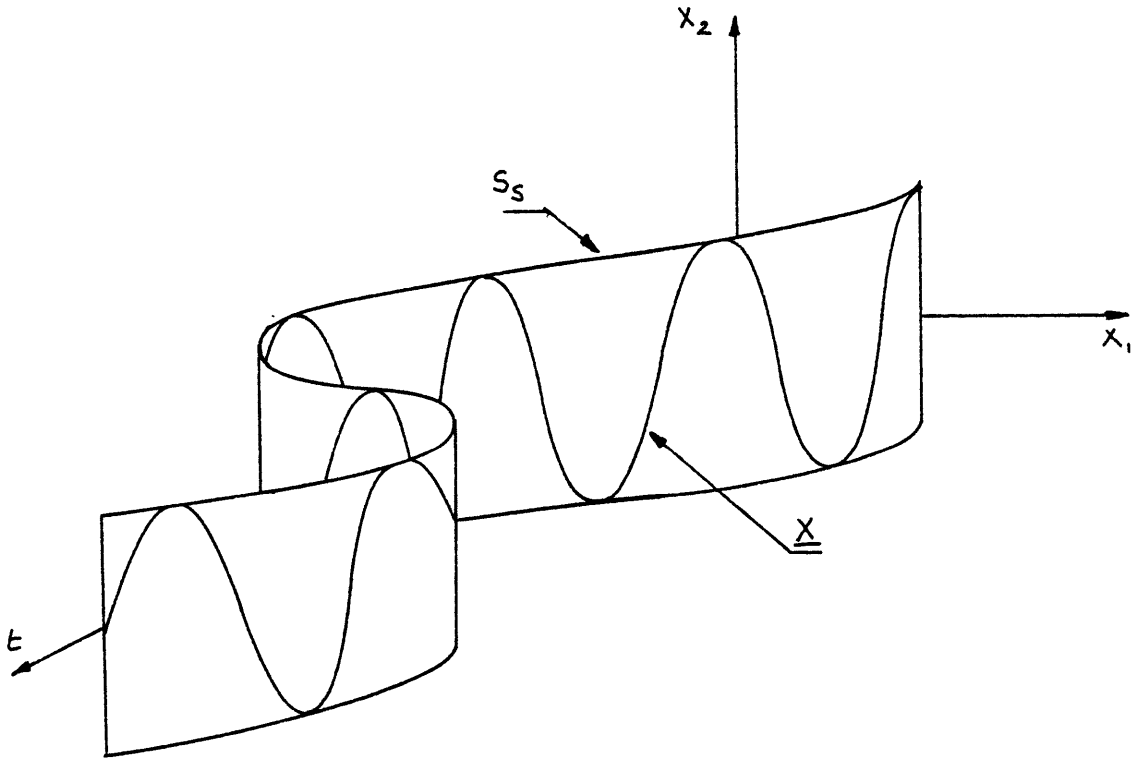

Fig. 9 - Surface envelope S_S in (X_1,X_2,t)-space

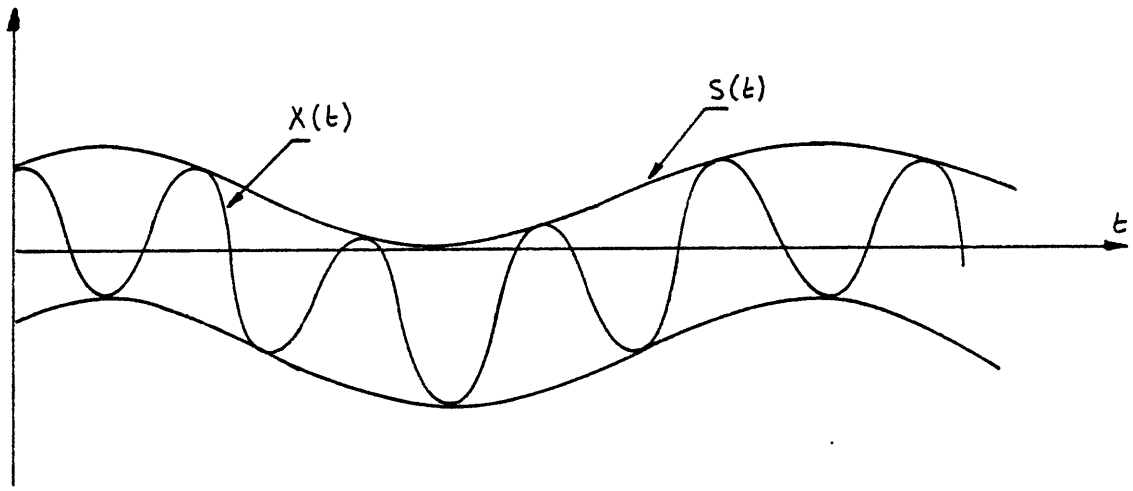

Fig. 10 - One-dimensional envelope associated with the surface envelope of Fig. 9

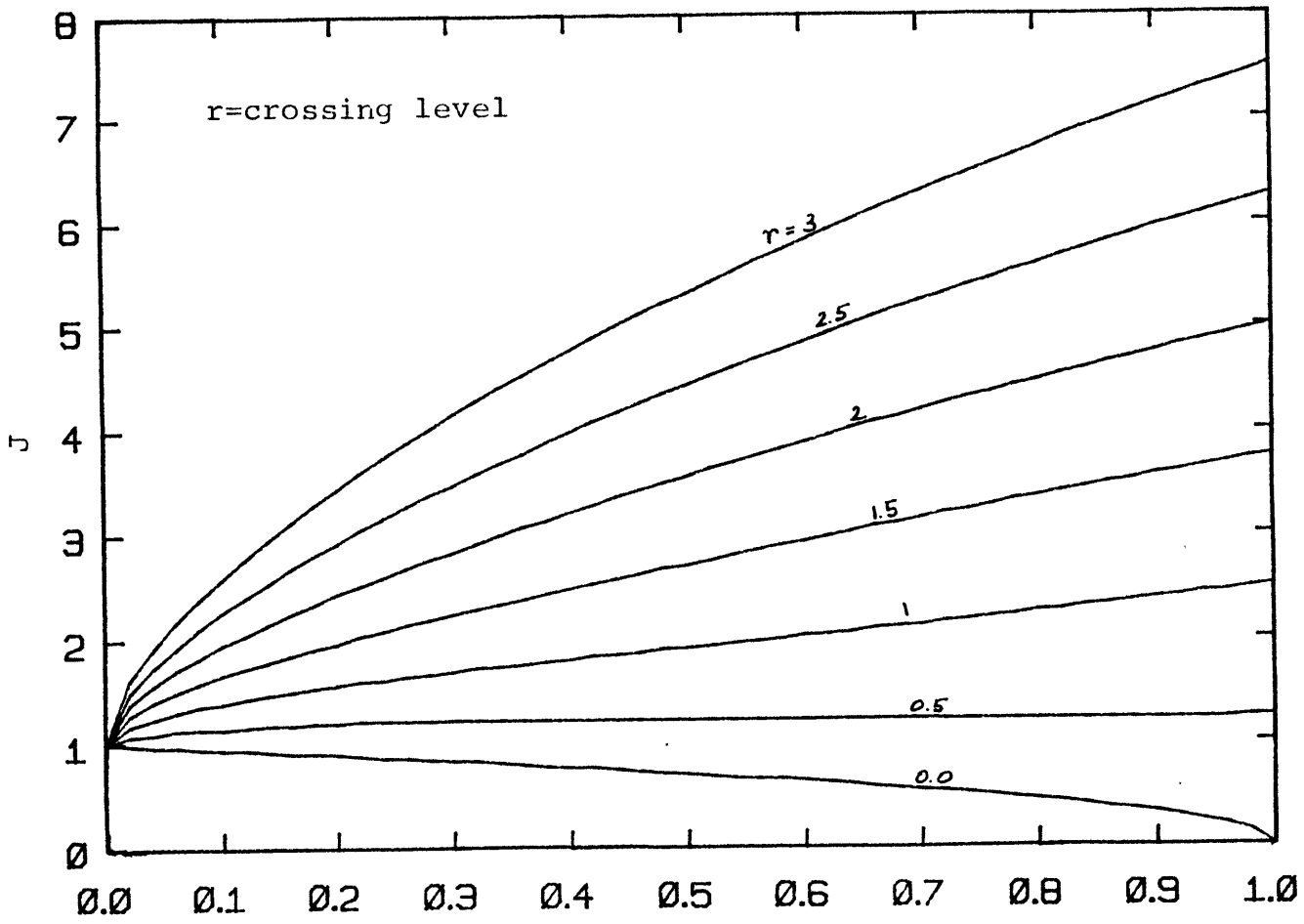

Fig. 11 - Factor J of Eq. 42 as a function of $\lambda_{0,2}$

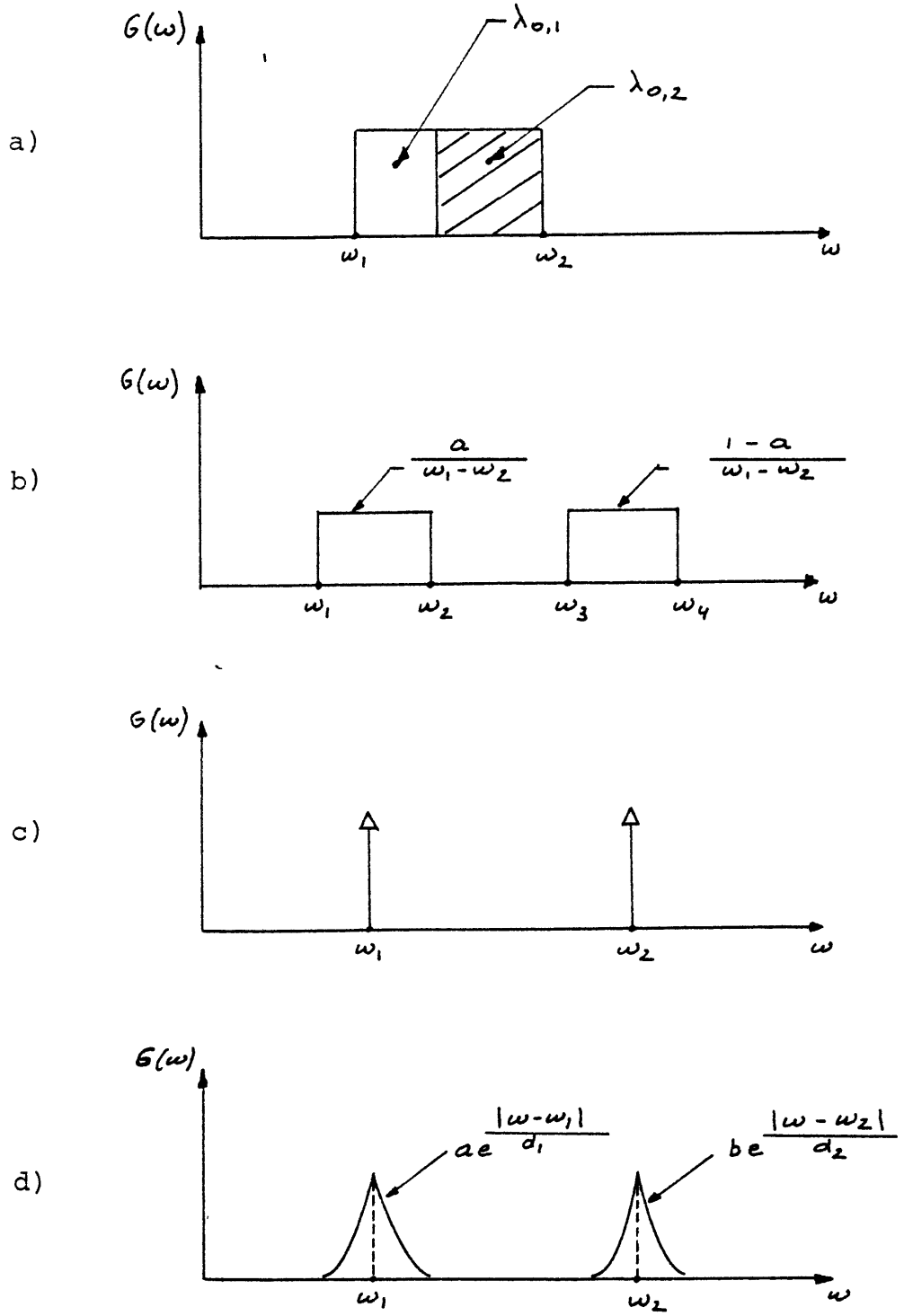

Fig. 12 - Spectral densities used for the calculation of the mean crossing rate ratio ν_s/ν_x

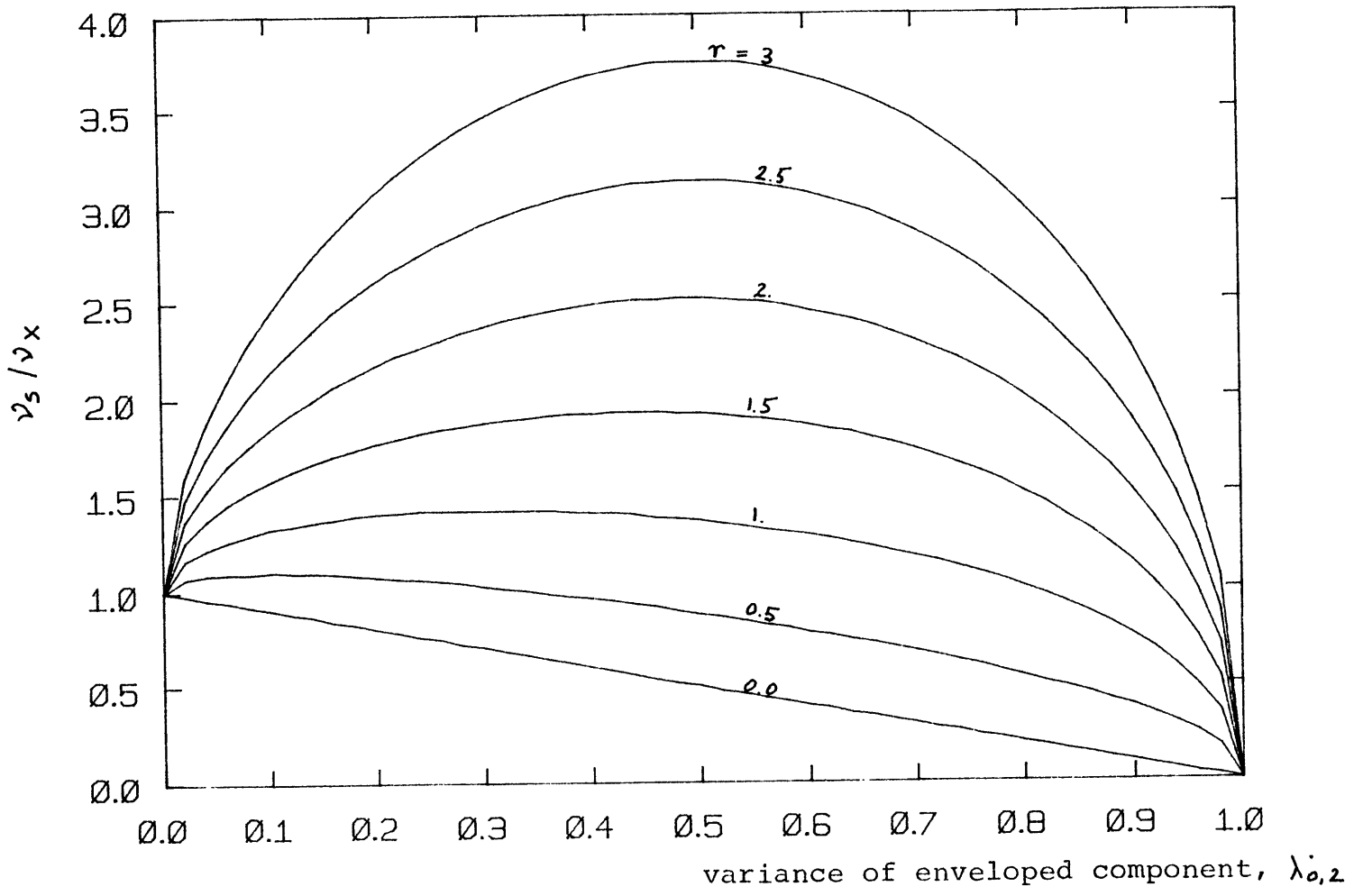

Fig. 13 - Ratio ν_s/ν_x for a rectangular spectrum, $\omega_2/\omega_1 = 1$

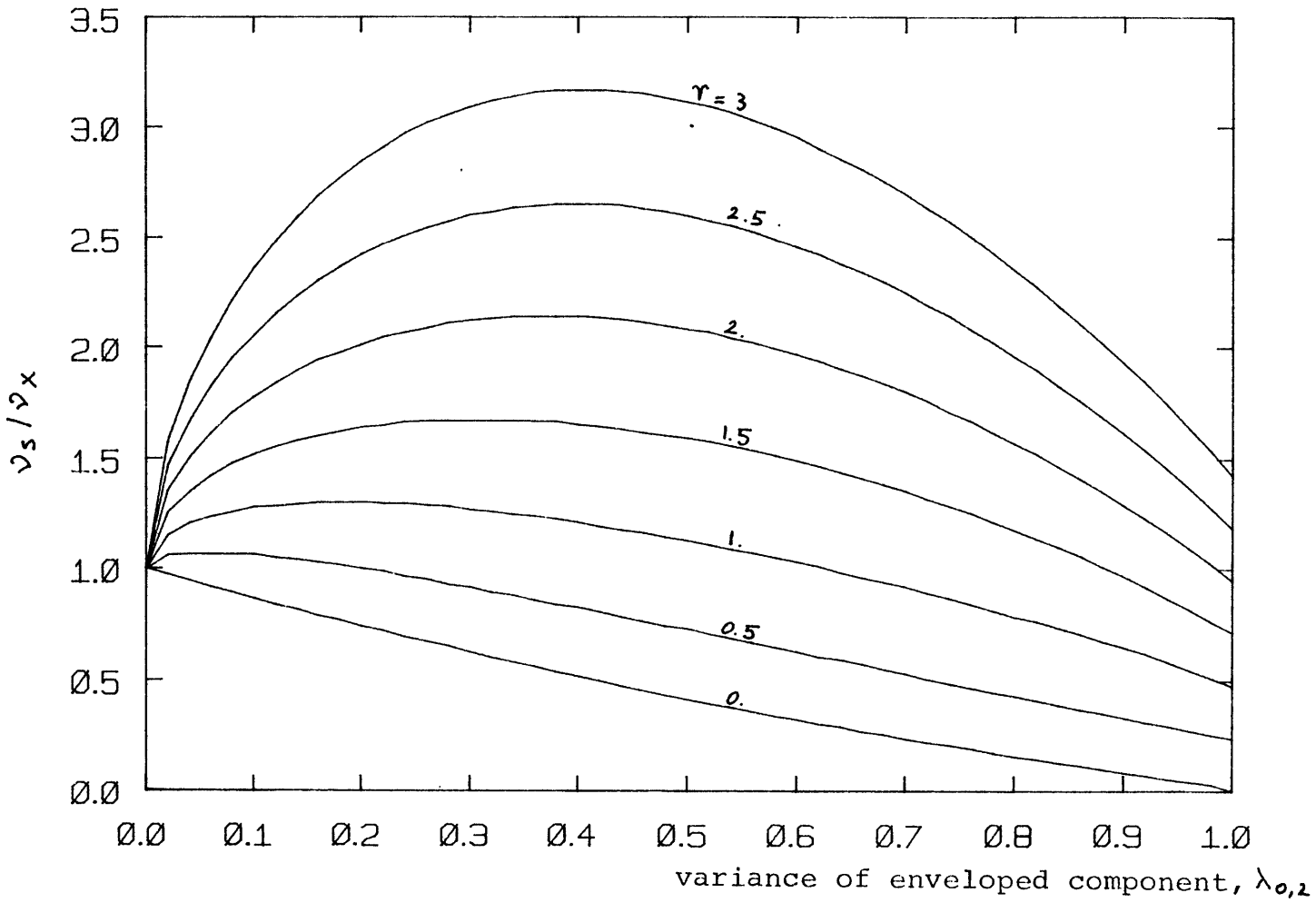

Fig. 14 - Ratio ν_s/ν_x for a rectangular spectrum, $\omega_2/\omega_1 = 2$

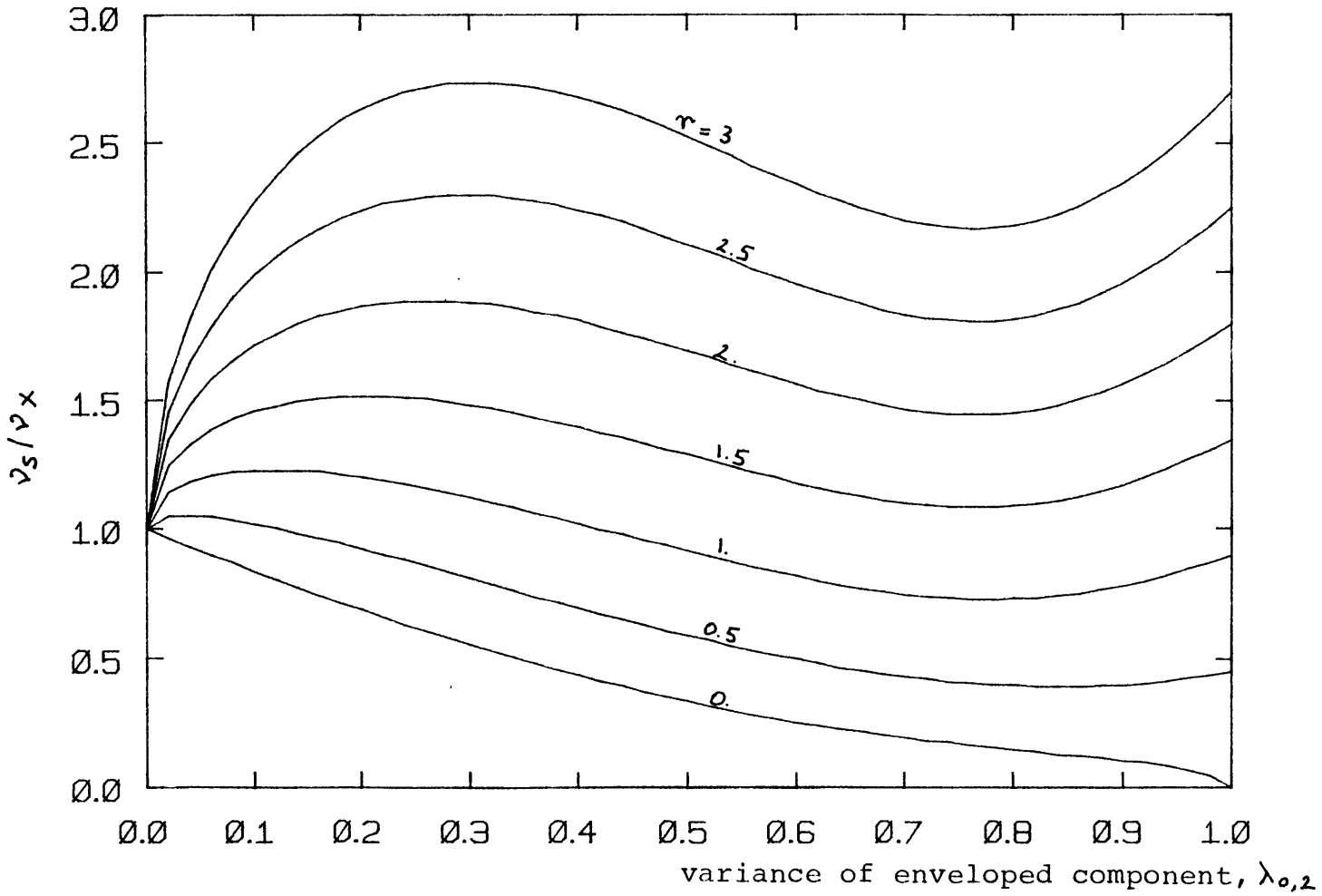

Fig. 15 - Ratio ν_s/ν_x for a rectangular spectrum, ω_2/ω_1 =5

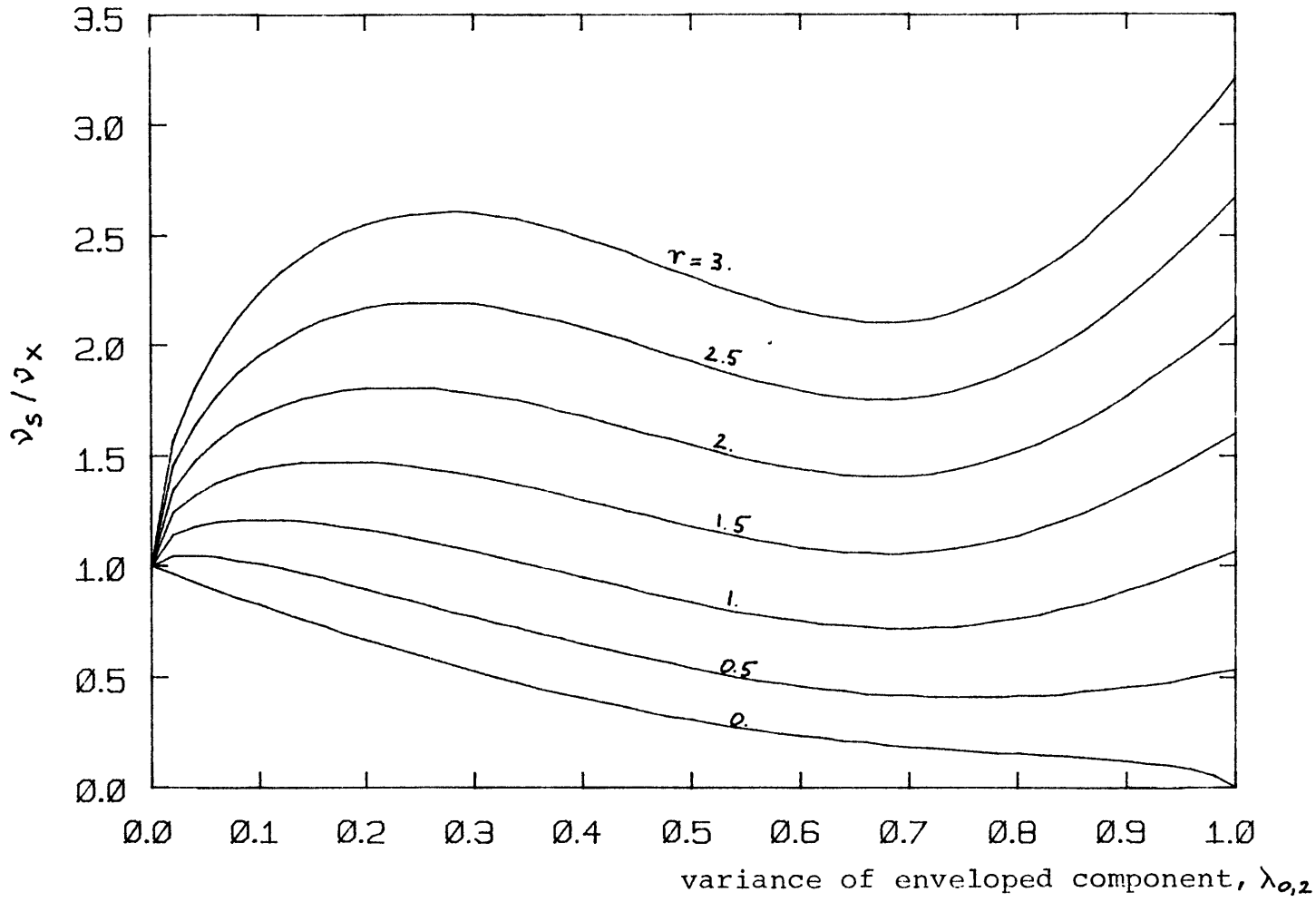

Fig. 16 - Ratio ν_s/ν_x for a rectangular spectrum, $\omega_2/\omega_1 = 10$

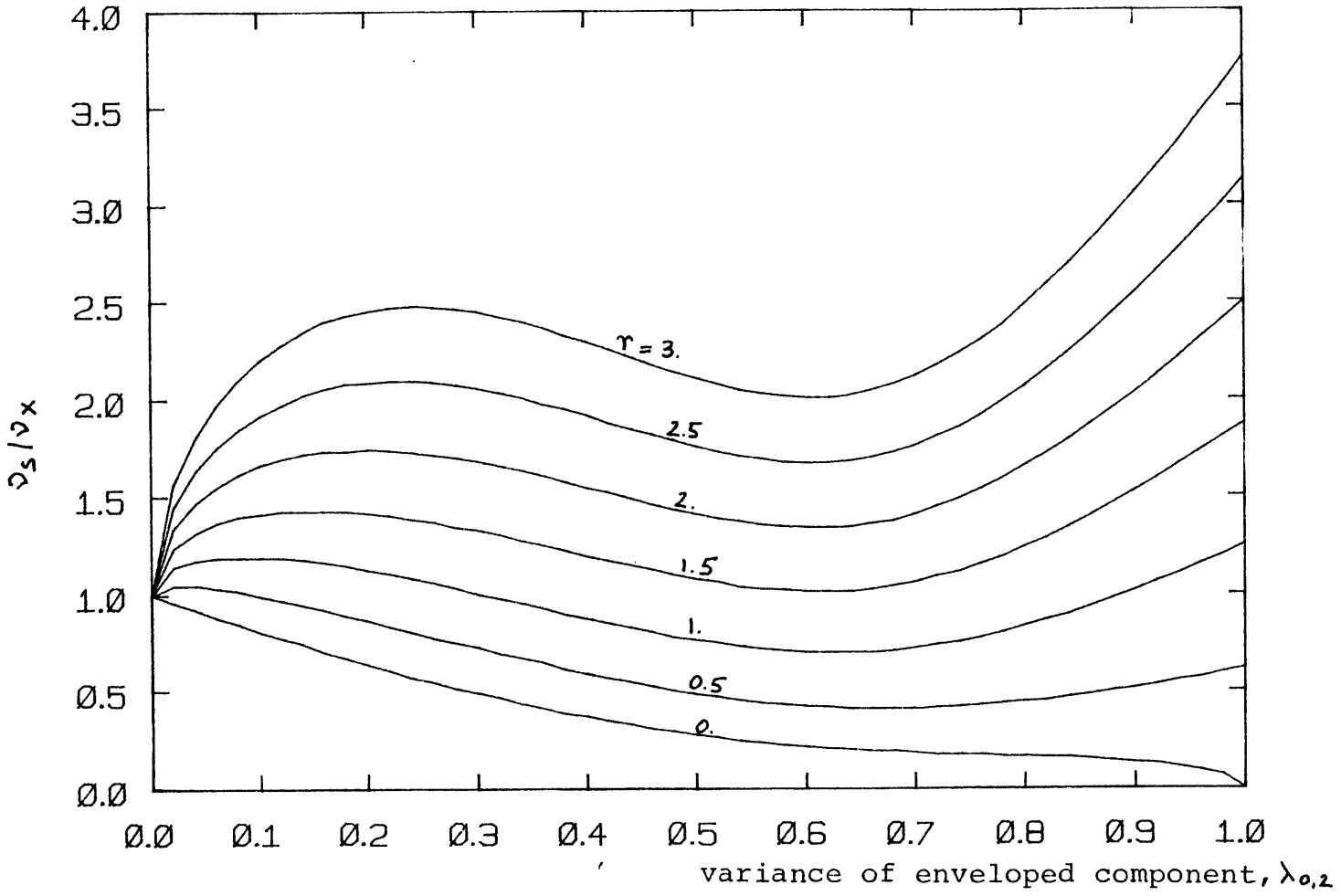

Fig. 17 - Ratio ν_s/ν_x for a rectangular spectrum, $\omega_2/\omega_1 = 10^4$

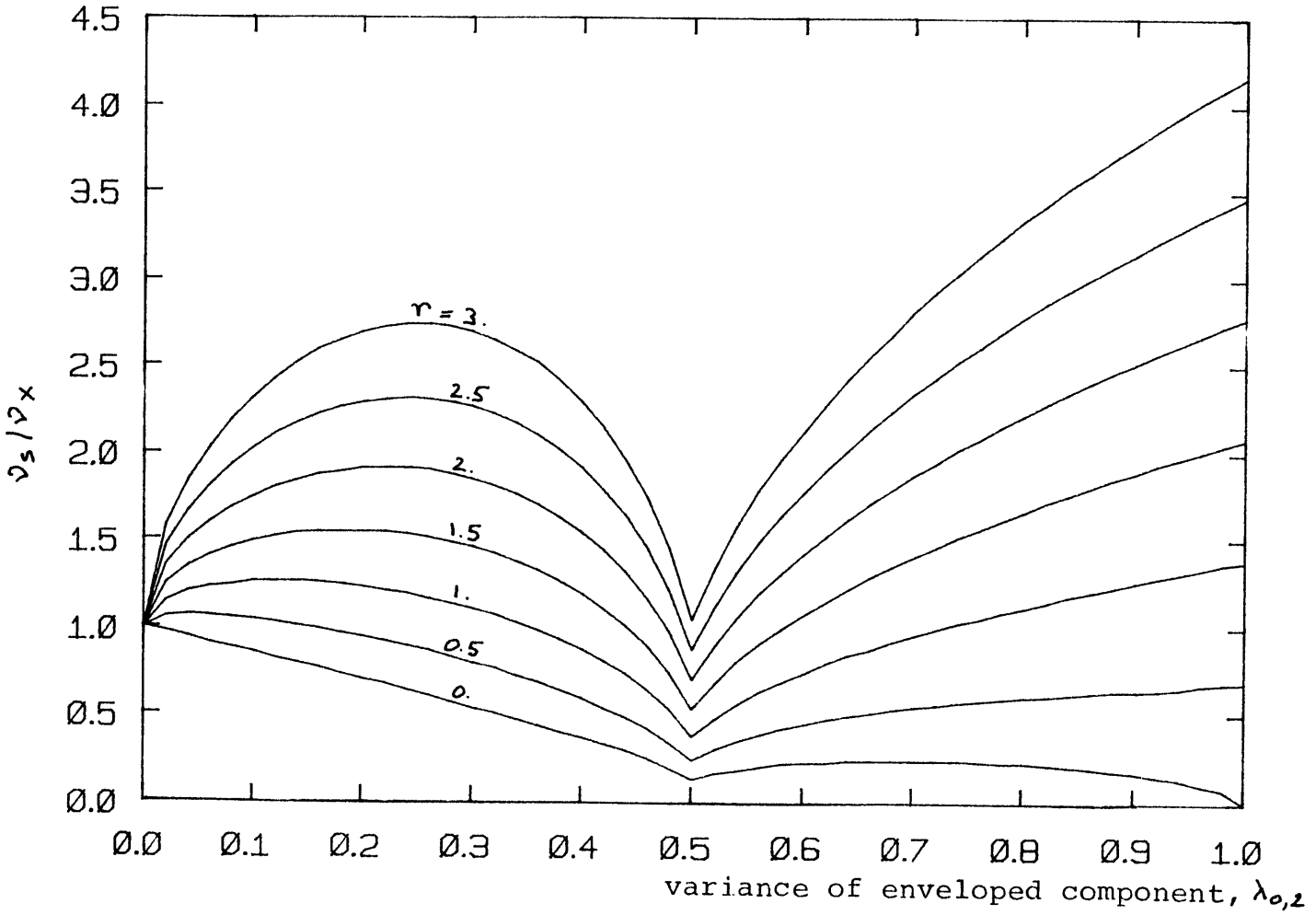

Fig. 18 - Ratio ν_s/ν_x for spectrum in Fig. 12b :

a=0.5, $\omega_1 = \omega_2$, $\omega_3 = 5\omega_1$, $\omega_3 = \omega_4$

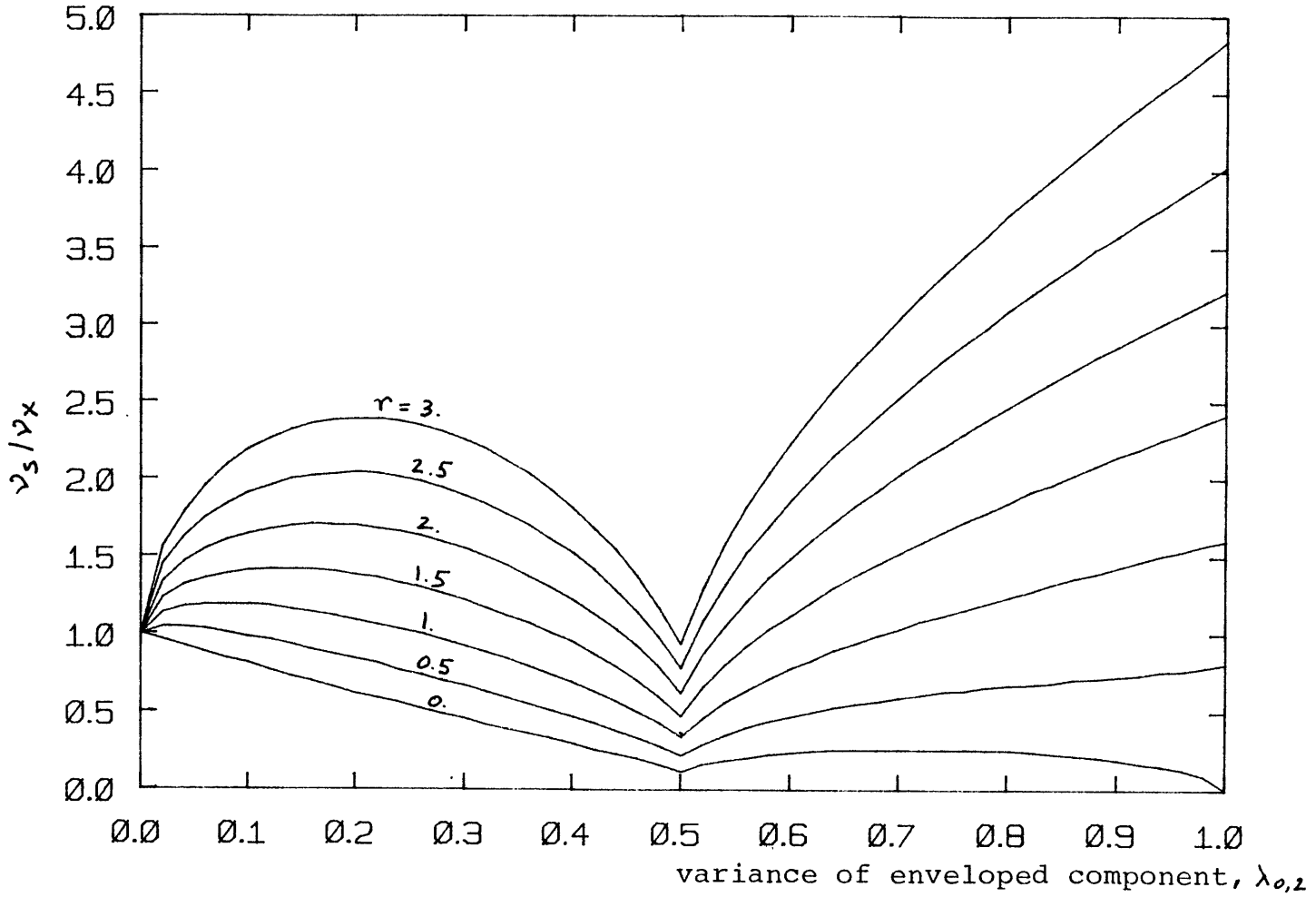

Fig. 19 - Ratio ν_s/ν_x for spectrum in Fig. 12b :

a=0.5, $\omega_2 = 3\,\omega_1$, $\omega_3 = 5\,\omega_2$, $\omega_4 = \frac{5}{3}\,\omega_3$

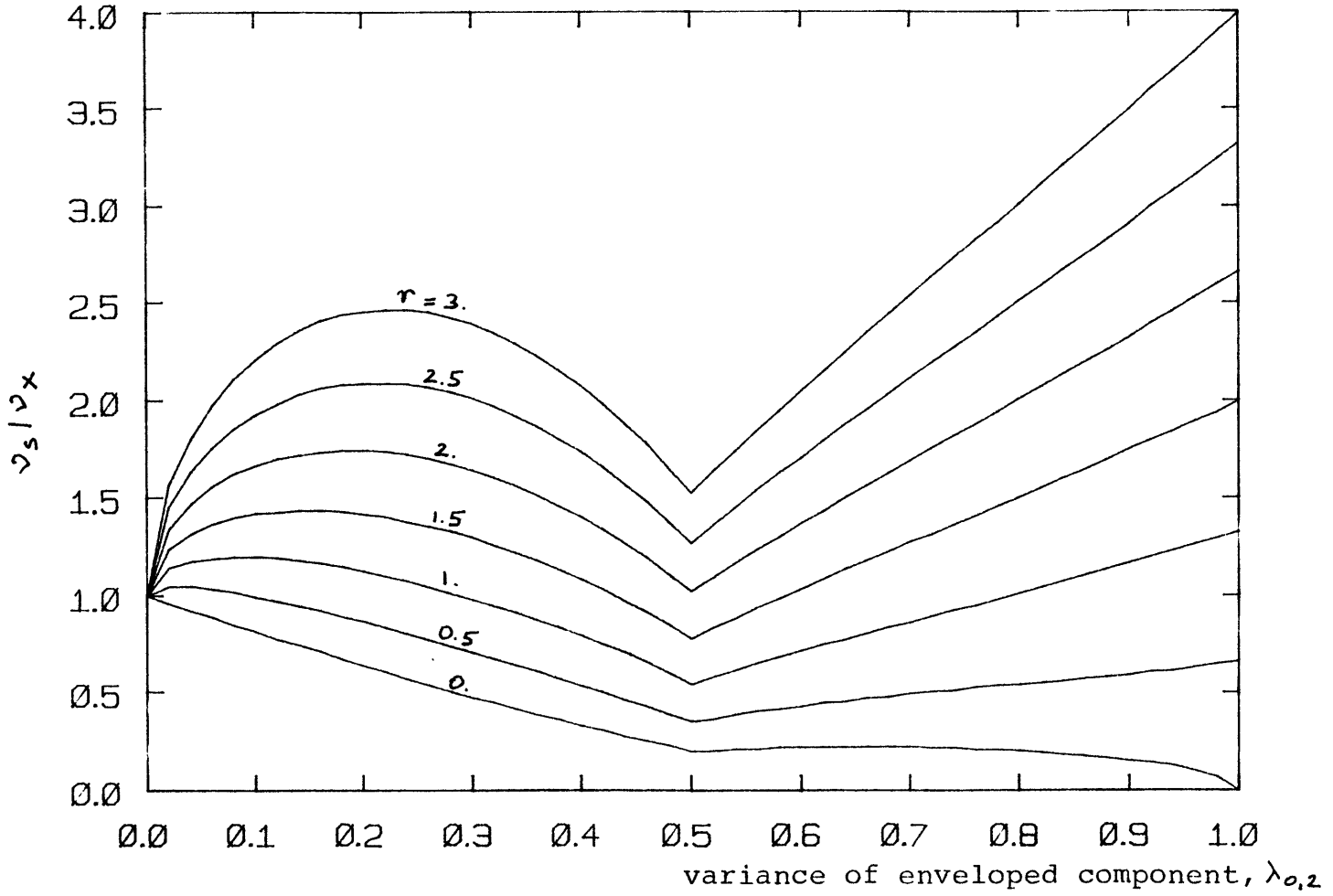

Fig. 20 - Ratio ν_s/ν_x for spectrum in Fig. 12b :

a=0.5, $\omega_2 = 3\omega_1$, $\omega_3 = 2\omega_2$, $\omega_4 = \frac{5}{3}\omega_3$

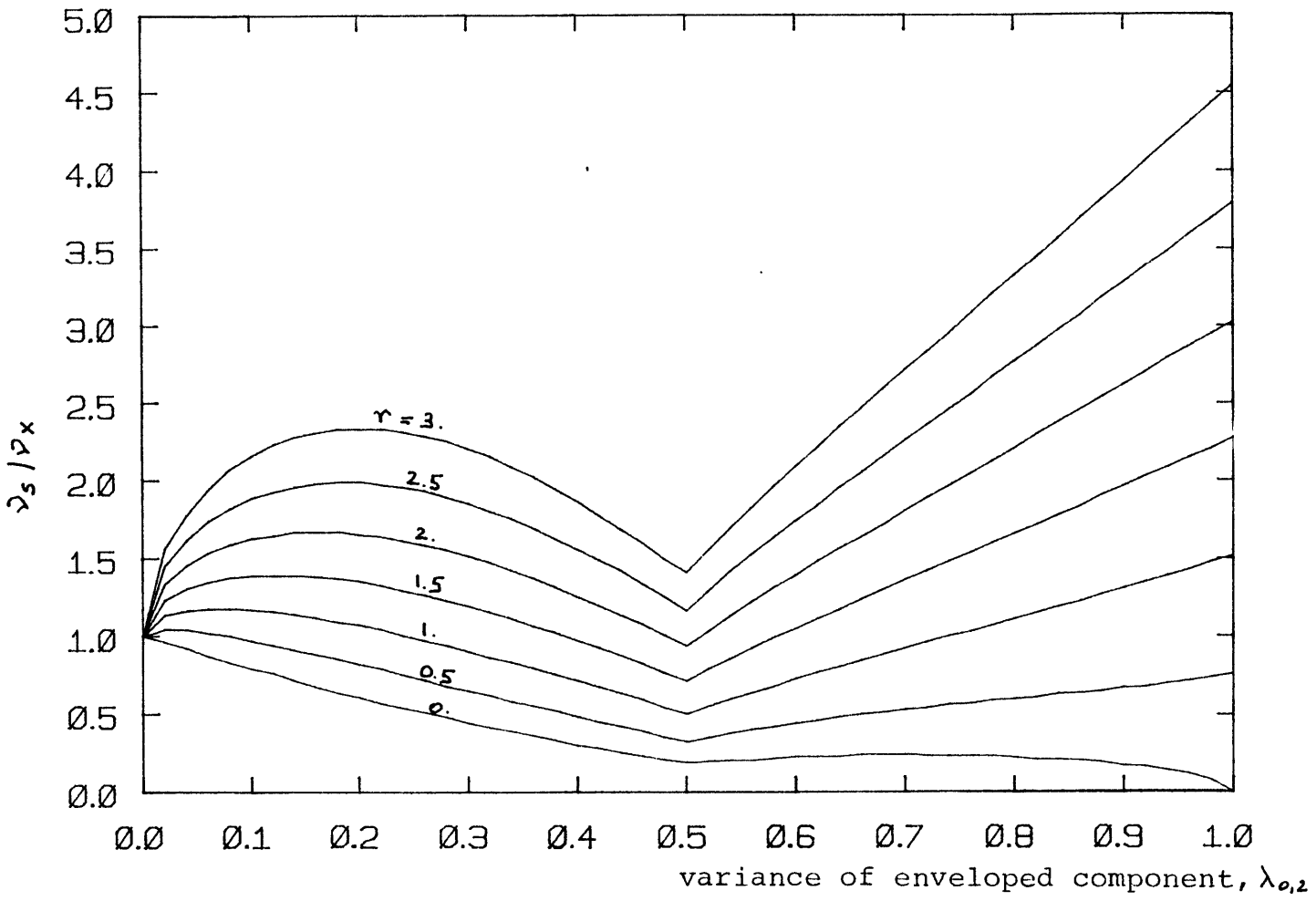

Fig. 21 - Ratio ν_s/ν_x for spectrum in Fig. 12b :

a=0.5, $\omega_2 = 5000\,\omega_1$, $\omega_3 = 2\,\omega_2$, $\omega_4 = 2\,\omega_3$

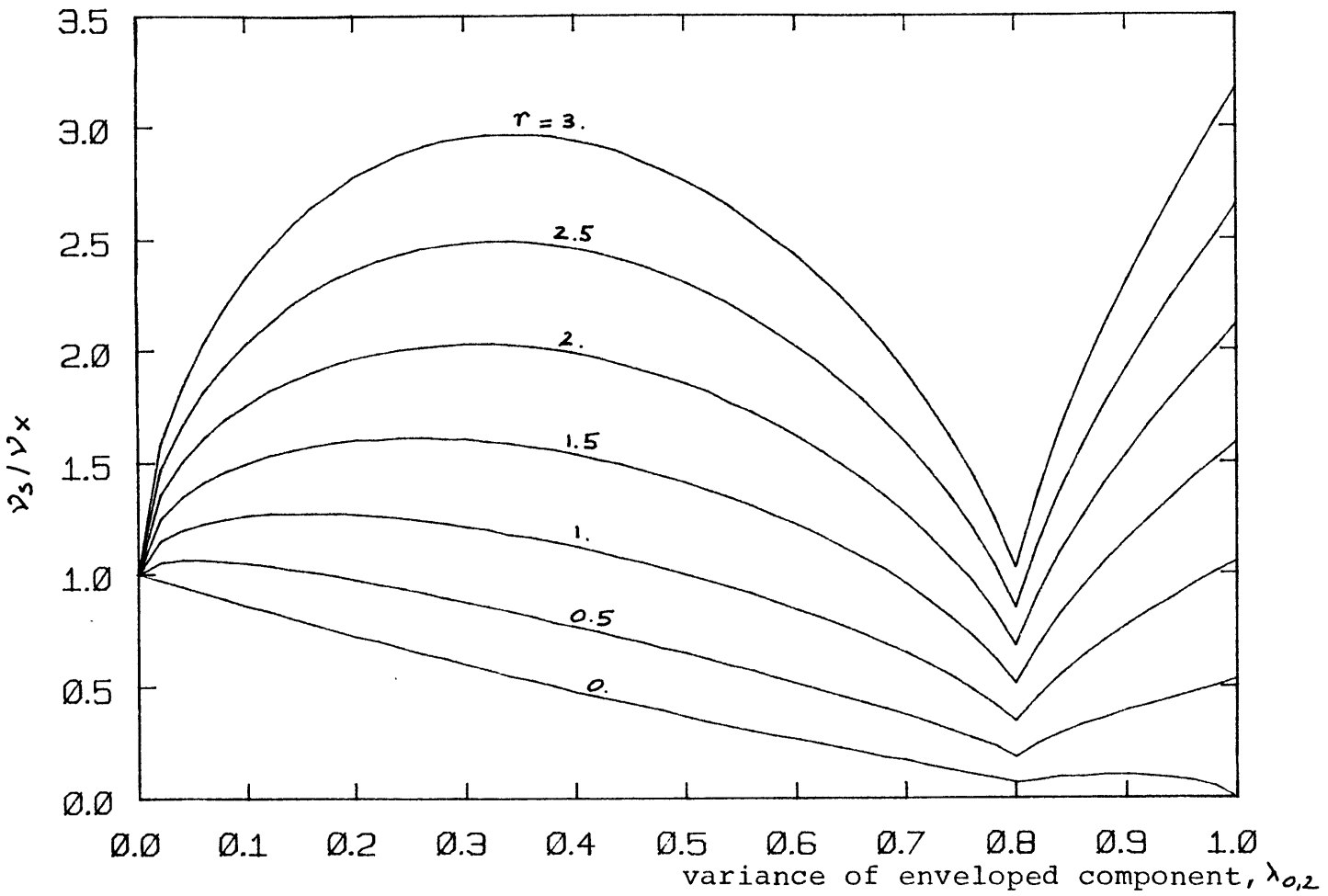

Fig. 22 - Ratio ν_s / ν_x for spectrum in Fig. 12b :

a=0.2, $\omega_2 = 3\omega_1$, $\omega_3 = 5\omega_2$, $\omega_4 = \frac{5}{3}\omega_3$

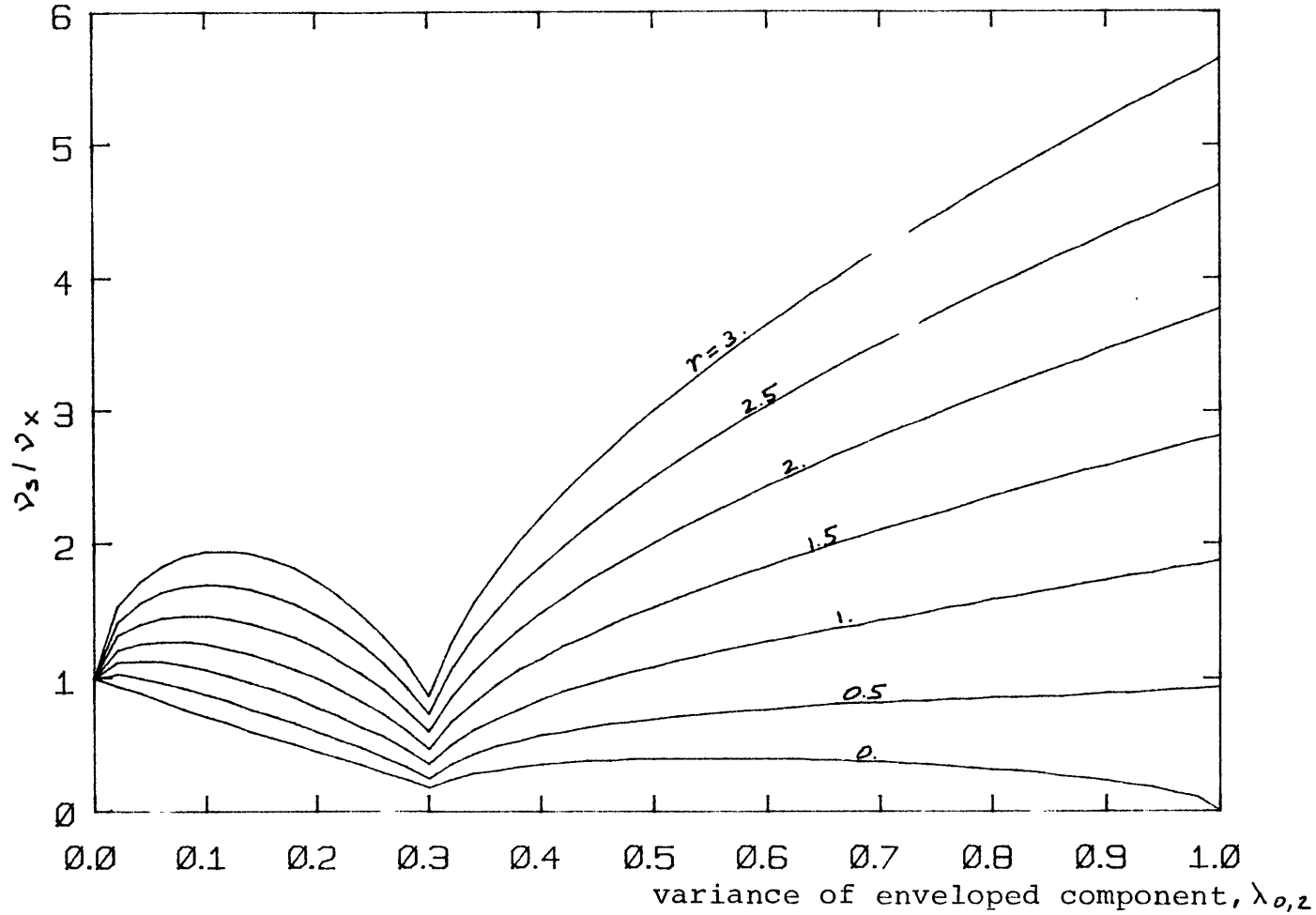

Fig. 23 - Ratio ν_s/ν_x for spectrum in Fig. 12b :

a=0.7, $\omega_2 = 3\omega_1$, $\omega_3 = 5\omega_2$, $\omega_4 = \frac{5}{3}\omega_3$

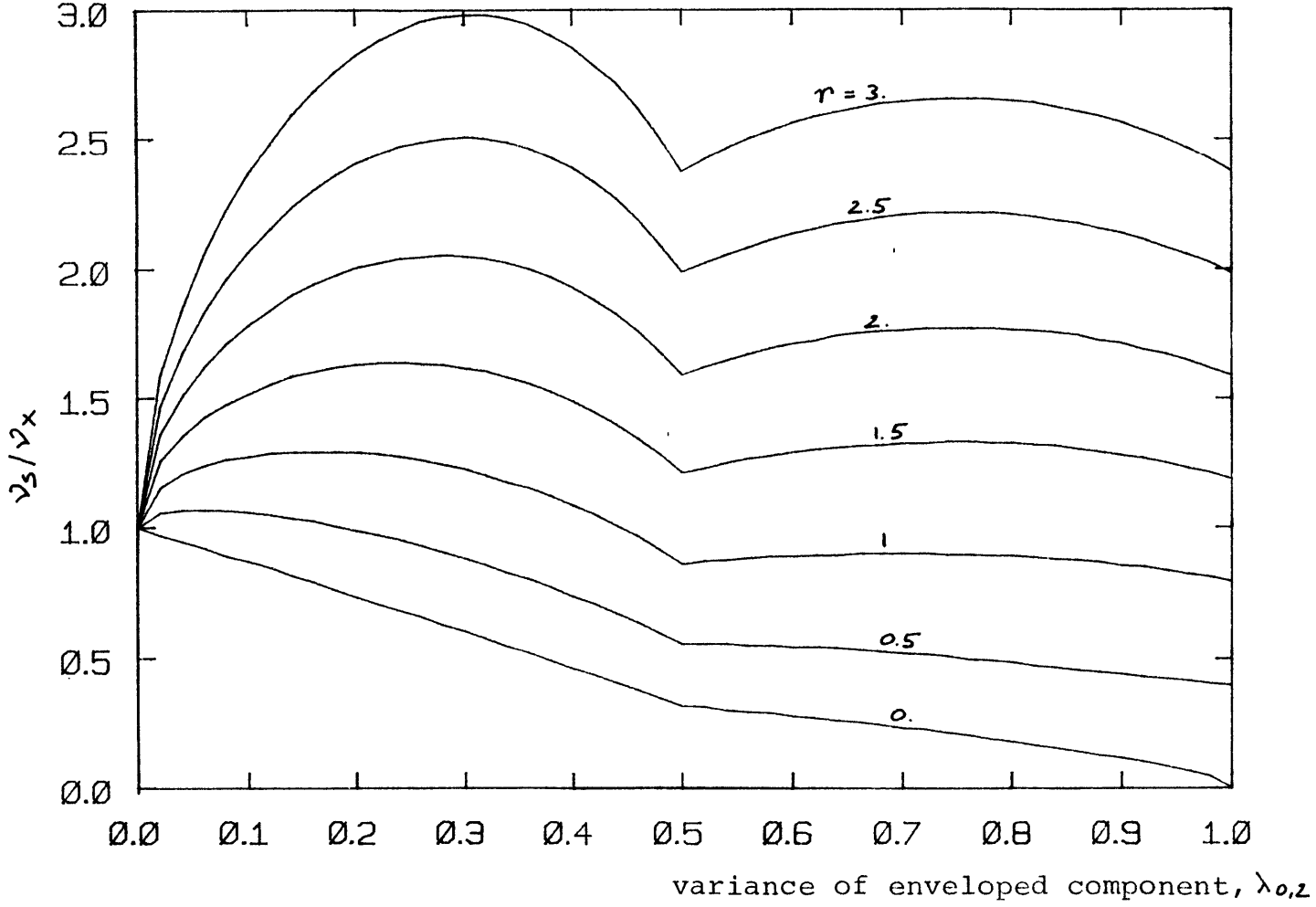

Fig. 24 - Ratio ν_3/ν_x for discrete spectrum, $\omega_2/\omega_1 = 2$

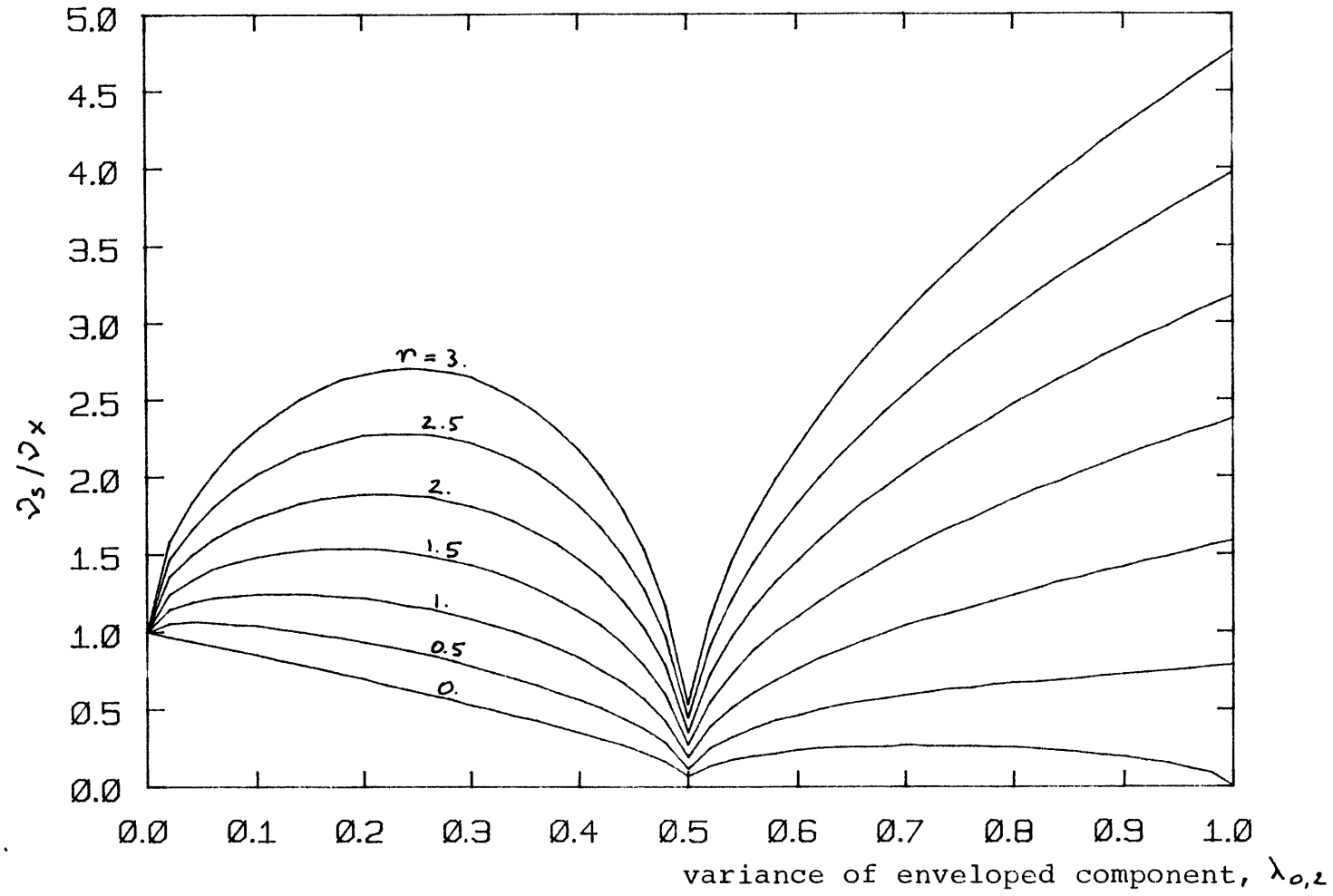

Fig. 25 - Ratio ν_s/ν_x for discrete spectrum, $\omega_2/\omega_1 = 10$

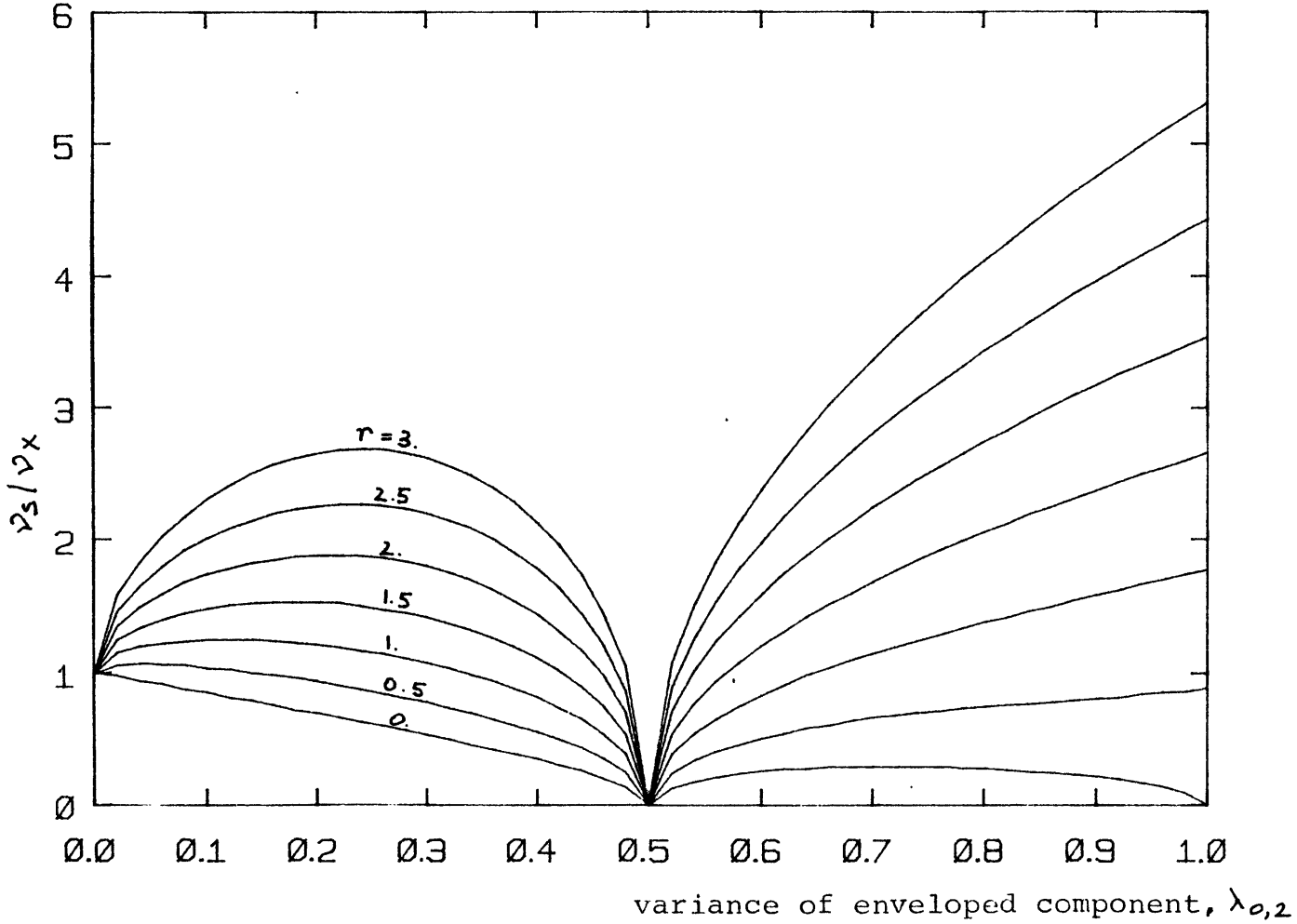

Fig. 26 - Ratio ν_s/ν_x for discrete spectrum, $\omega_2/\omega_1 = 10^4$

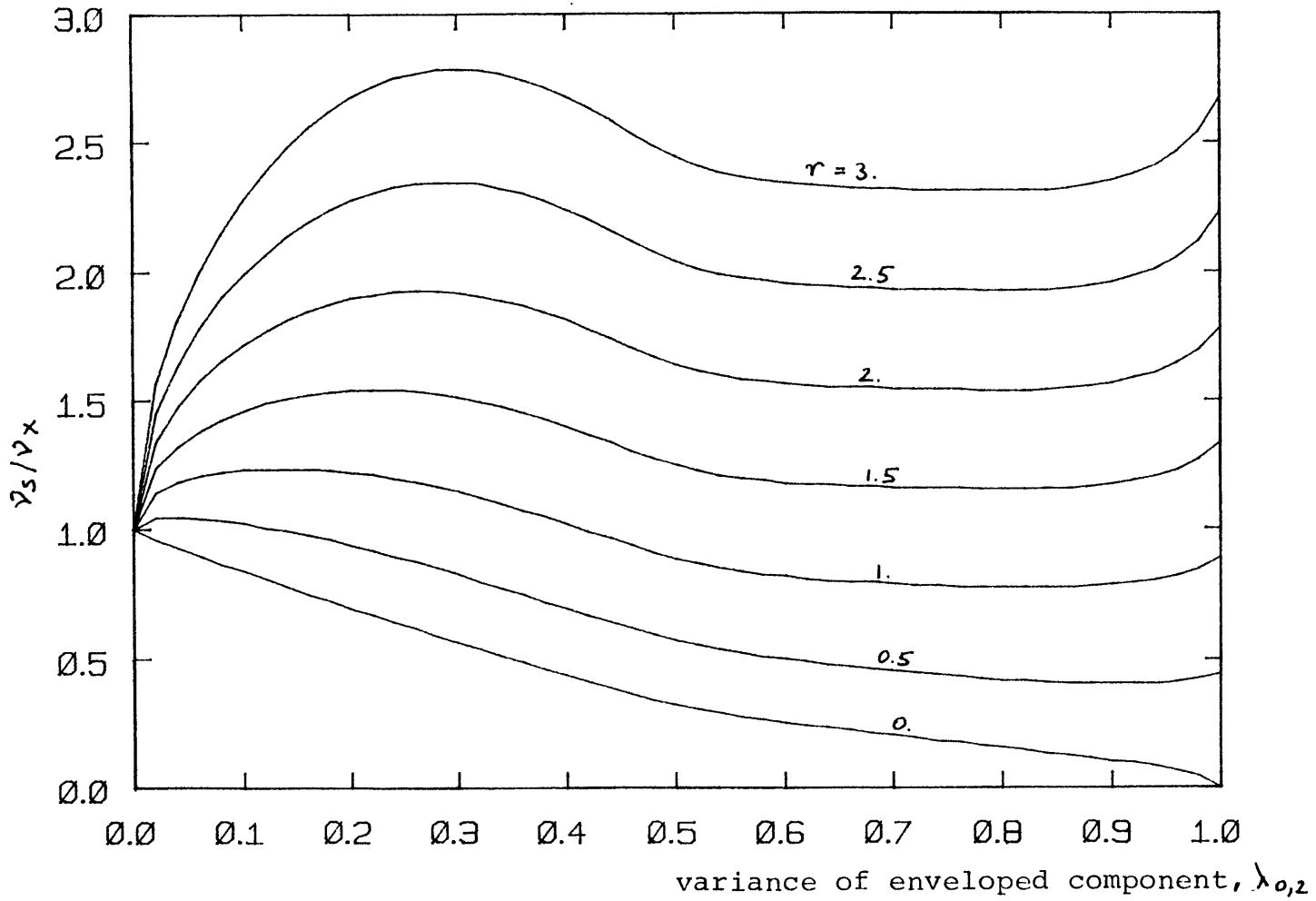

Fig. 27 - Ratio ν_s/ν_x for $G(\omega)=0.25e^{-|\omega-5|}+0.25e^{-|\omega-10|}$

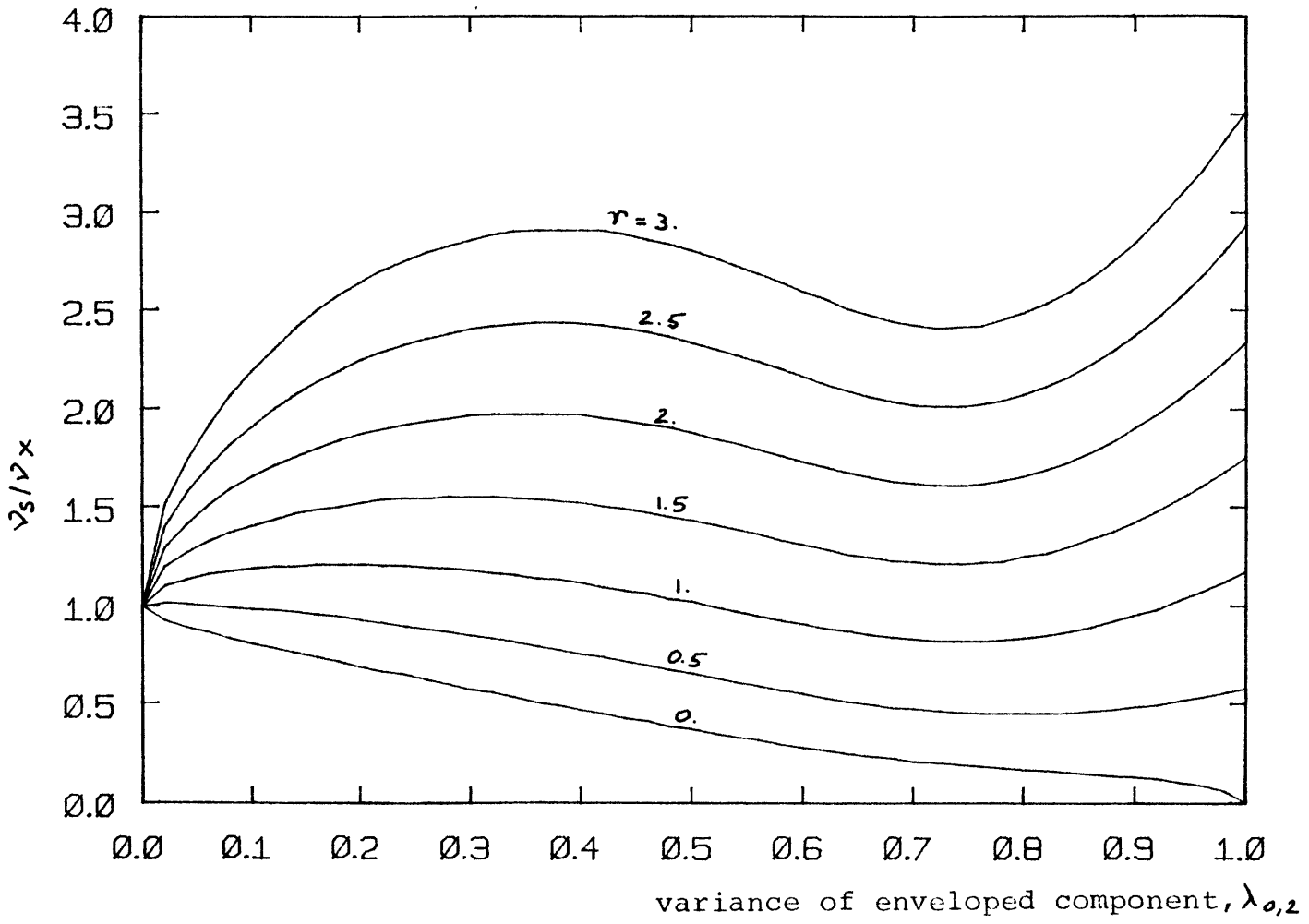

Fig. 28 - Ratio ν_s/ν_x for $G(\omega)=0.05e^{-\frac{|\omega-5|}{5}}+0.25e^{-|\omega-10|}$

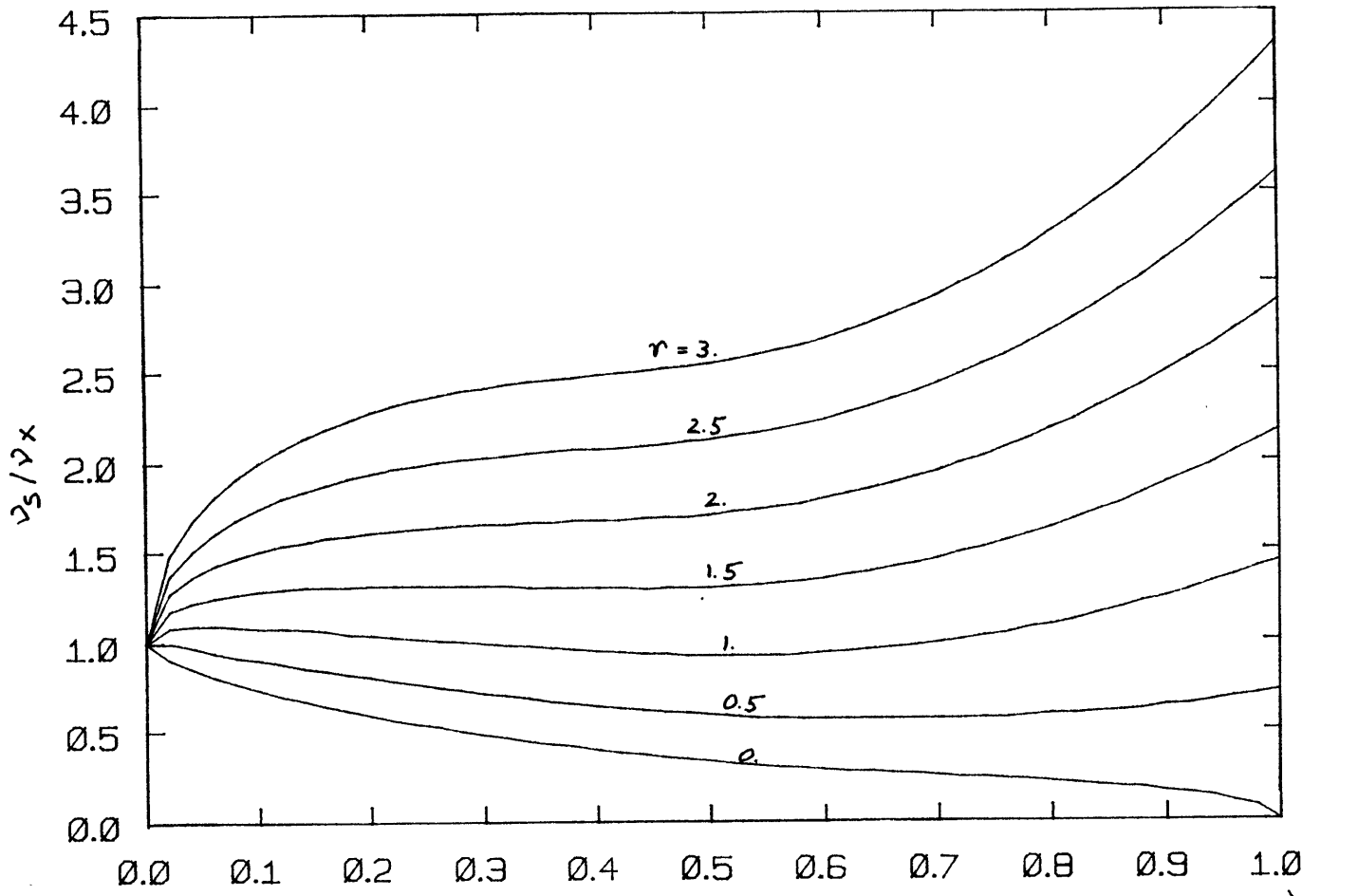

Fig. 29 - Ratio ν_s/ν_x for $G(\omega)=0.05e^{-\frac{|\omega-5|}{5}}+0.05e^{-\frac{|\omega-10|}{5}}$

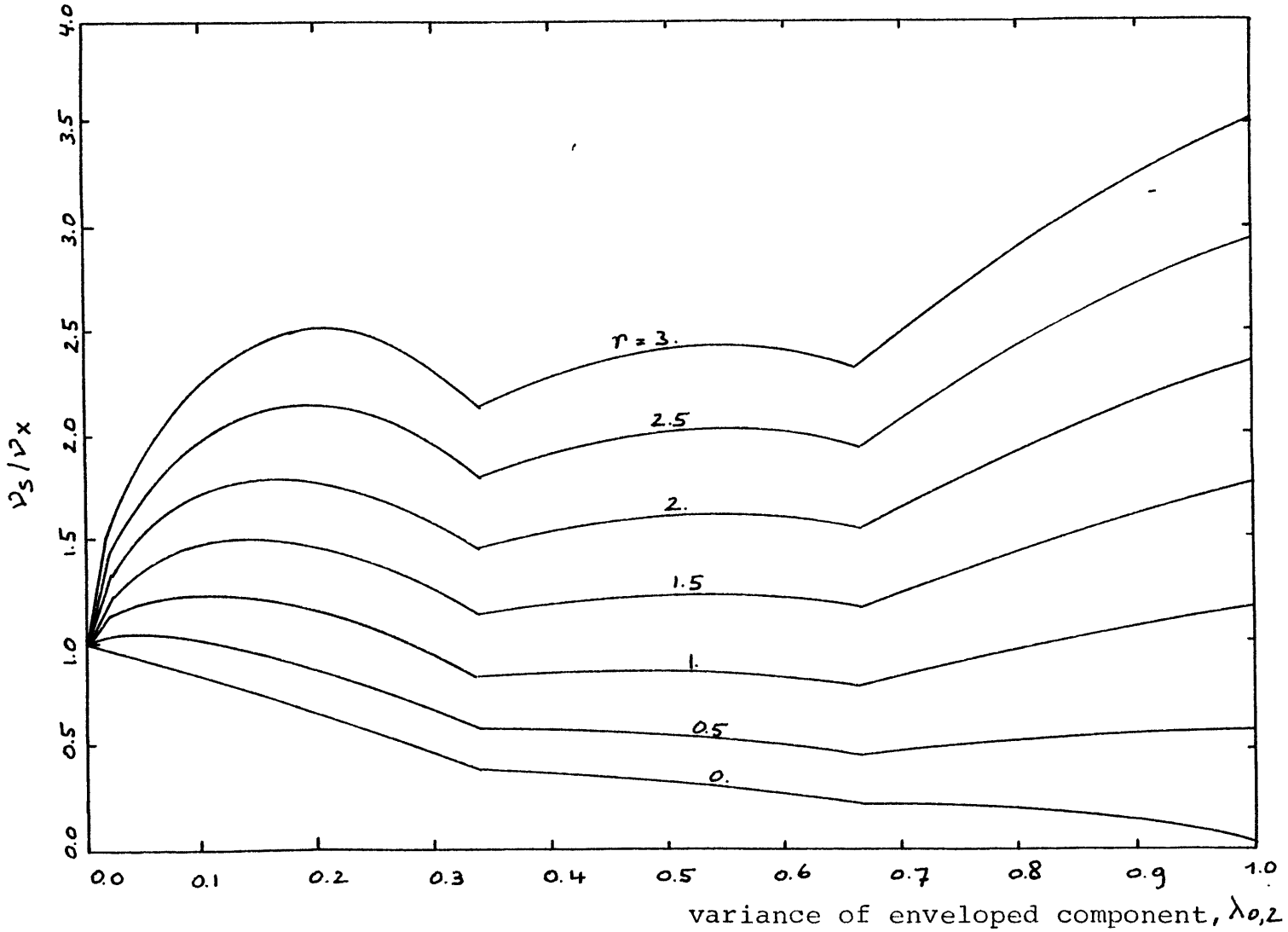

Fig. 30 - Ratio ν_s/ν_x for discrete spectrum, $\omega_2/\omega_1 = 2$, $\omega_3/\omega_2 = 2$

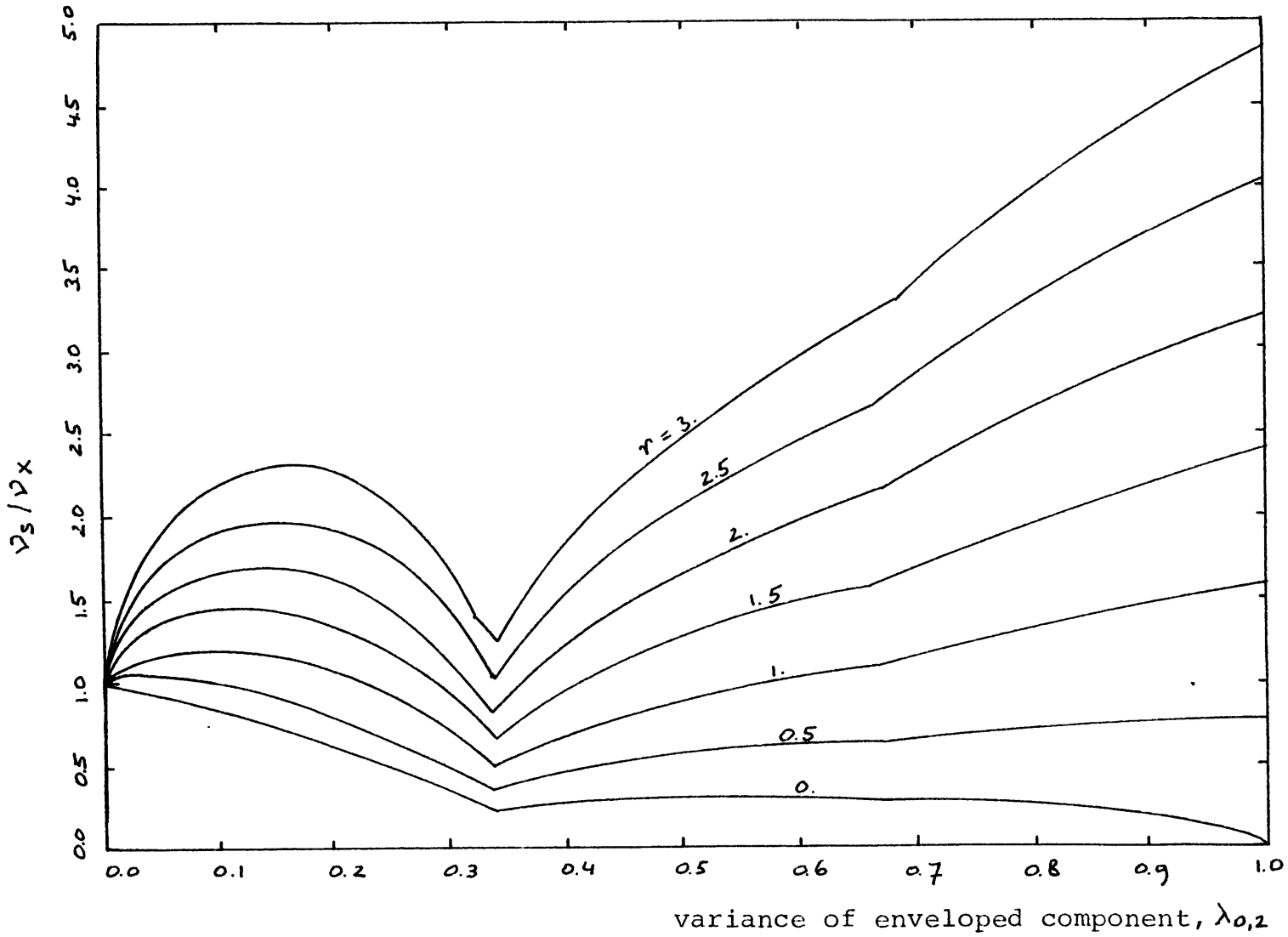

Fig. 31 - Ratio ν_s/ν_x for discrete spectrum, $\omega_2/\omega_1=2$, $\omega_3/\omega_2=4$

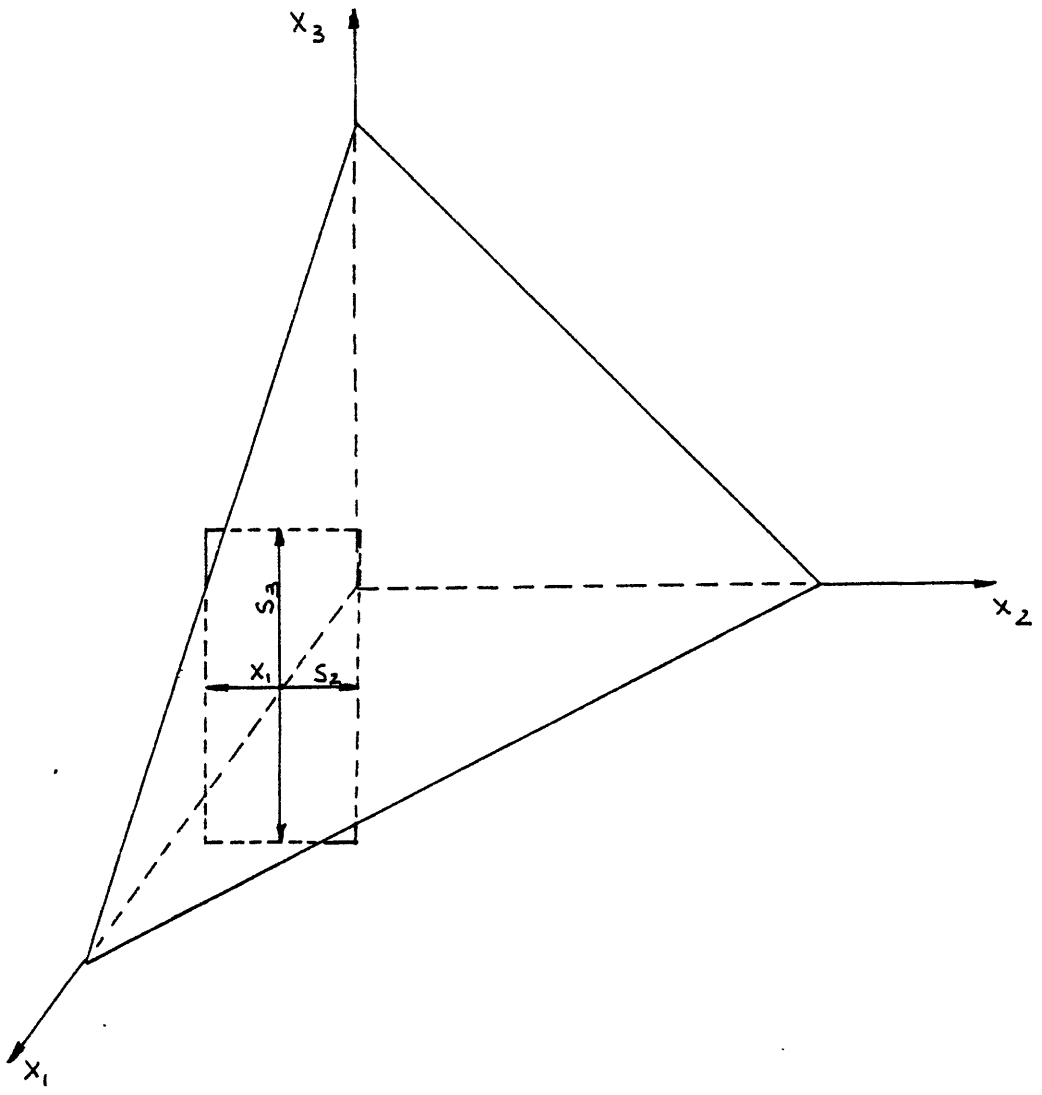

Fig. 32 - Decomposition of X(t) into three components and partial enveloping

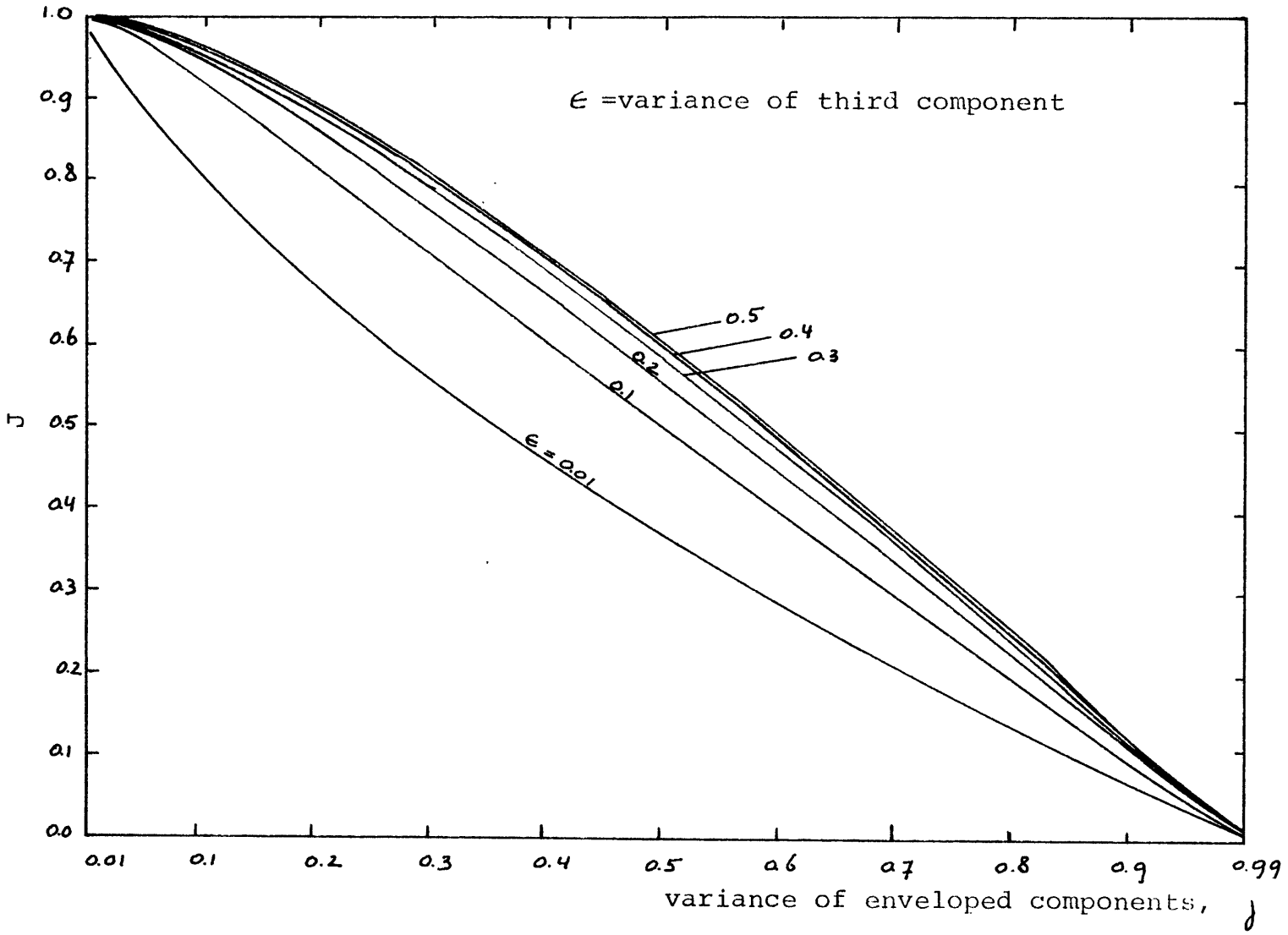

Fig. 33 - Factor J of Eq. 48 for level r=0.

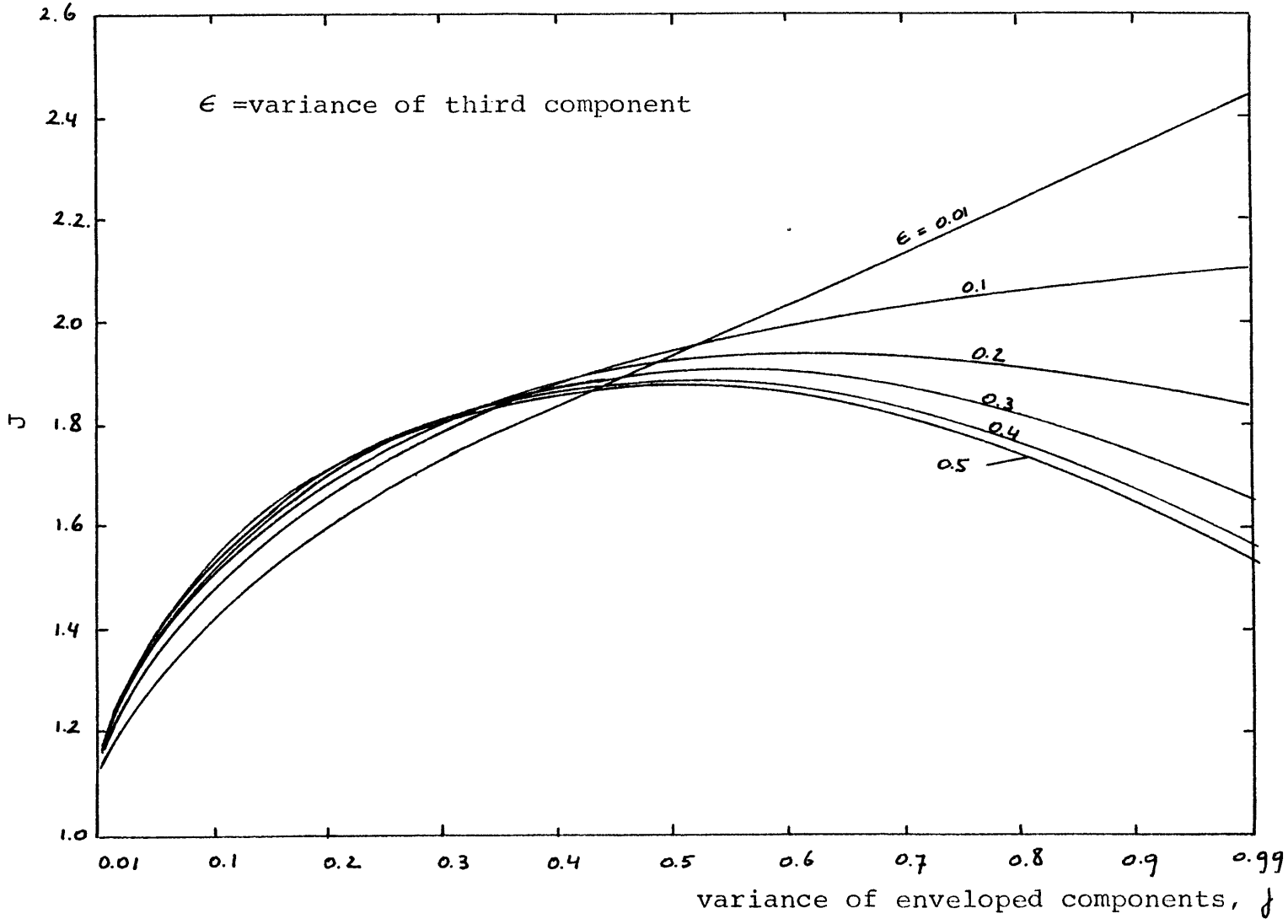

Fig. 34 - Factor J of Eq. 48 for level r=1.

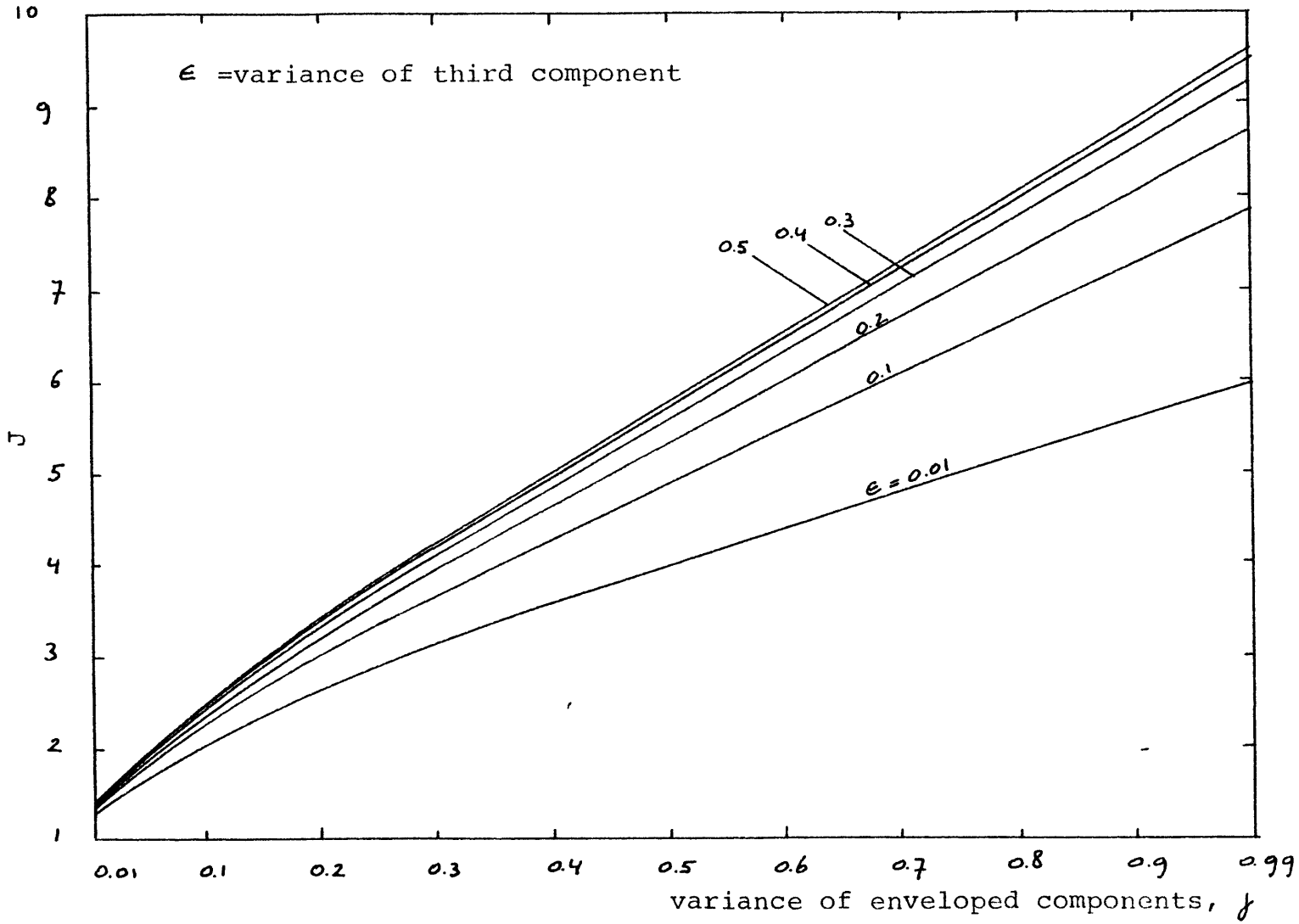

Fig. 35 - Factor J of Eq. 48 for level r=2.

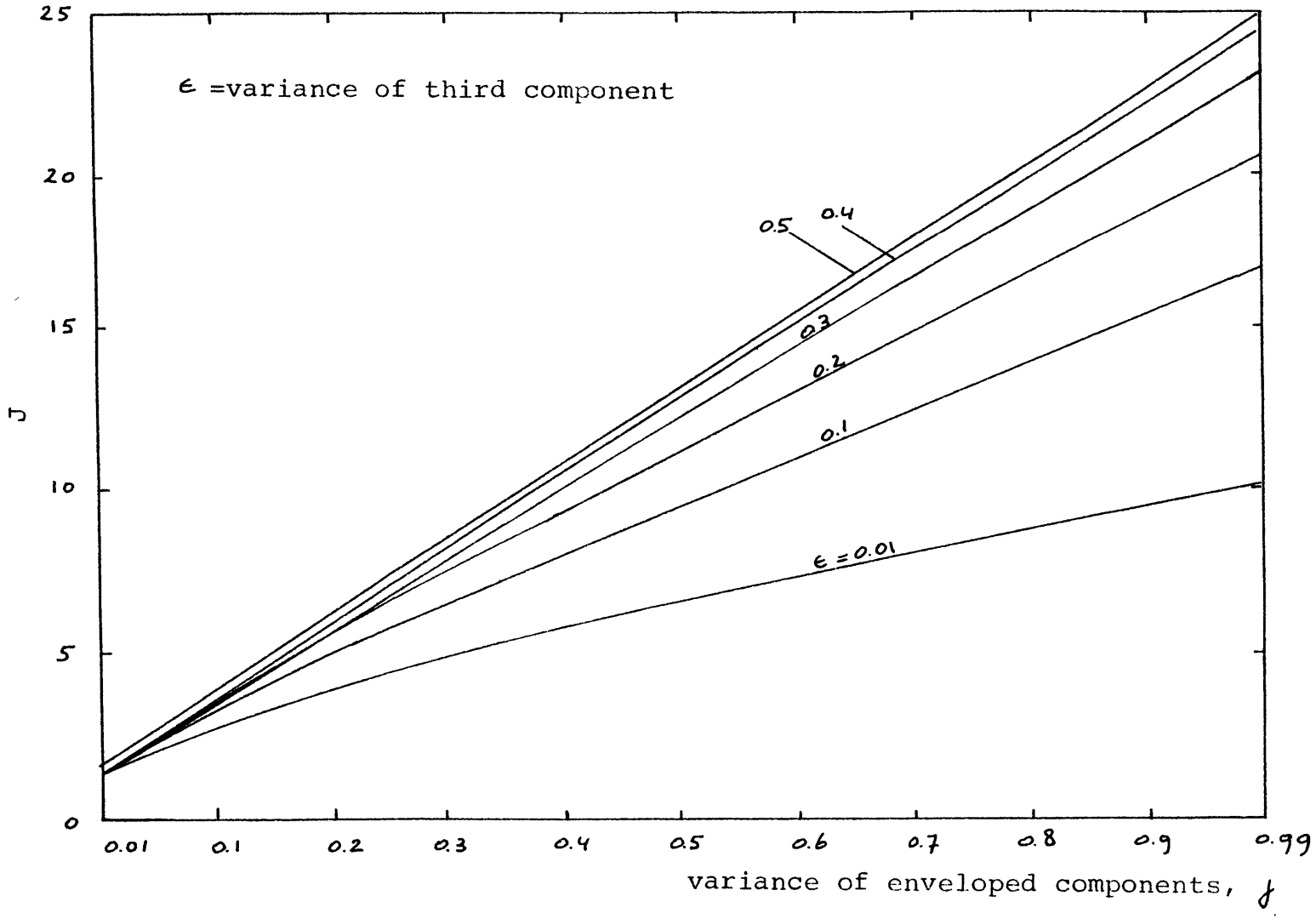

Fig. 36 - Factor J of Eq. 48 for level r=3.

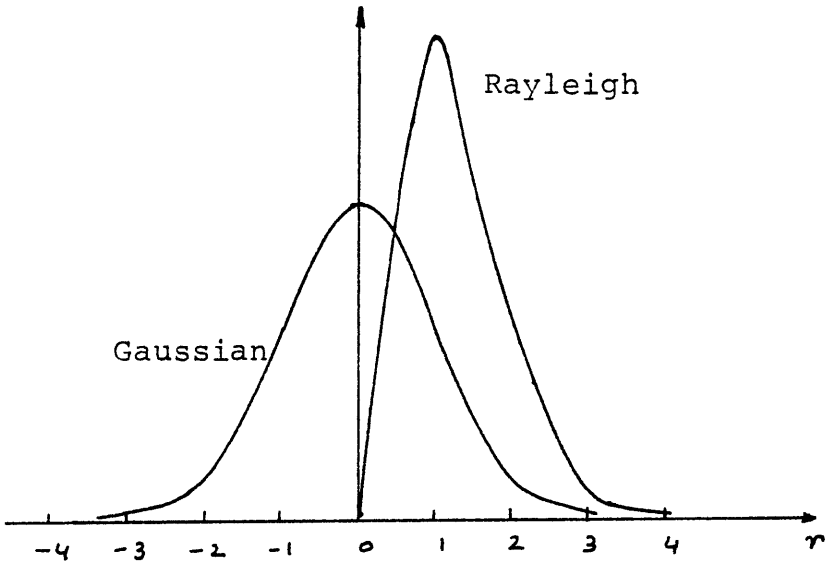

Fig. 37 - Normalised Gaussian and Rayleigh densities

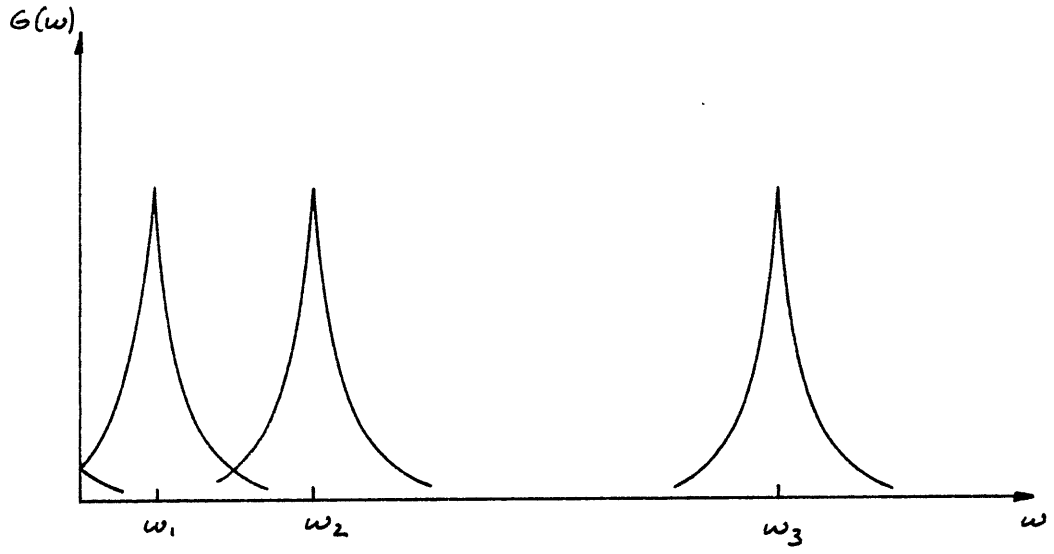

Fig. 38 - Spectral density composed of three exponential peaks

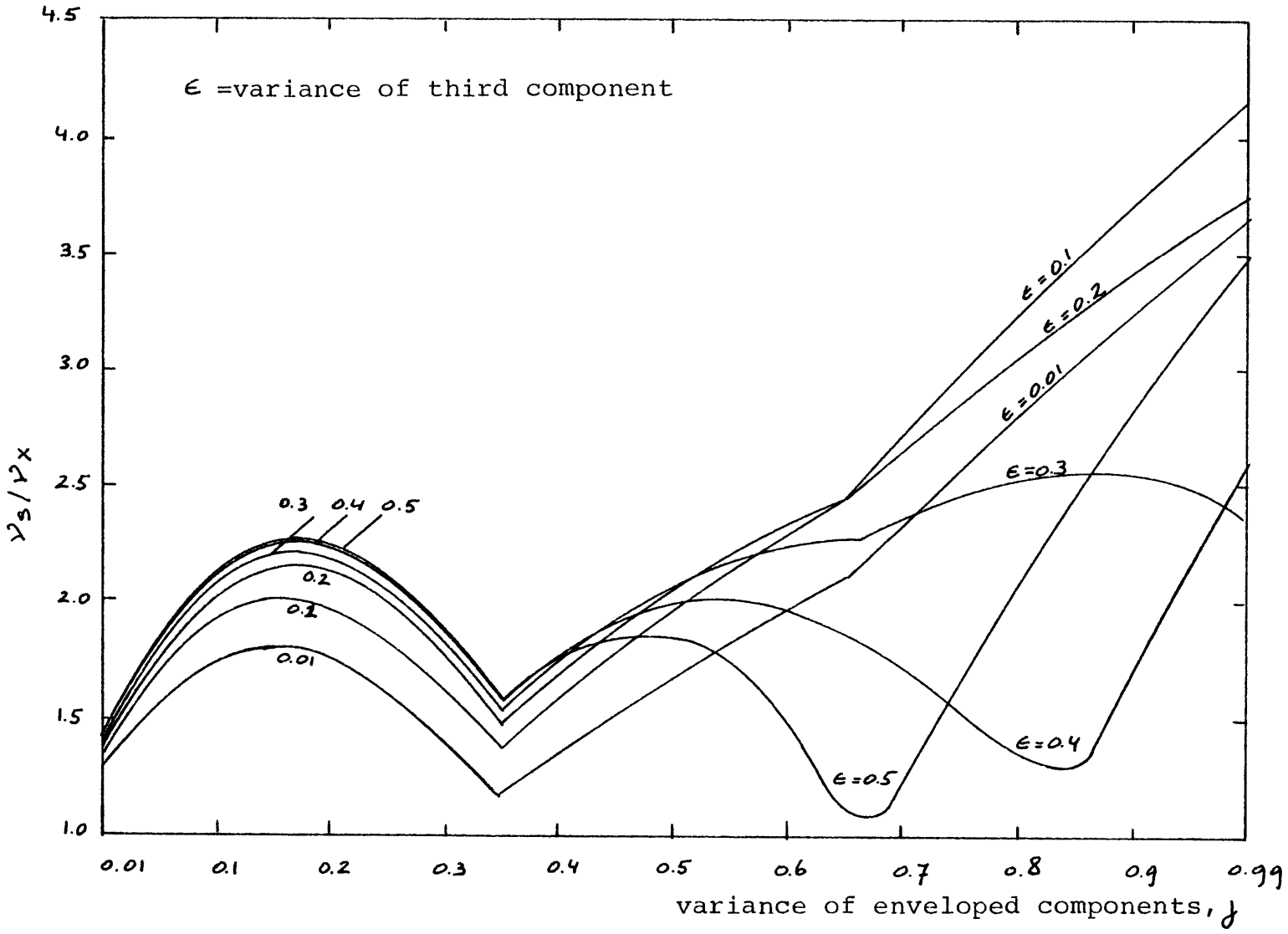

Fig. 39 - Ratio ν_s/ν_x for spectrum in Fig. 38 :

$\omega_1=1$, $\omega_2=3$, $\omega_3=9$; level r=2.

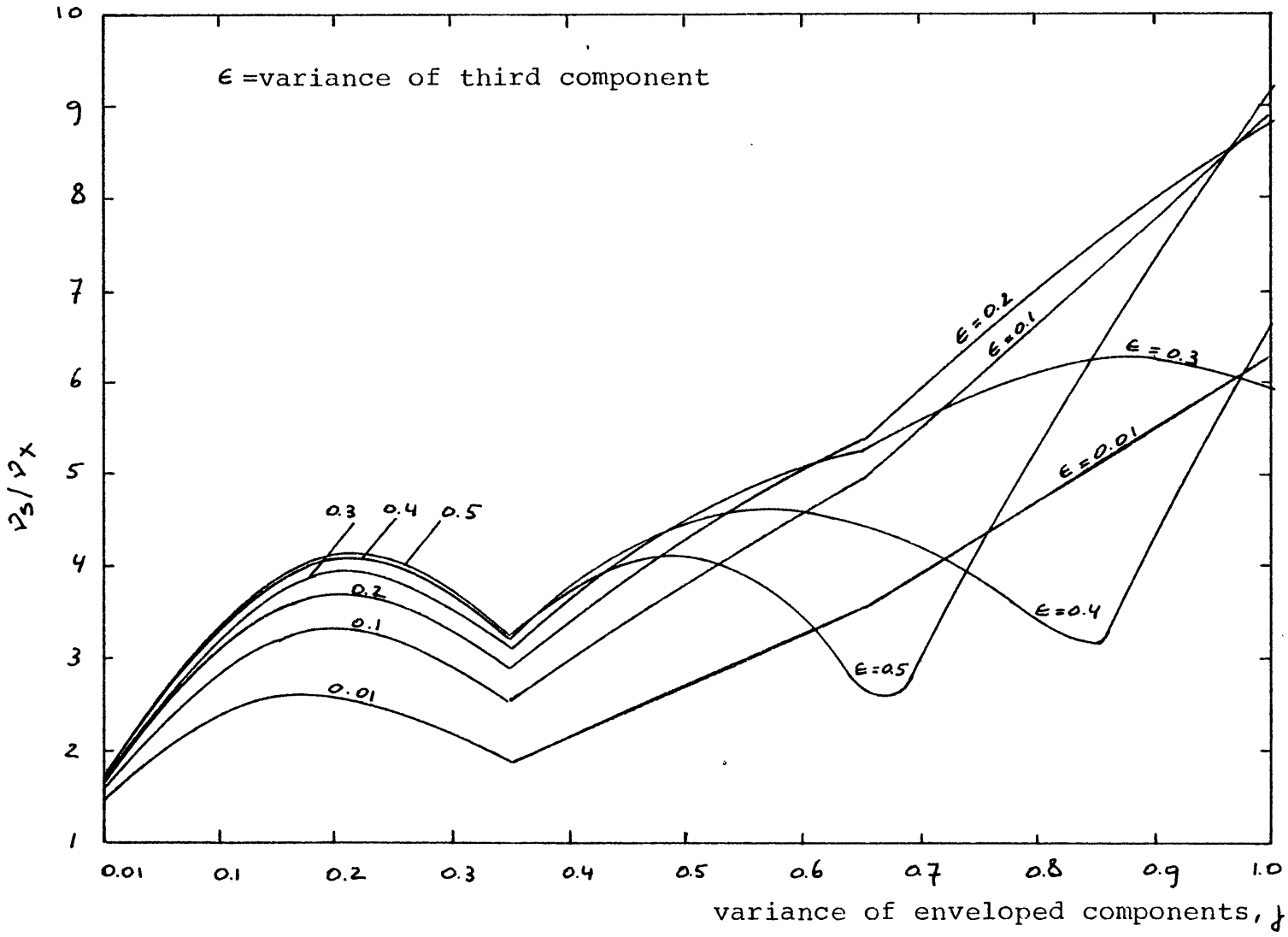

Fig. 40 - Ratio ν_s/ν_x for spectrum in Fig. 38 :

$\omega_1=1$, $\omega_2=3$, $\omega_3=9$; level r=3.

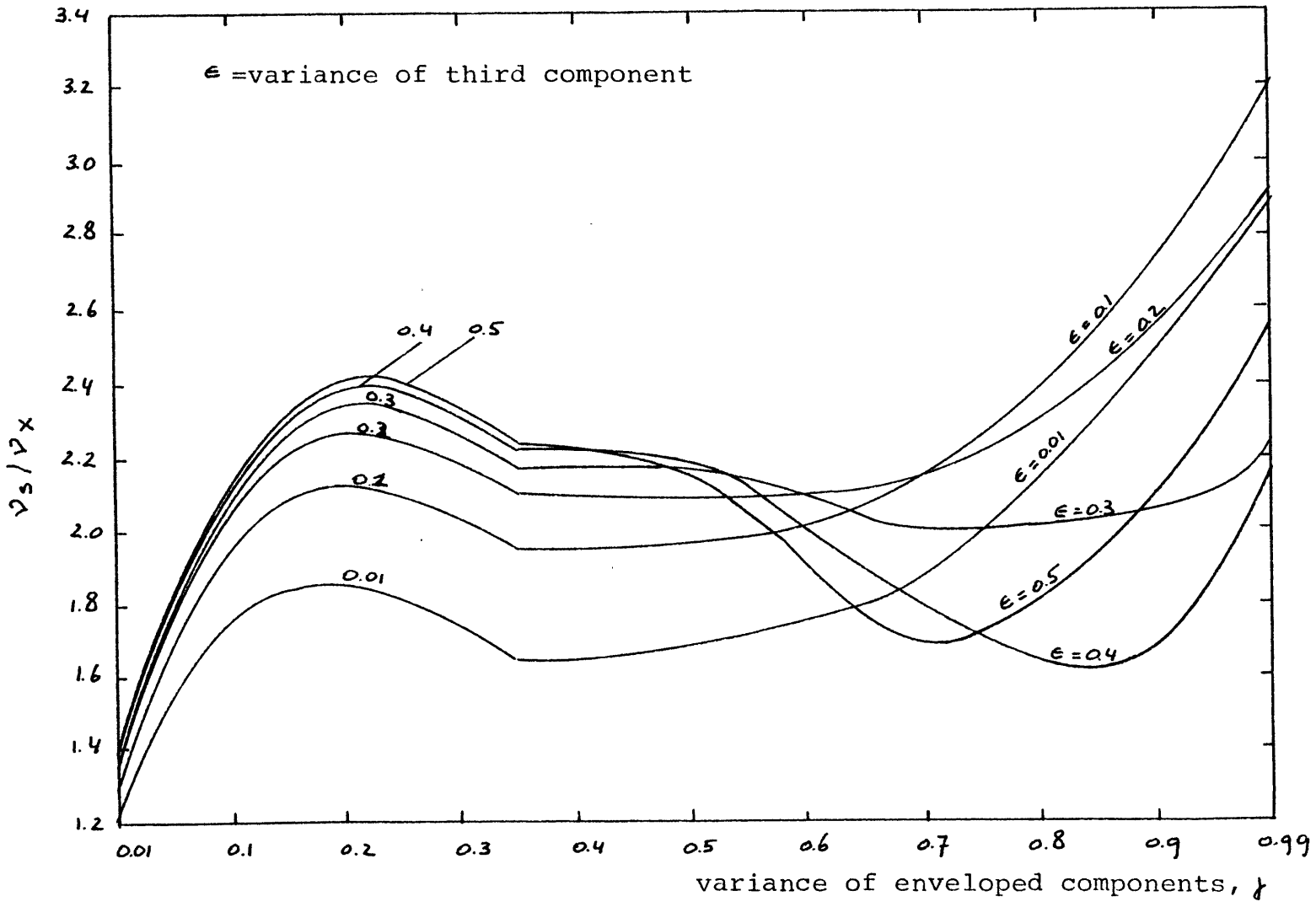

Fig. 41 - Ratio ν_s/ν_x for spectrum in Fig. 38 :

$\omega_1=1$, $\omega_2=2$, $\omega_3=4$; level r =2.

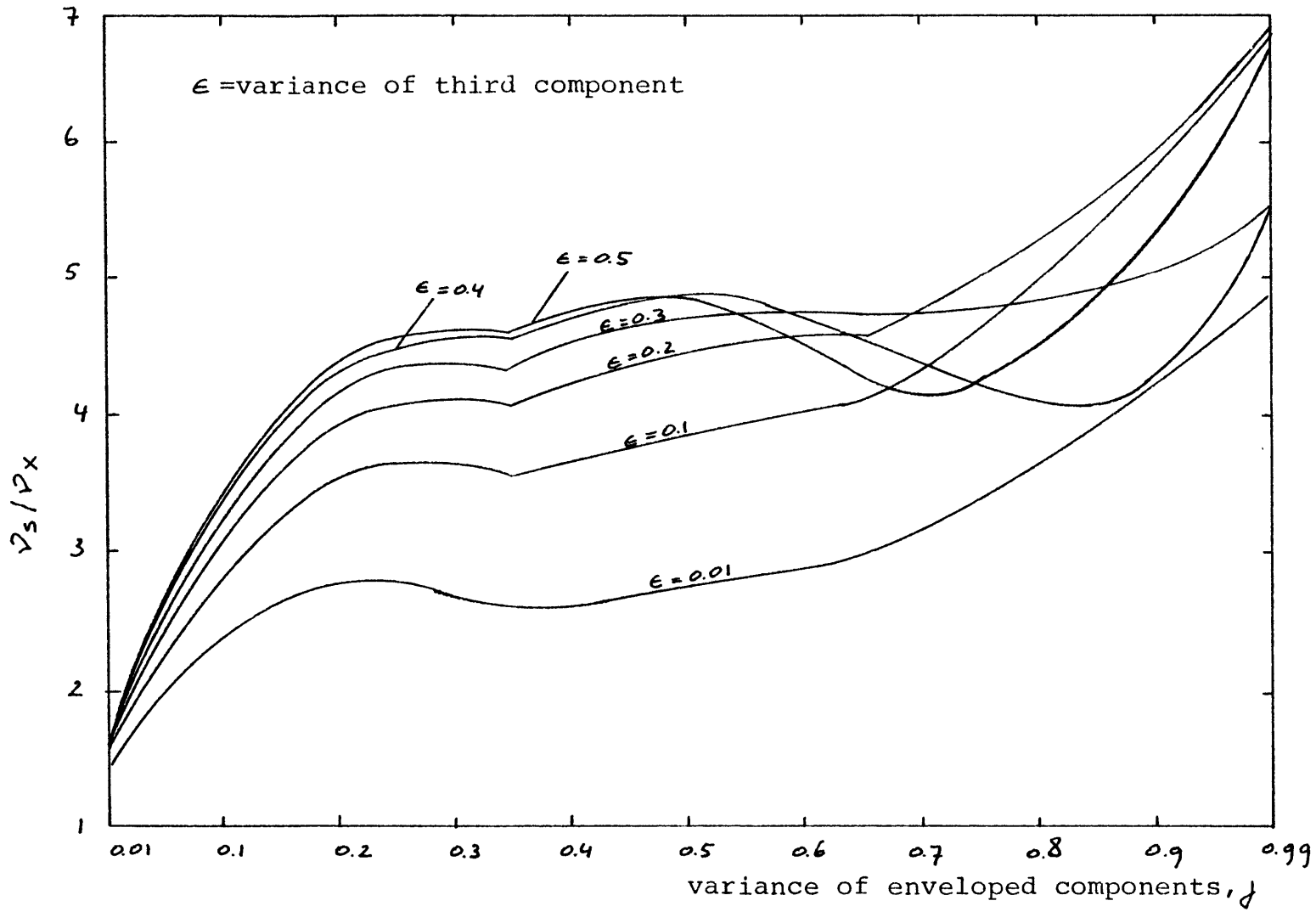

Fig. 42 - Ratio ν_3/ν_x for spectrum in Fig. 38 :

$\omega_1=1$, $\omega_2=2$, $\omega_3=4$; level r=3.

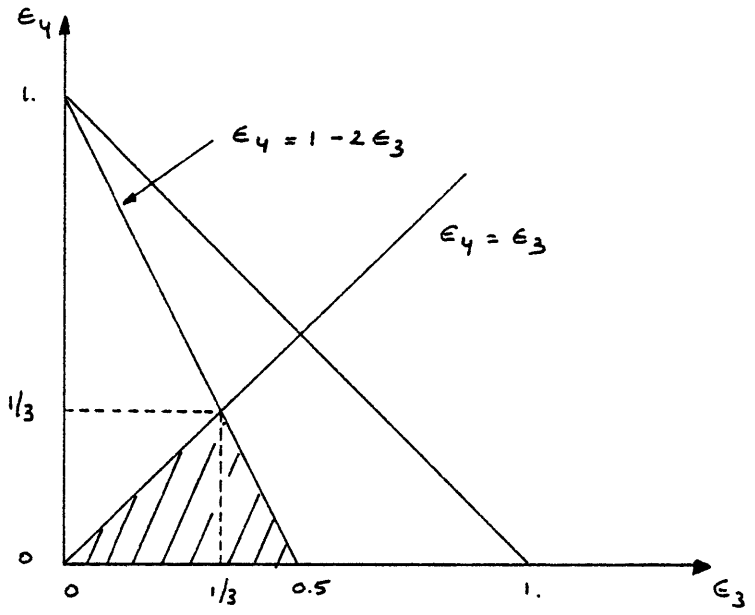

Fig. 43 - Symmetry lines in the (ϵ_3, ϵ_4)-plane for the calculation of J

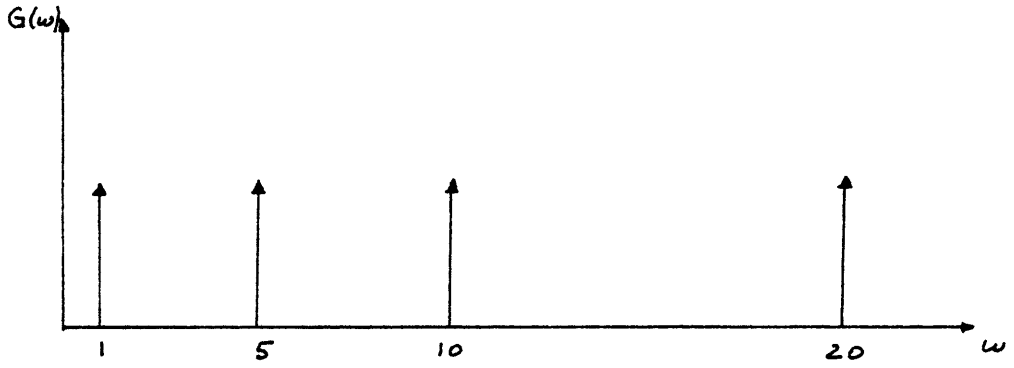

$$G(\omega) = \frac{1}{4}\left[\delta(\omega-1) + \delta(\omega-5) + \delta(\omega-10) + \delta(\omega-20)\right]$$

Fig. 44 - Discrete spectral density

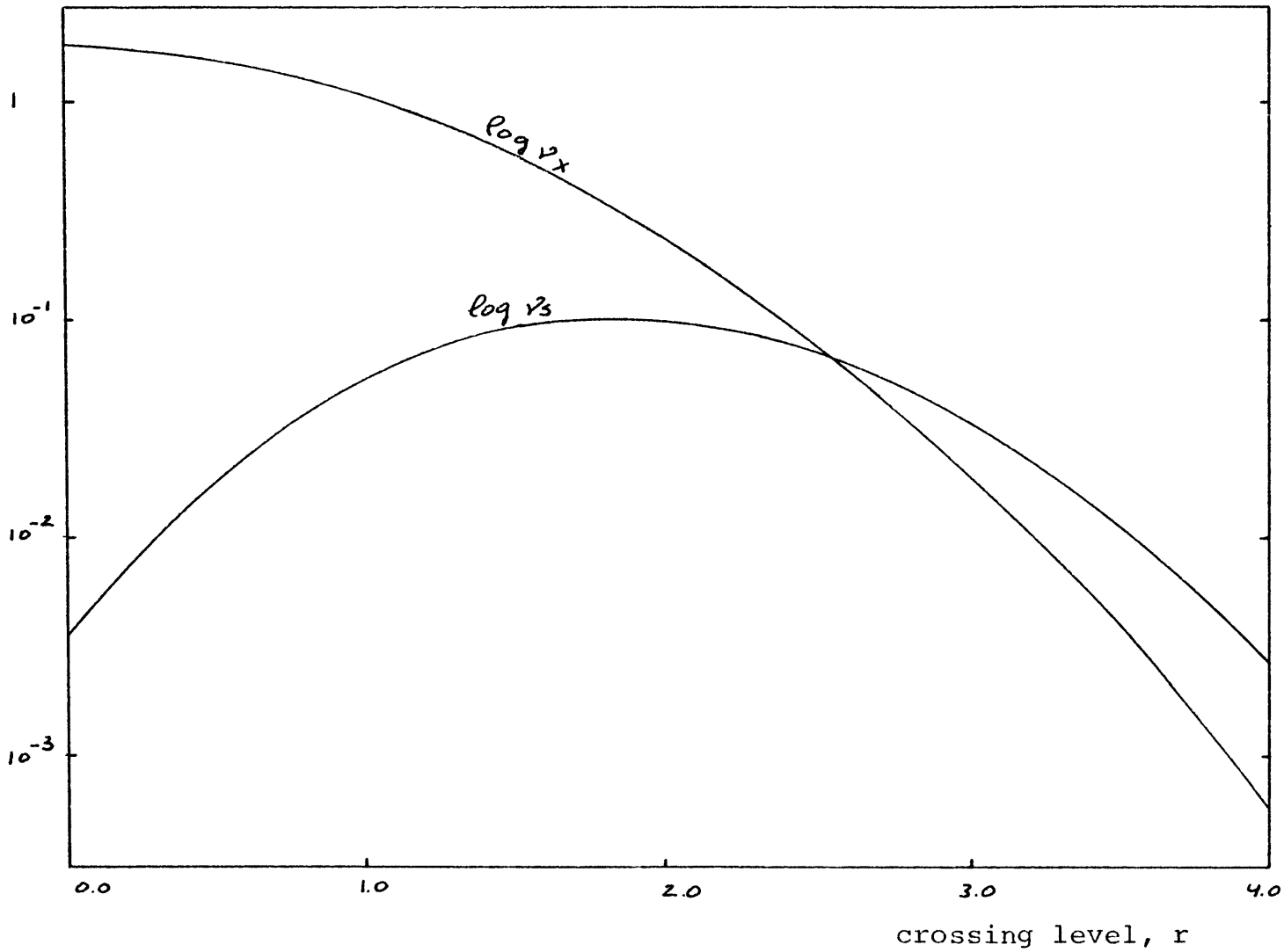

Fig. 45 - Crossing rates of the process X(t) and the envelope S(t) as a function of r

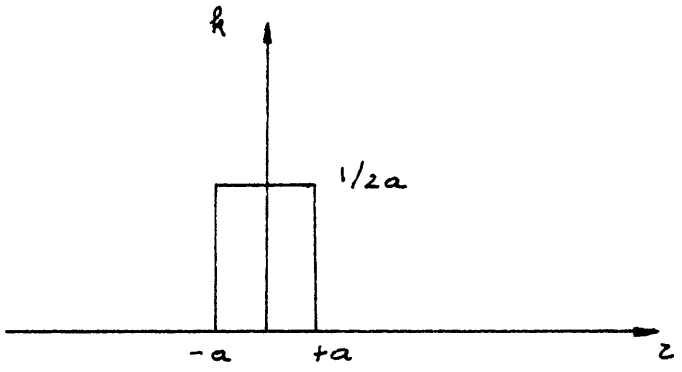

Fig. 46 - Example of a kernelfunction

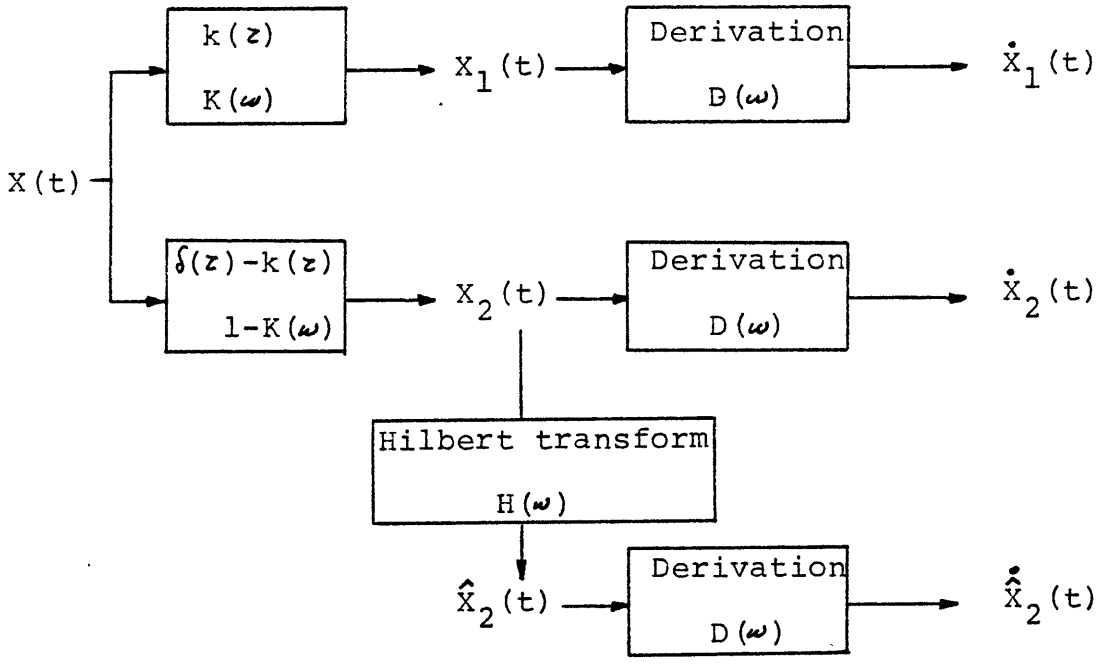

Fig. 47 - Sheme of linear, time-invariant transformations

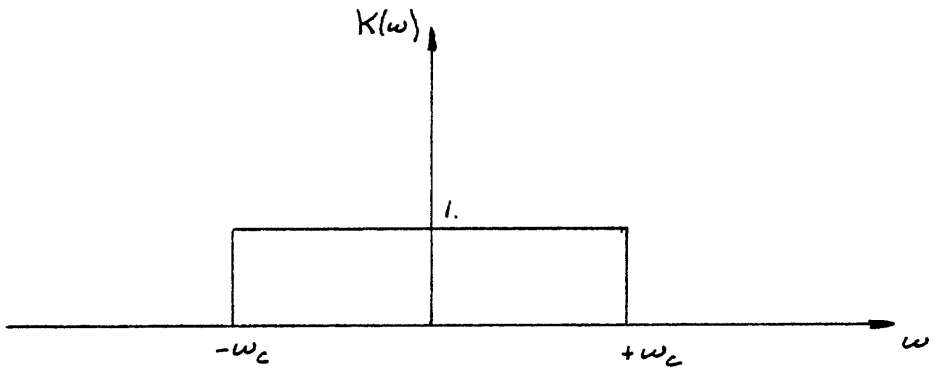

Fig. 48 - Low frequency filter

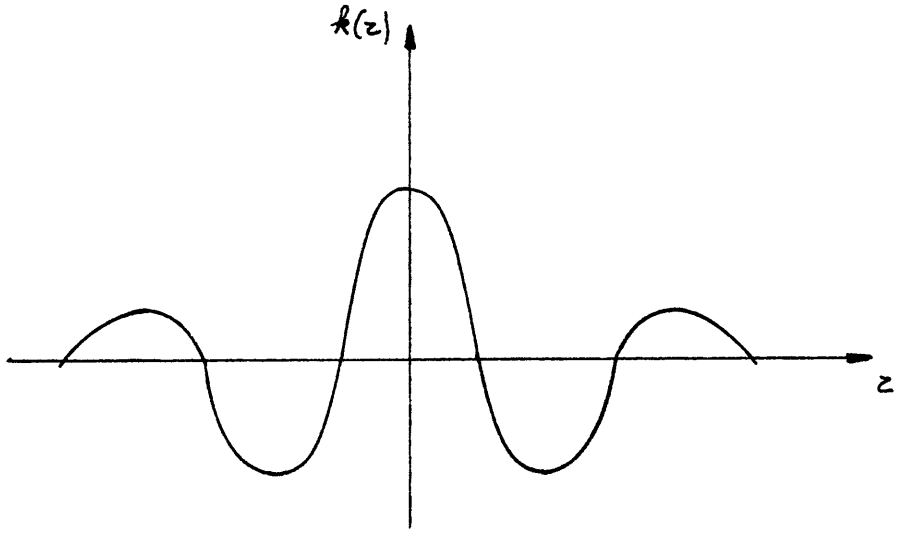

Fig. 49 - Kernelfunction associated with low frequency filter

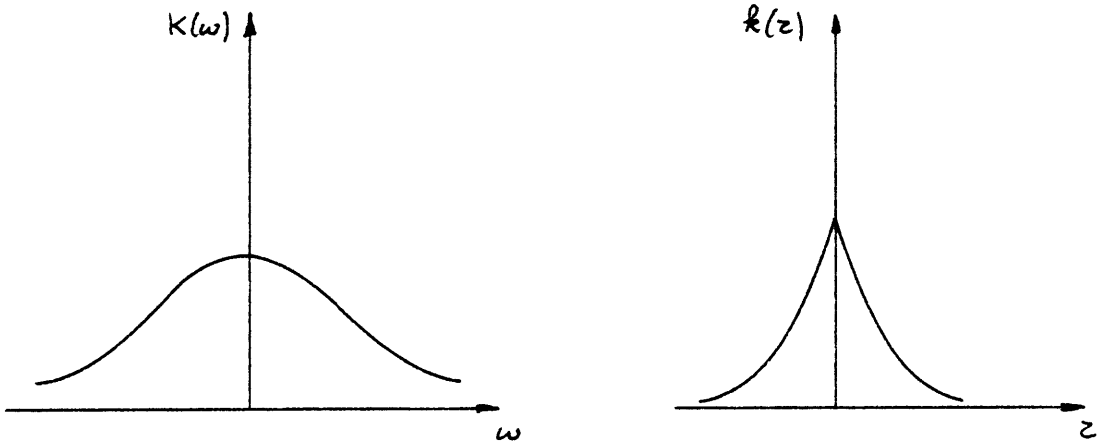

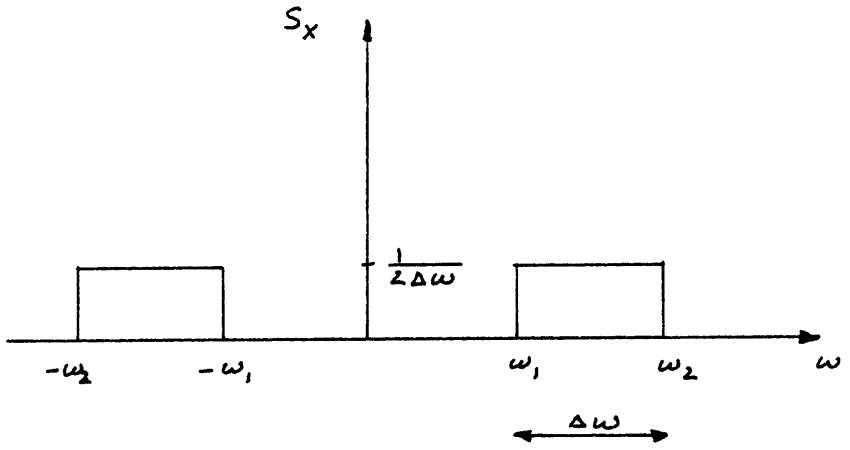

Fig. 50 - Case of exponential kernelfunction and rectangular spectral density

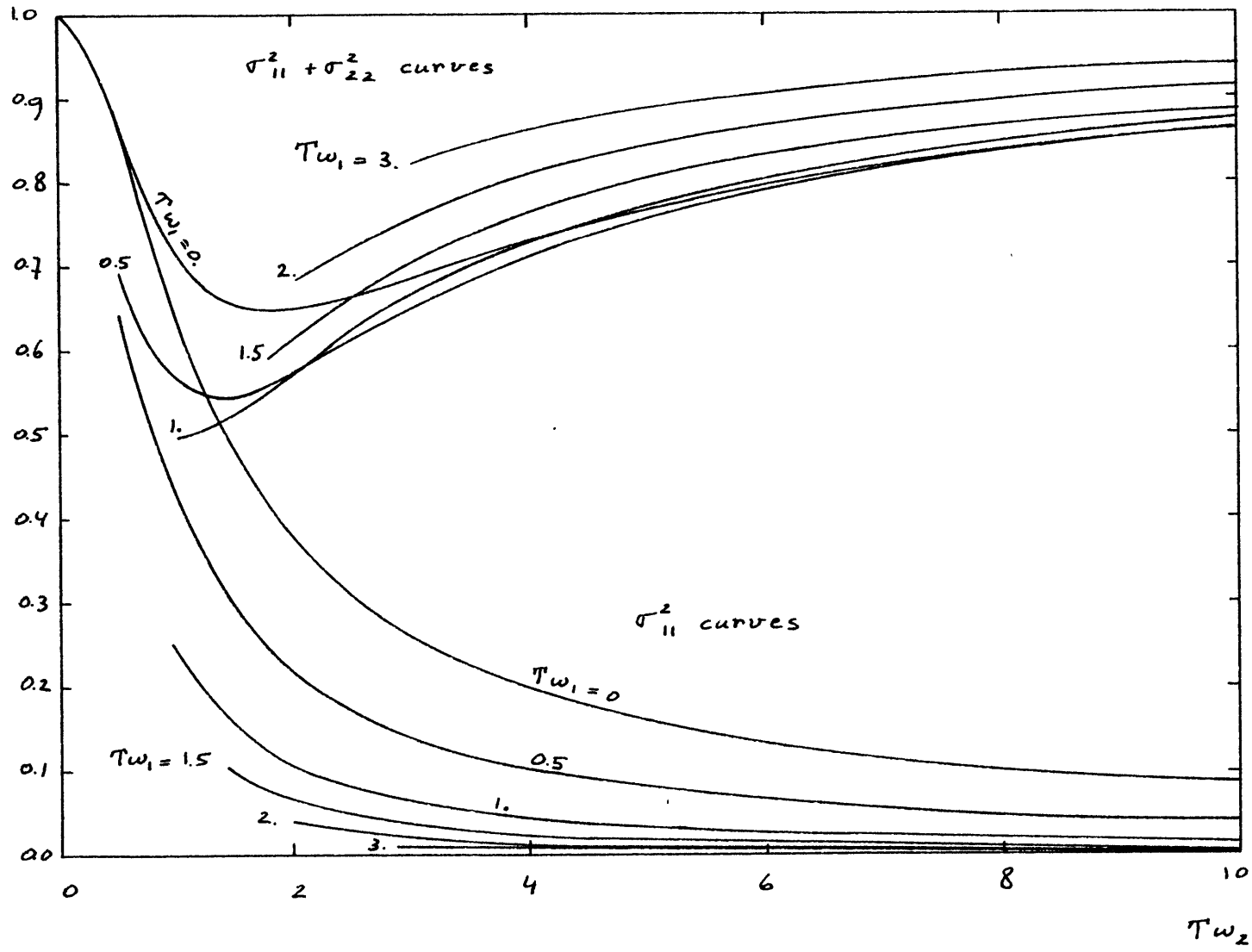

Fig. 51 - Variance of the time average process X_1 and sum of the variances of X_1 and X_2

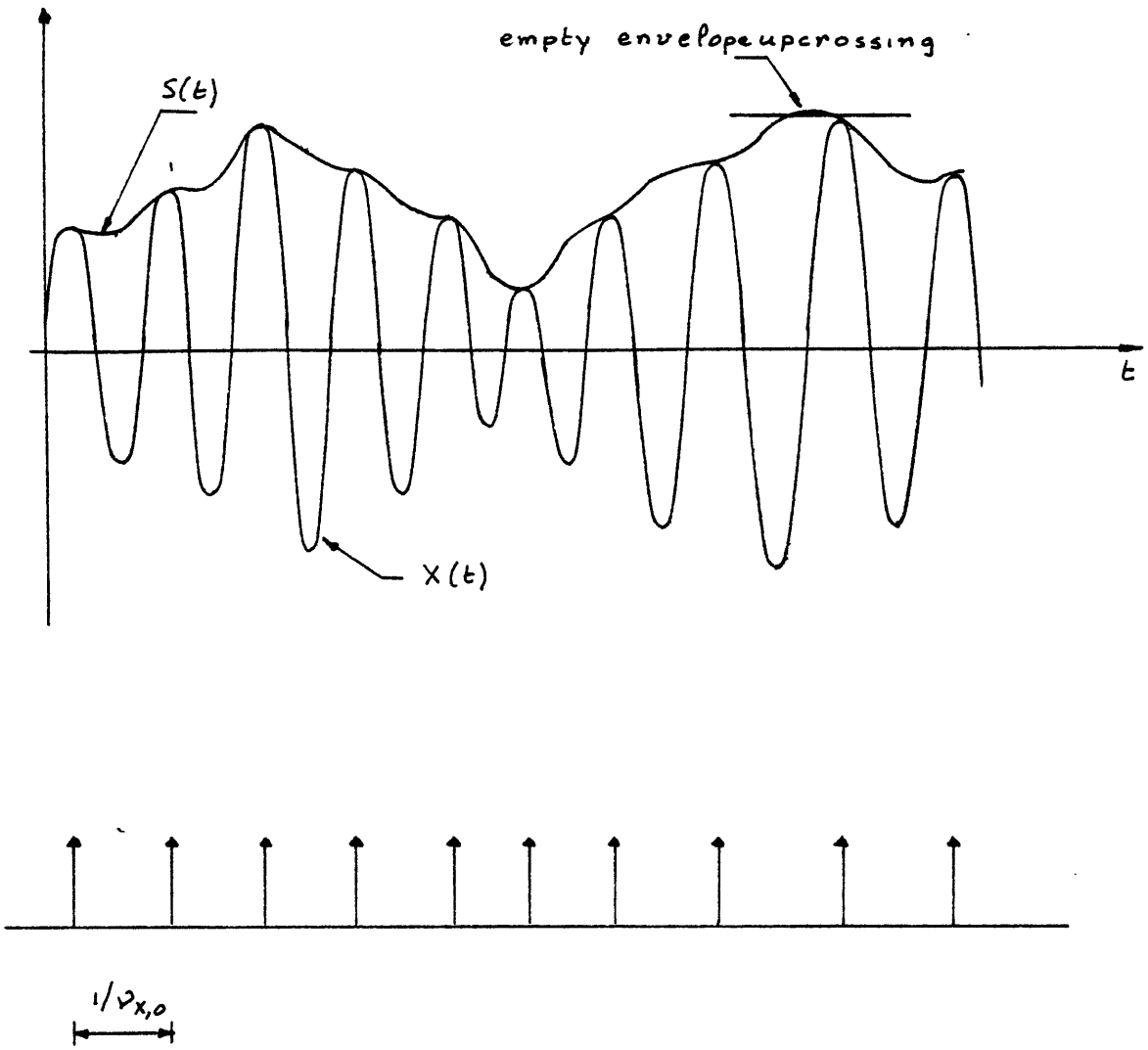

Fig. 52 - Narrow-band process X(t) and associated envelope S(t)

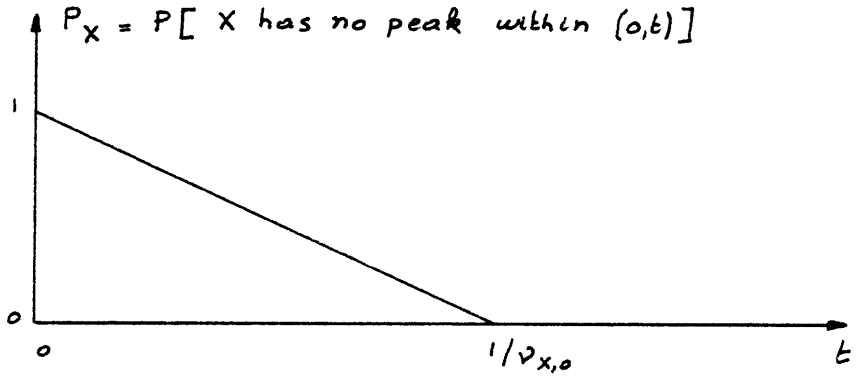

Fig. 53 - $P_X(t)$

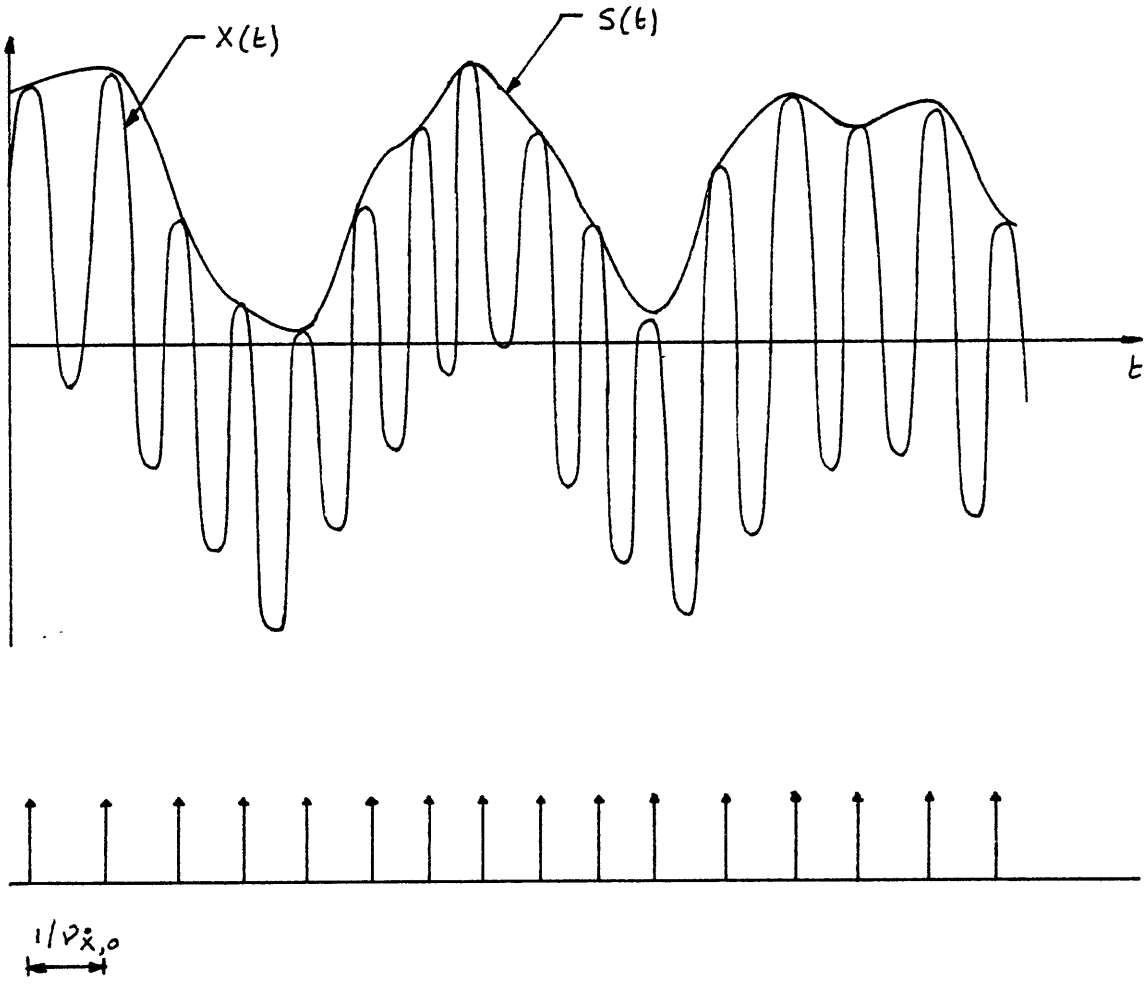

Fig. 54 - Broad-band process X(t) and associated envelope S(t)

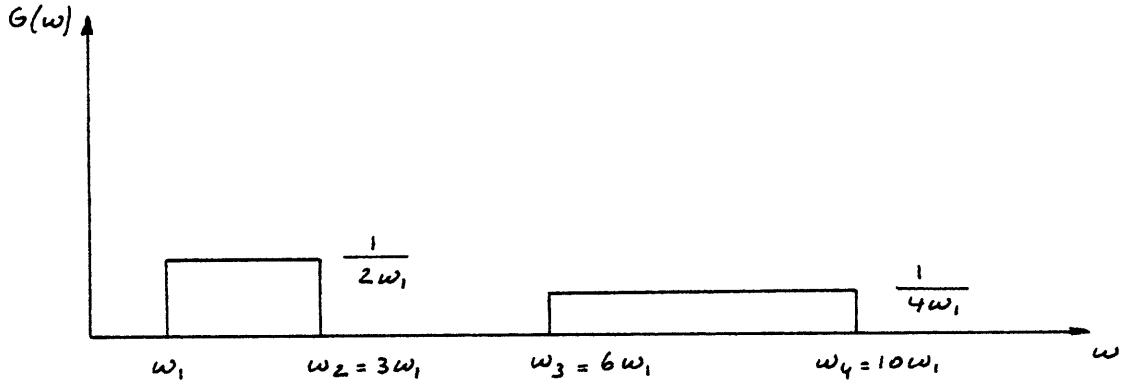

Fig. 55 - Spectrum composed of two rectangular blocks

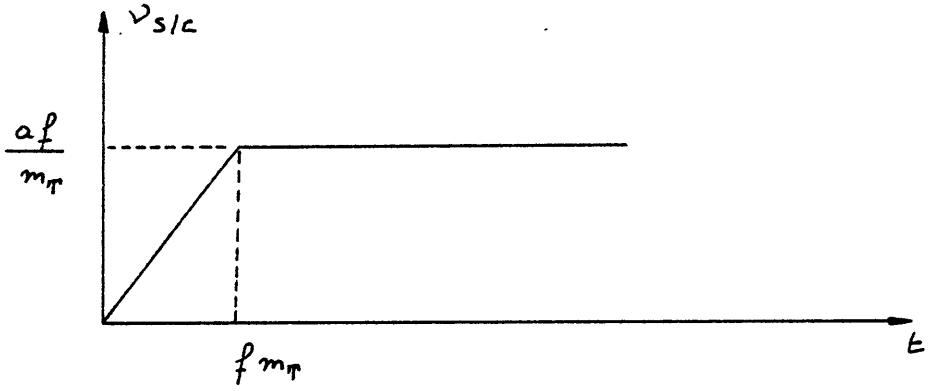

Fig. 56 - Conditional down crossing rate of the envelope during excursion

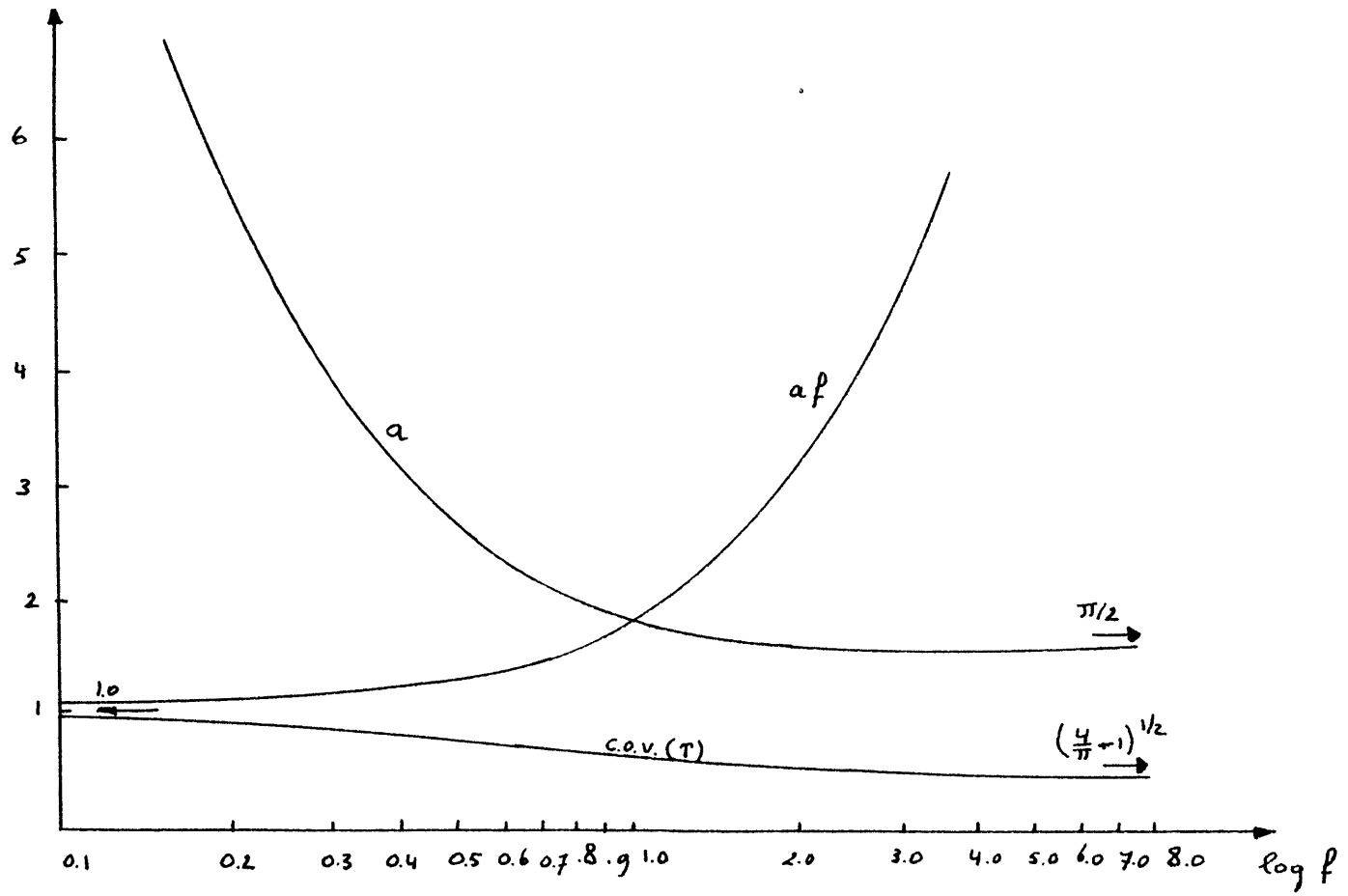

Fig. 57 - Parameters a, af and the coefficient of variation of T (the excursion length of the envelope) as a function of log f

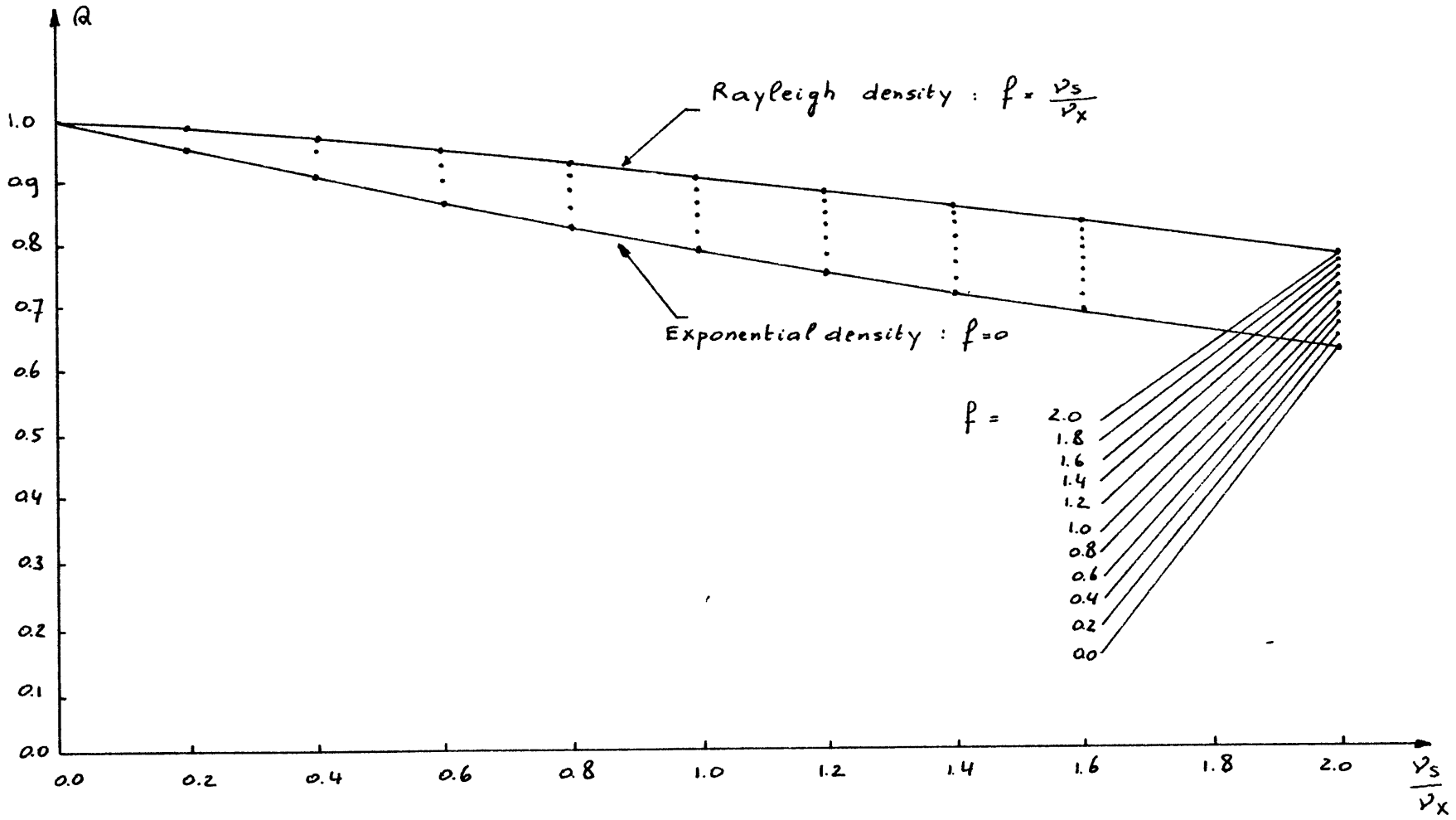

Fig. 58 - Ratio Q for different assumptions about the density function of the excursion length as a function of ν_s/ν_x

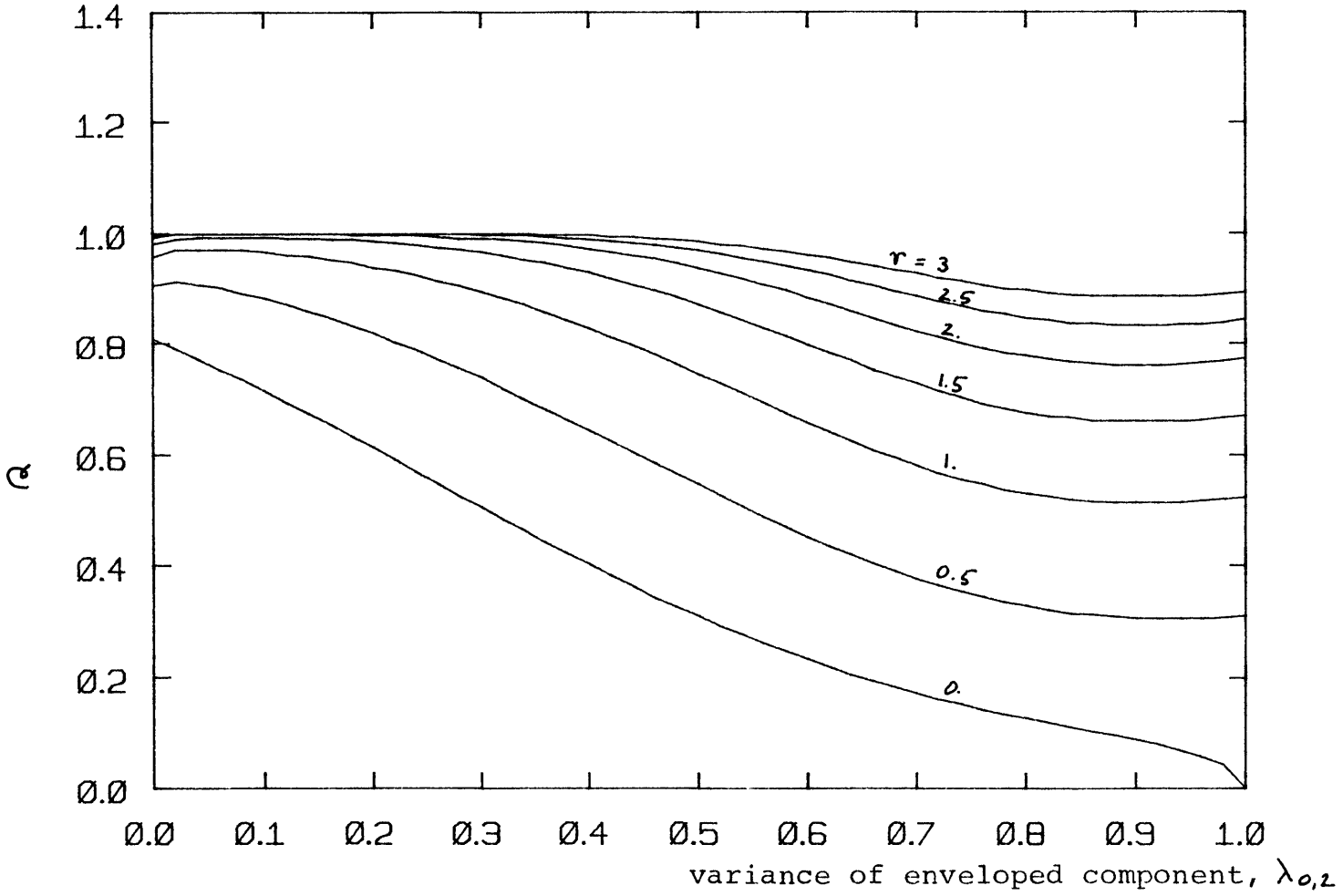

Fig. 59 - Ratio Q (model A) for rectangular spectrum, $\omega_2/\omega_1=5$

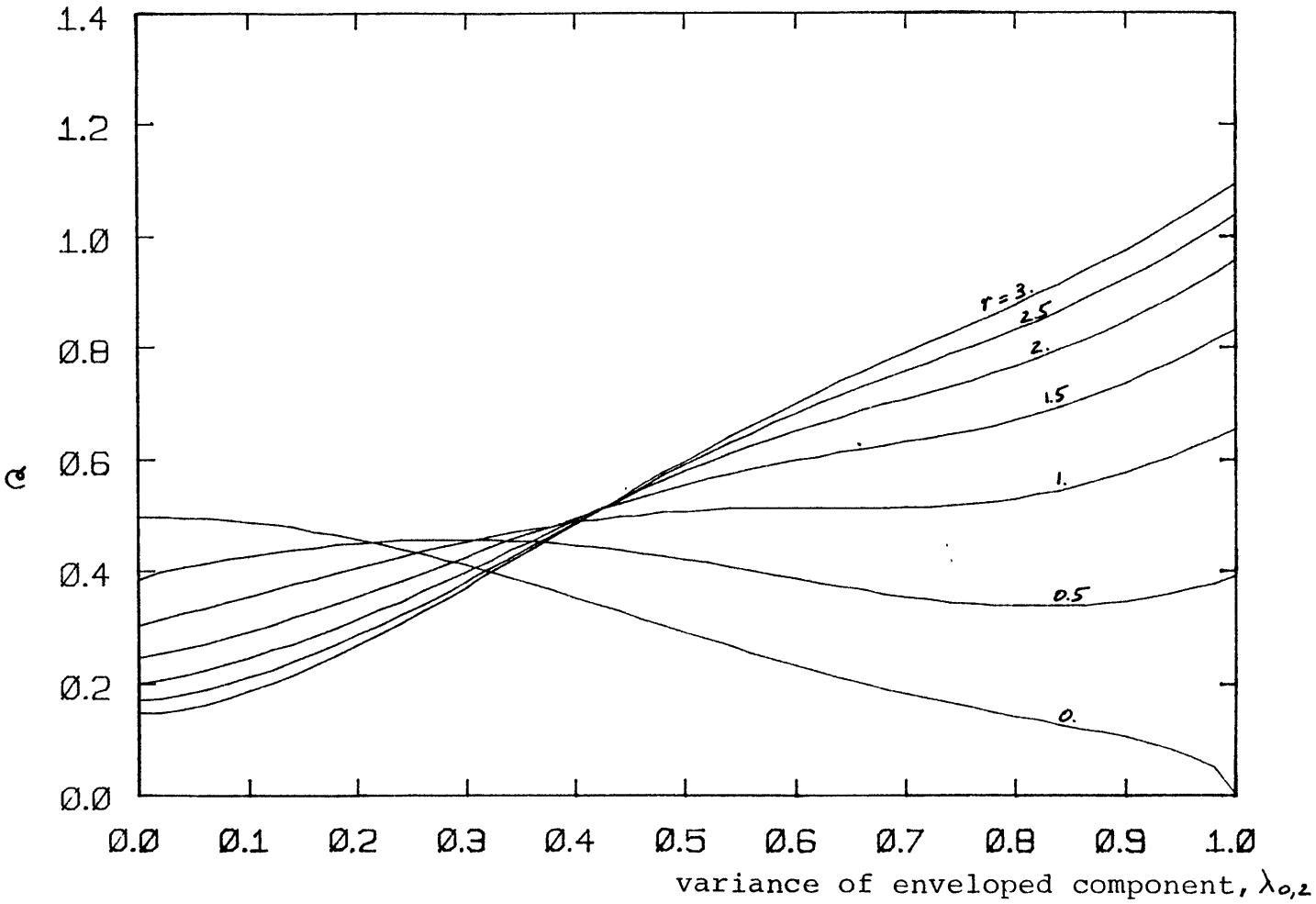

Fig. 60 - Ratio Q (model B, f=0.1) for rectangular spectrum, $\omega_2/\omega_1 = 5$

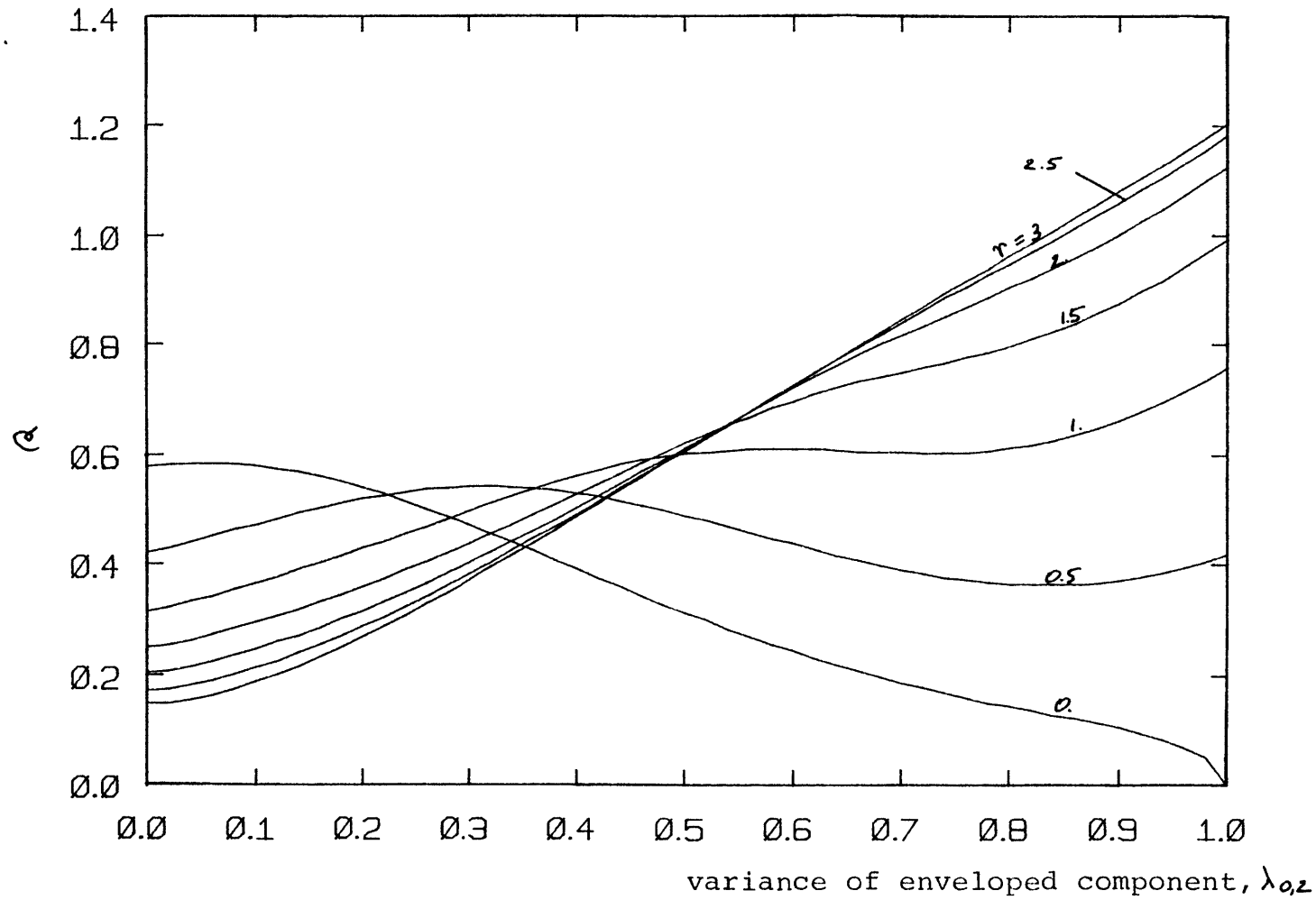

Fig. 61 - Ratio Q (model B, f=10.) for a rectangular spectrum, $\omega_2/\omega_1=5$

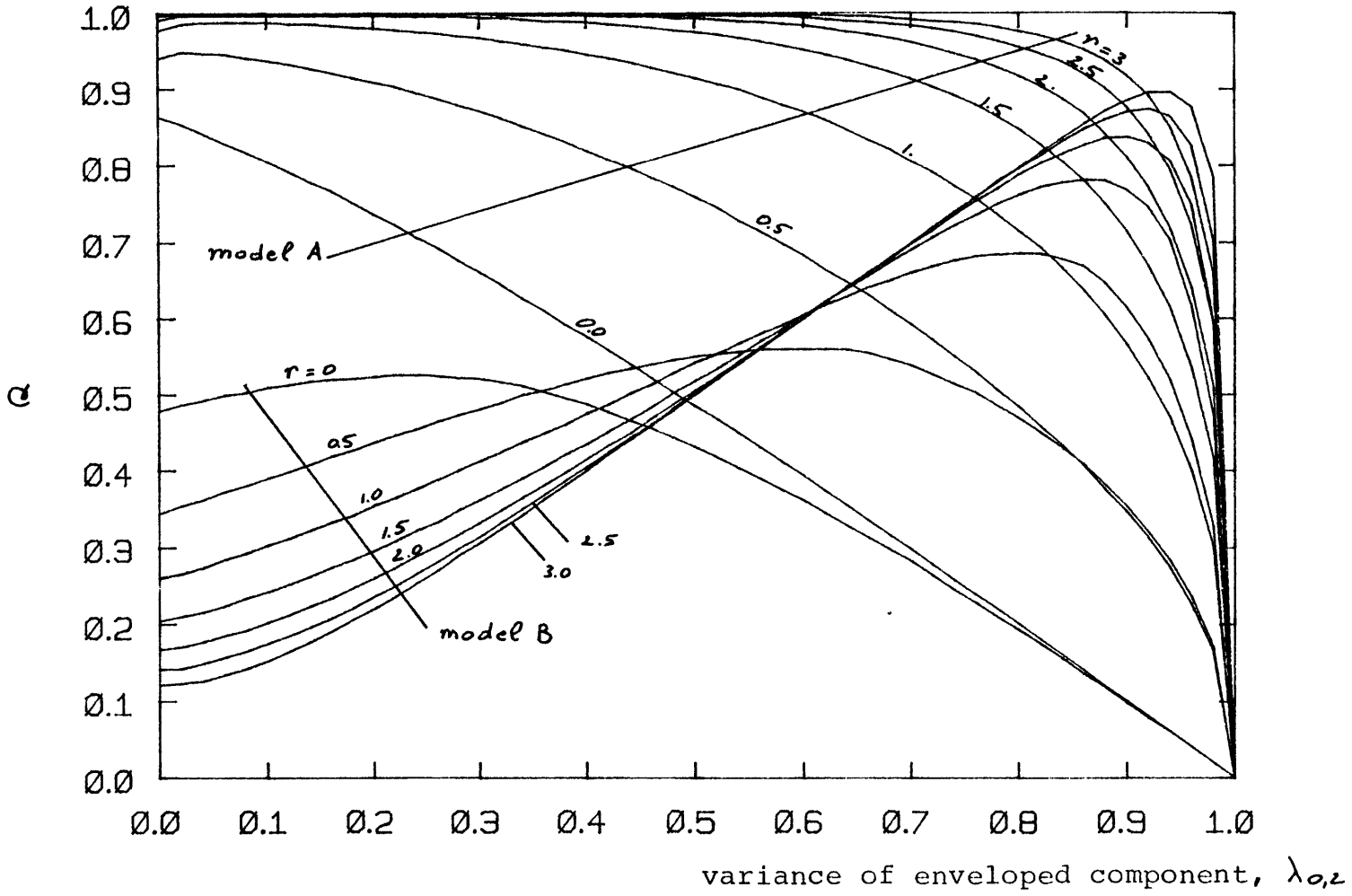

Fig. 62 - Ratio Q for rectangular spectrum, $\omega_2/\omega_1 = 1$

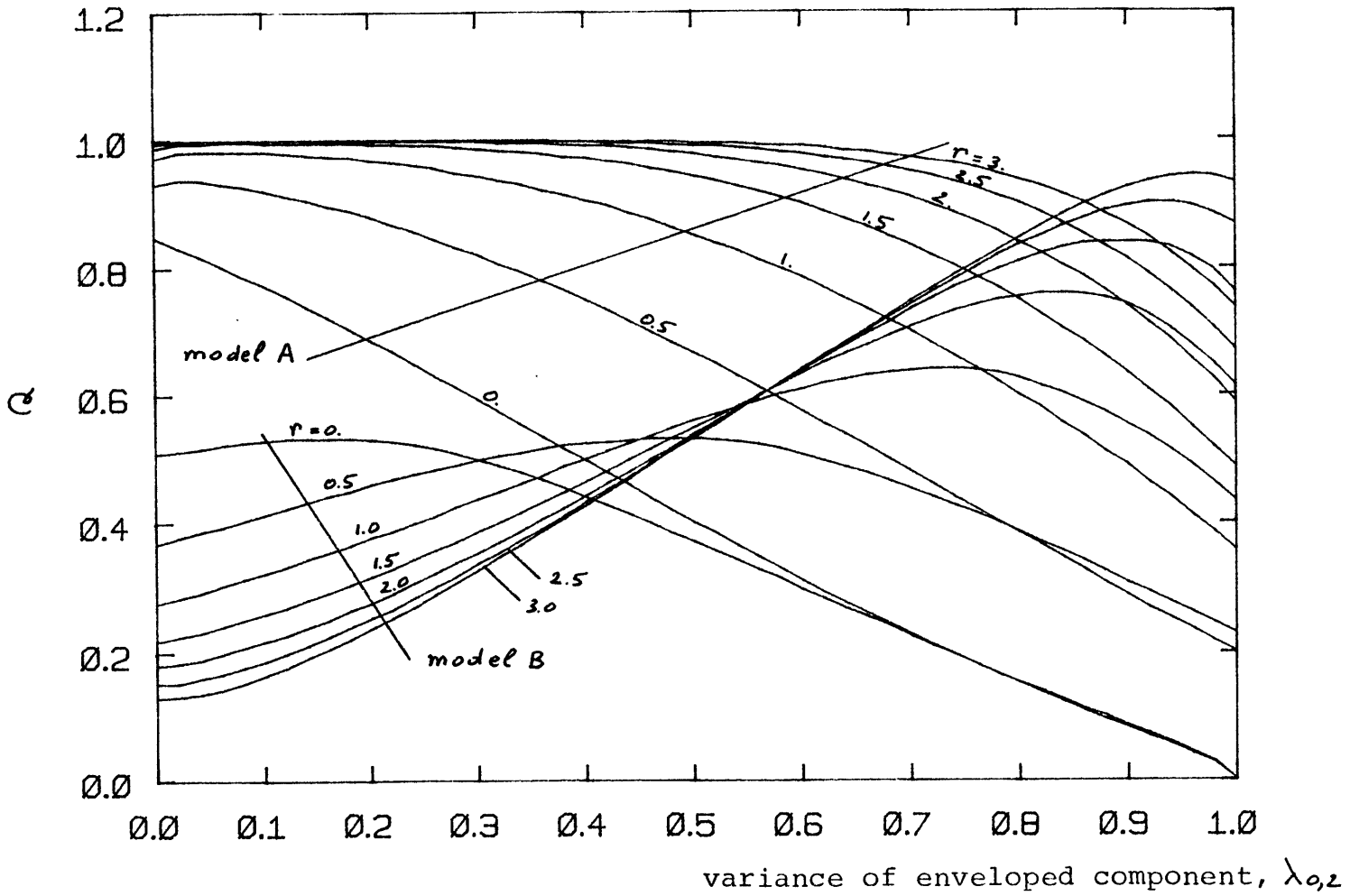

Fig. 63 - Ratio Q for rectangular spectrum, $\omega_2/\omega_1 = 2$

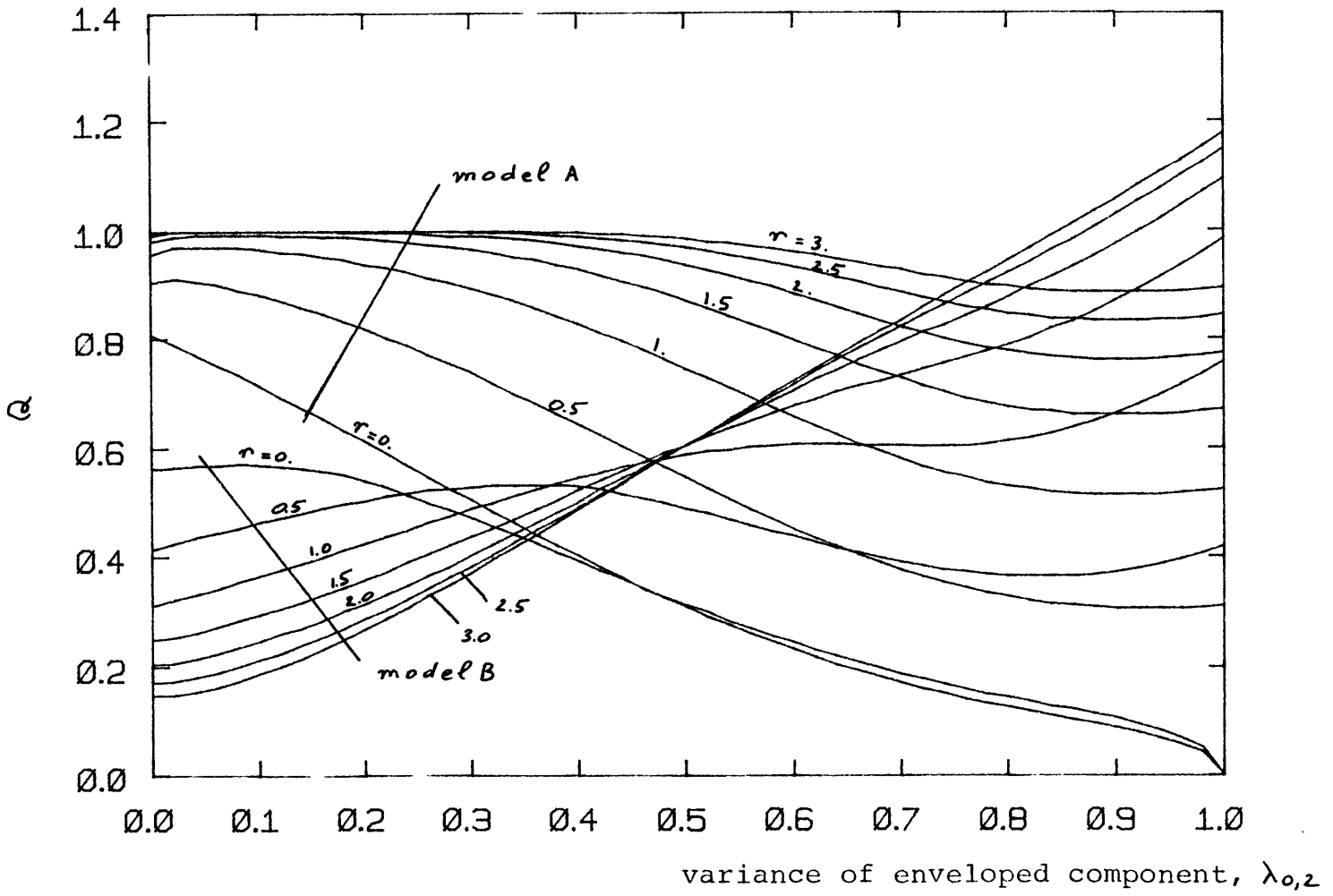

Fig. 64 - Ratio Q for rectangular spectrum, $\omega_2/\omega_1 = 5$

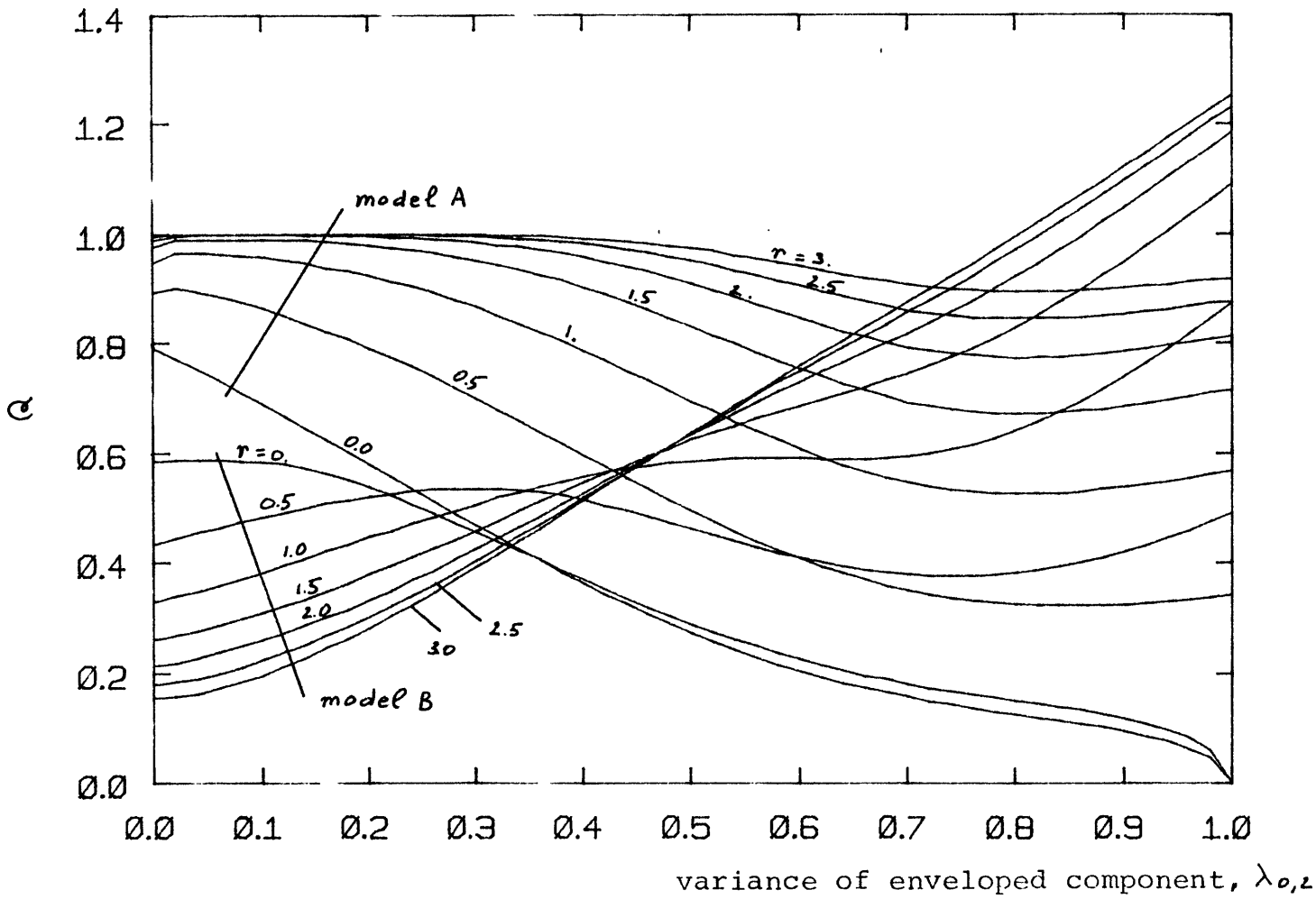

Fig. 65 - Ratio Q for rectangular spectrum, $\omega_2/\omega_1 = 10$

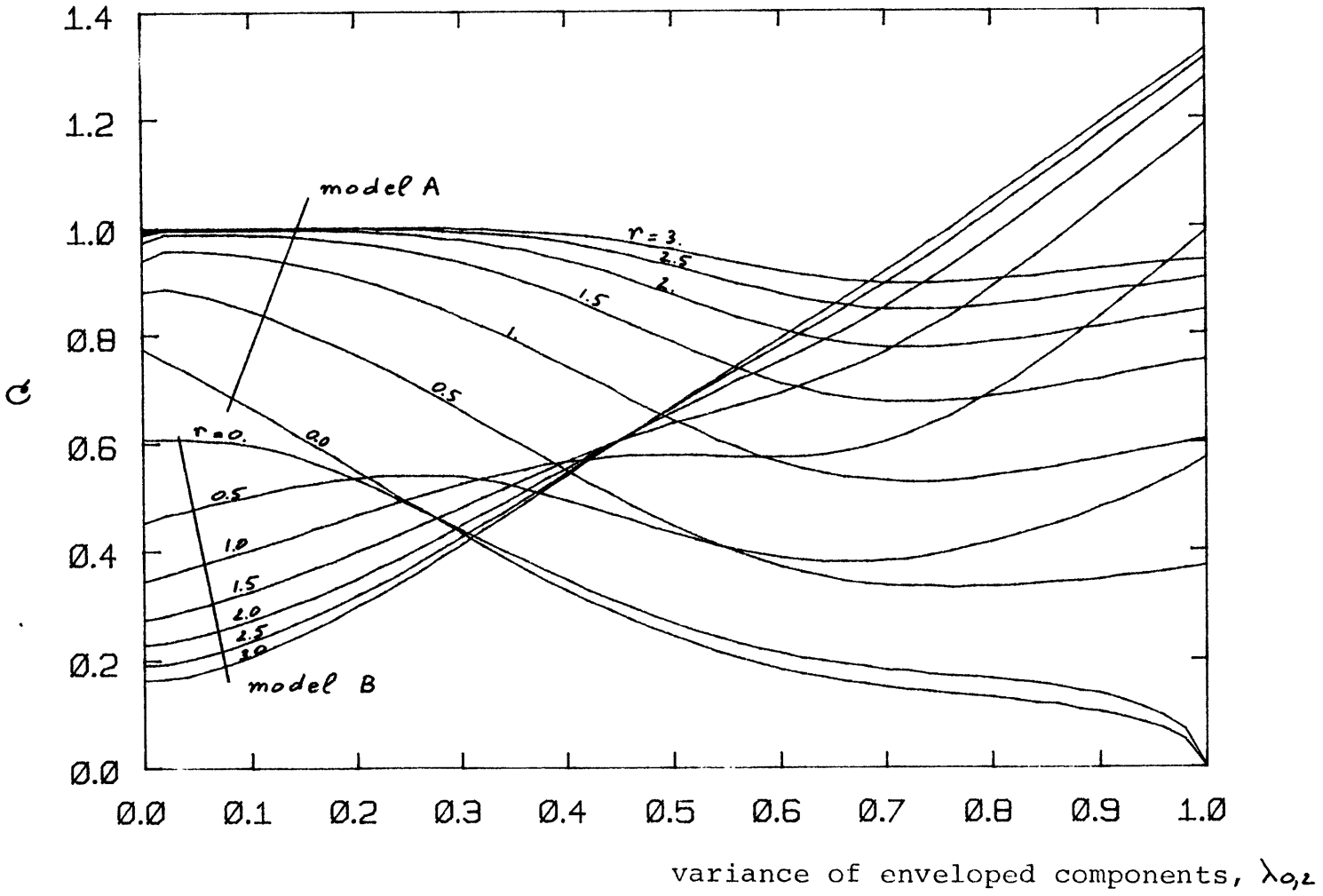

Fig. 66 - Ratio Q for rectangular spectrum, $\omega_2/\omega_1 = 10^4$

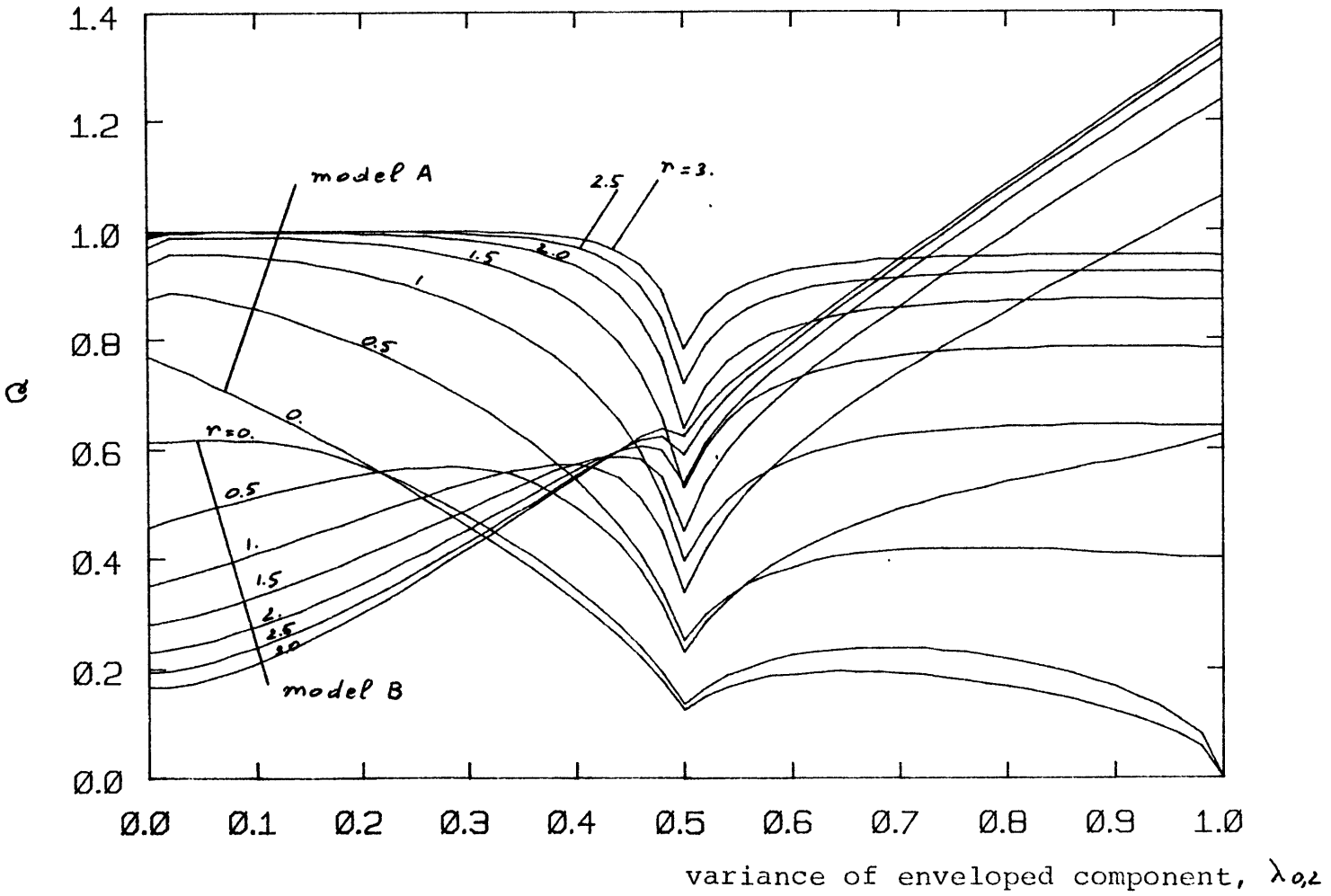

Fig. 67 - Factor Q for spectrum in Fig. 12b :

a=0.5, $\omega_1 = \omega_2$, $\omega_3 = 5\,\omega_2$, $\omega_3 = \omega_4$

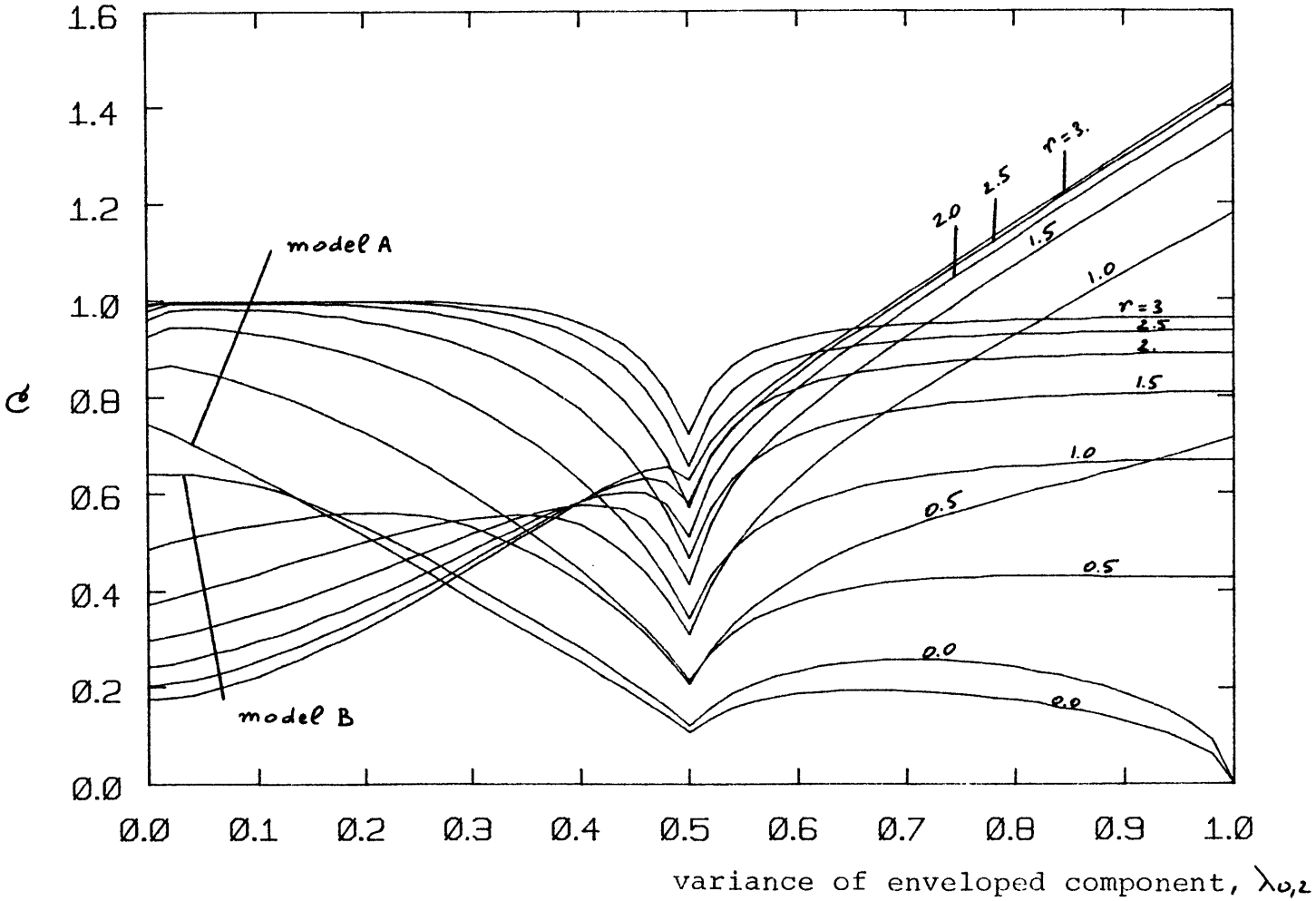

Fig. 68 - Factor Q for spectrum in Fig. 12b :

$a=0.5$, $\omega_2=3\,\omega_1$, $\omega_3=5\,\omega_2$, $\omega_4=\frac{5}{3}\,\omega_3$

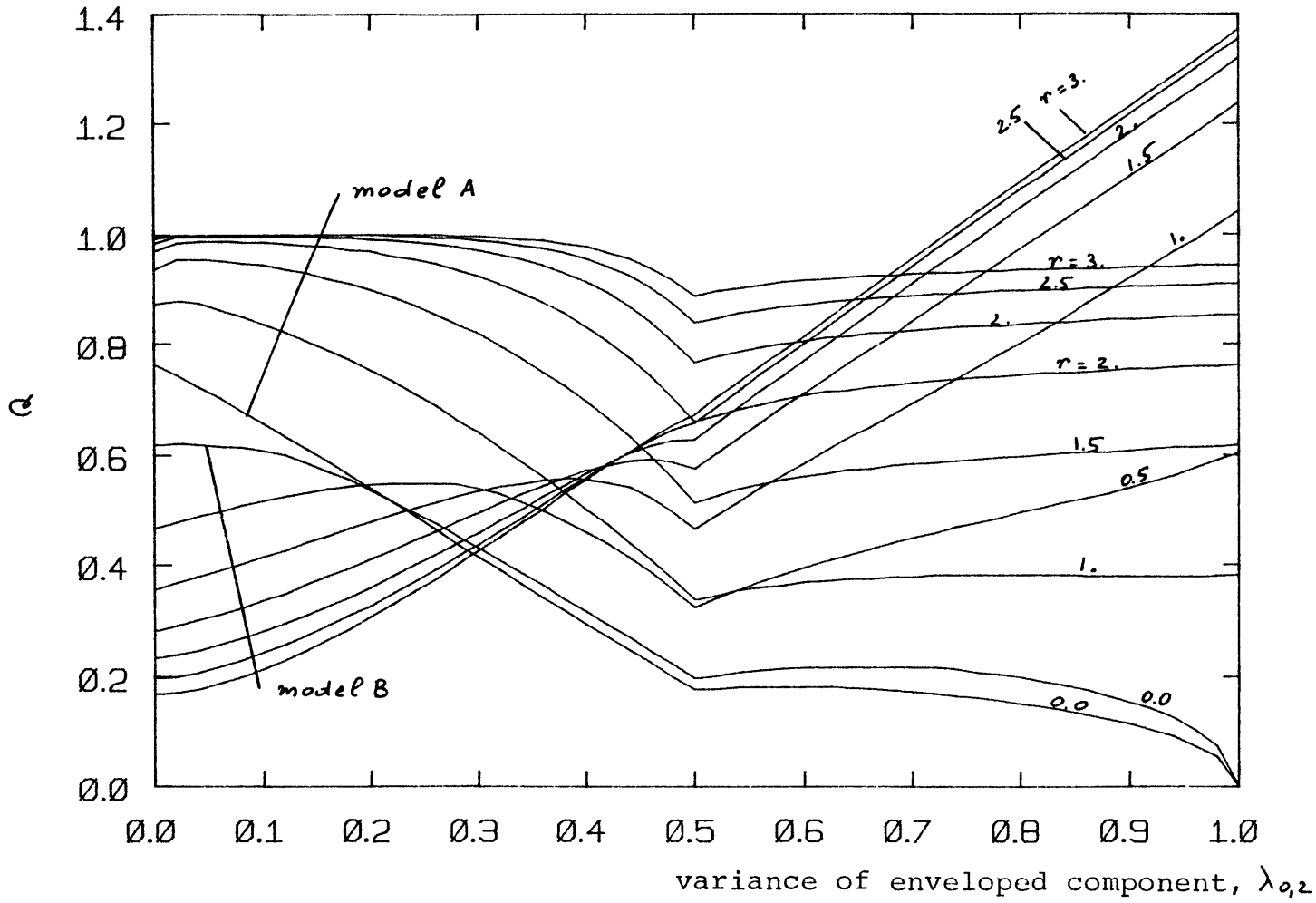

Fig. 69 - Factor Q for spectrum in Fig. 12b :

$a=0.5,\ \omega_2=3\omega_1\ ,\ \omega_3=2\omega_2\ ,\ \omega_4=\frac{5}{3}\omega_3$

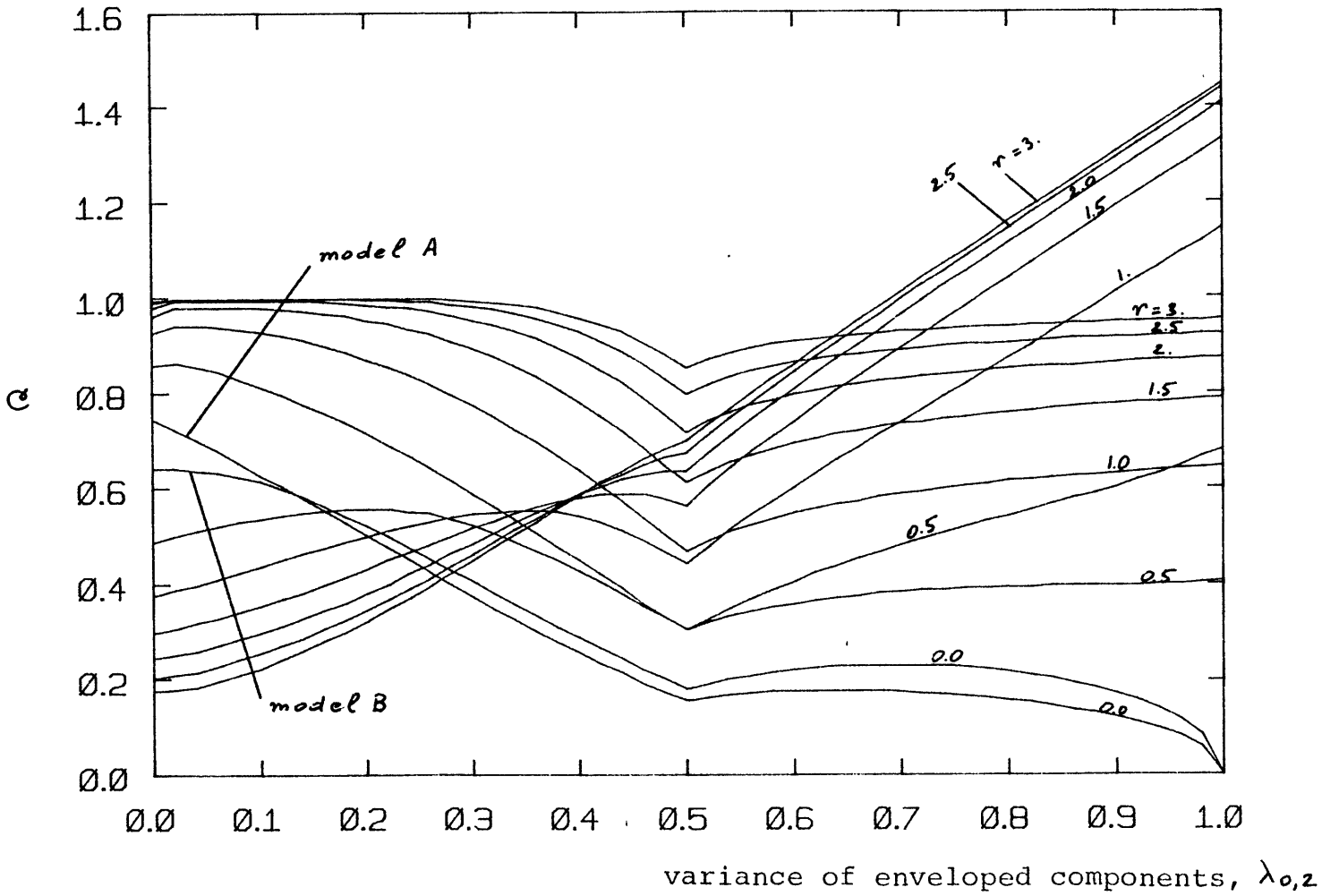

Fig. 70 - Factor Q for spectrum in Fig. 12b :

a=0.5, $\omega_2=5000\,\omega_1$, $\omega_3=2\,\omega_2$, $\omega_4=2\,\omega_3$

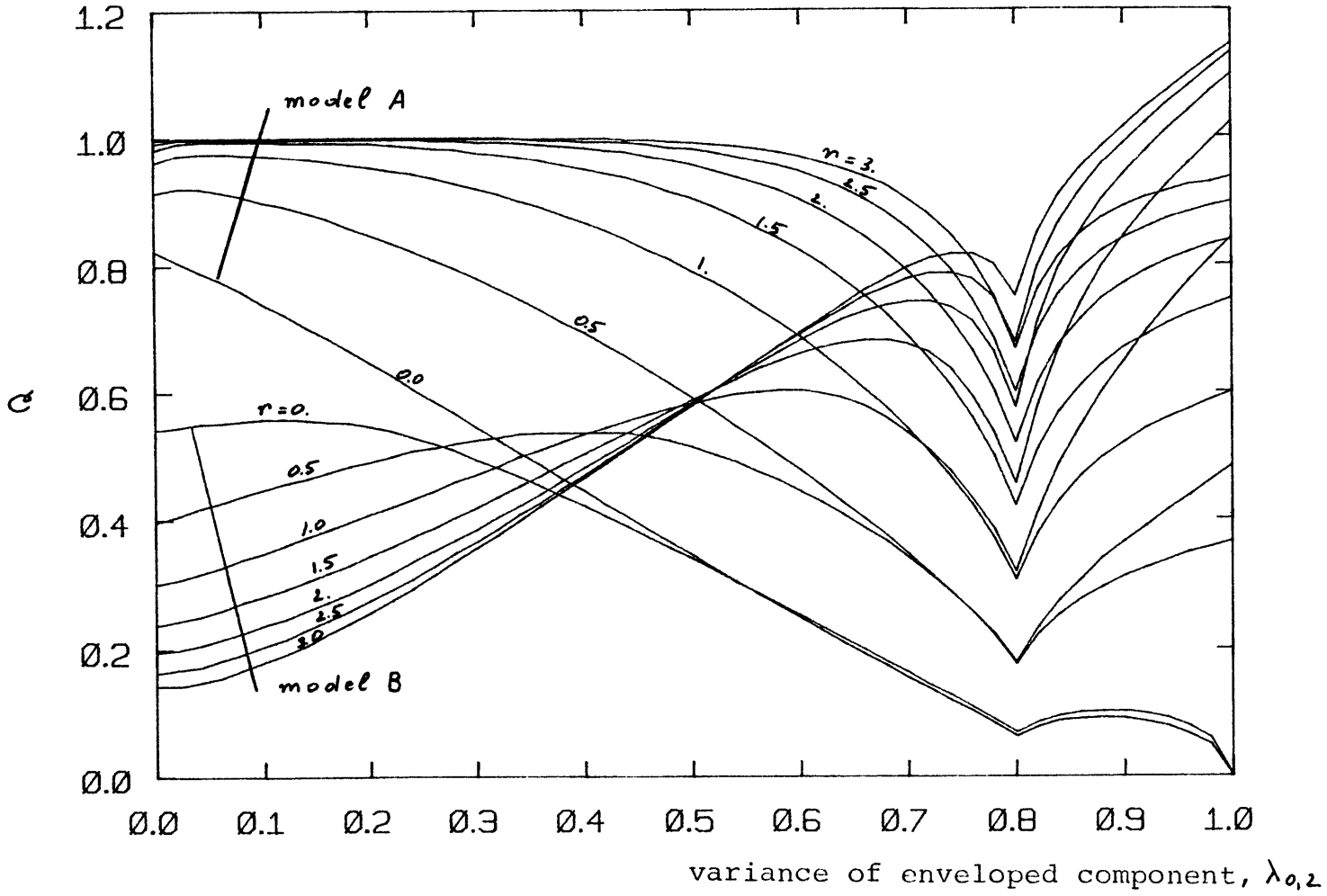

Fig. 71 - Factor Q for spectrum in Fig. 12b :

$a=0.2$, $\omega_2=3\omega_1$, $\omega_3=5\omega_2$, $\omega_4=\frac{5}{3}\omega_3$

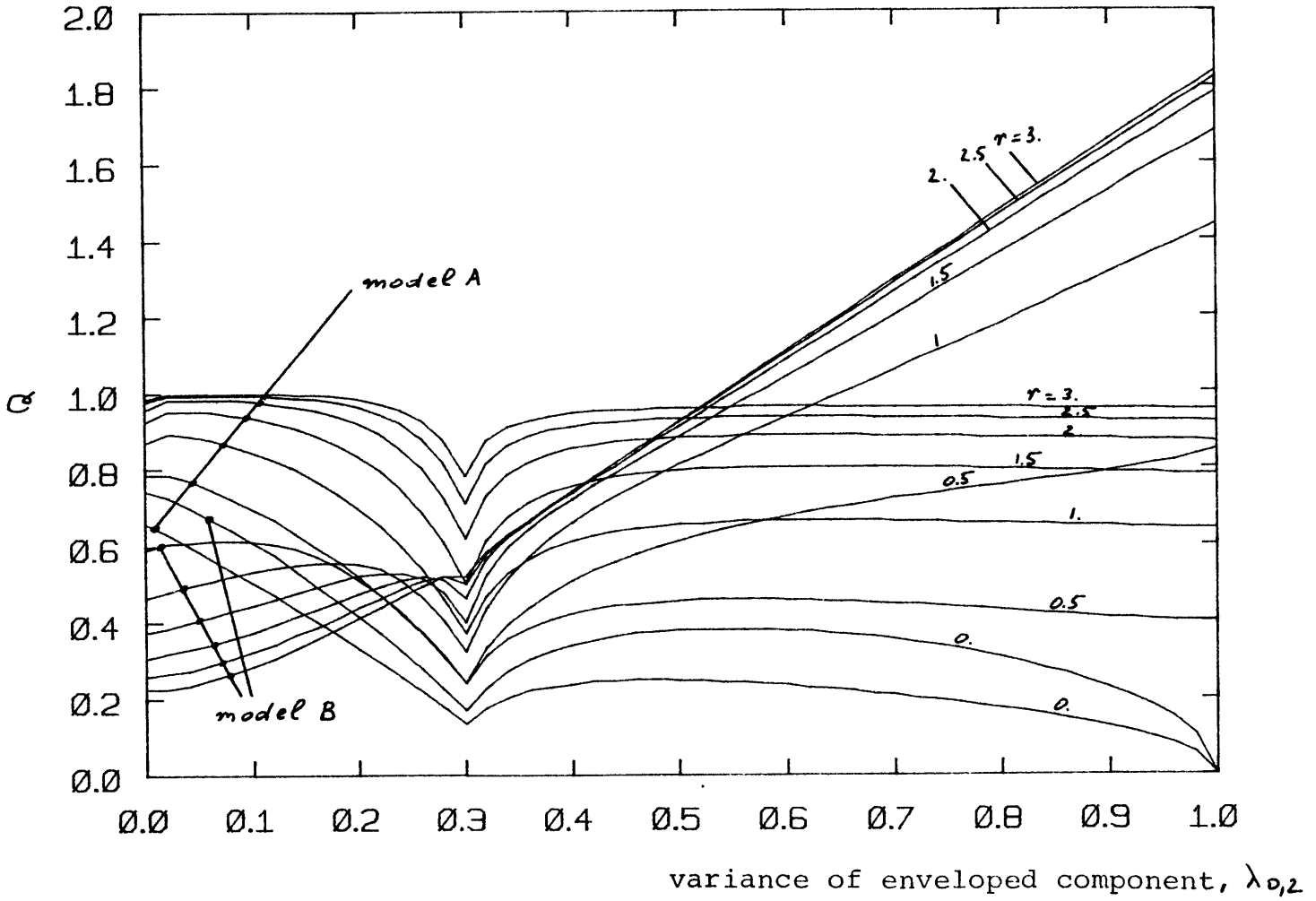

Fig. 72 - Factor Q for spectrum in Fig. 12b :

a=0.7, $\omega_2 = 3\omega_1$, $\omega_3 = 5\omega_2$, $\omega_4 = \frac{5}{3}\omega_3$

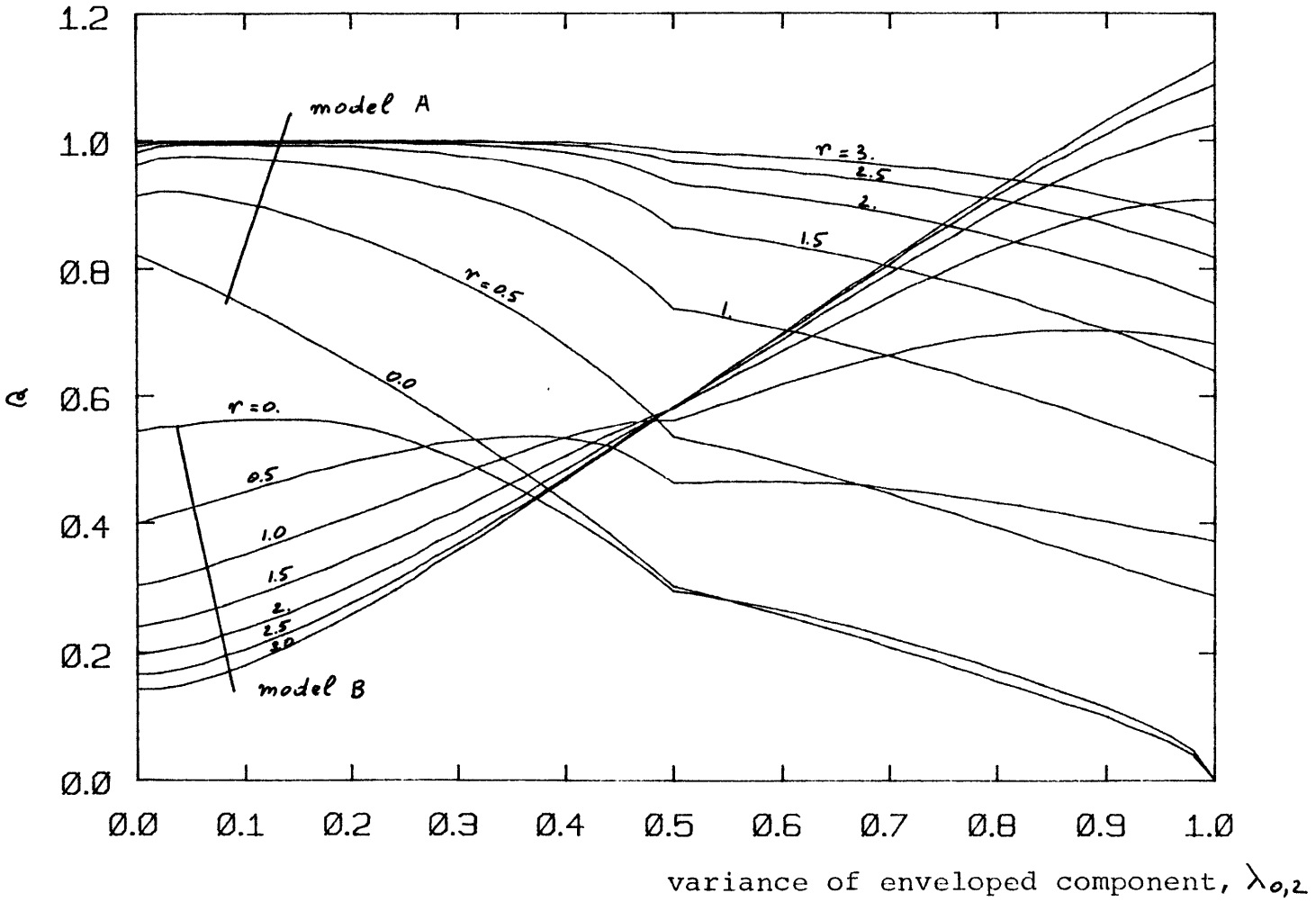

Fig. 73 - Factor Q for discrete spectrum, $\omega_2/\omega_1 = 2$

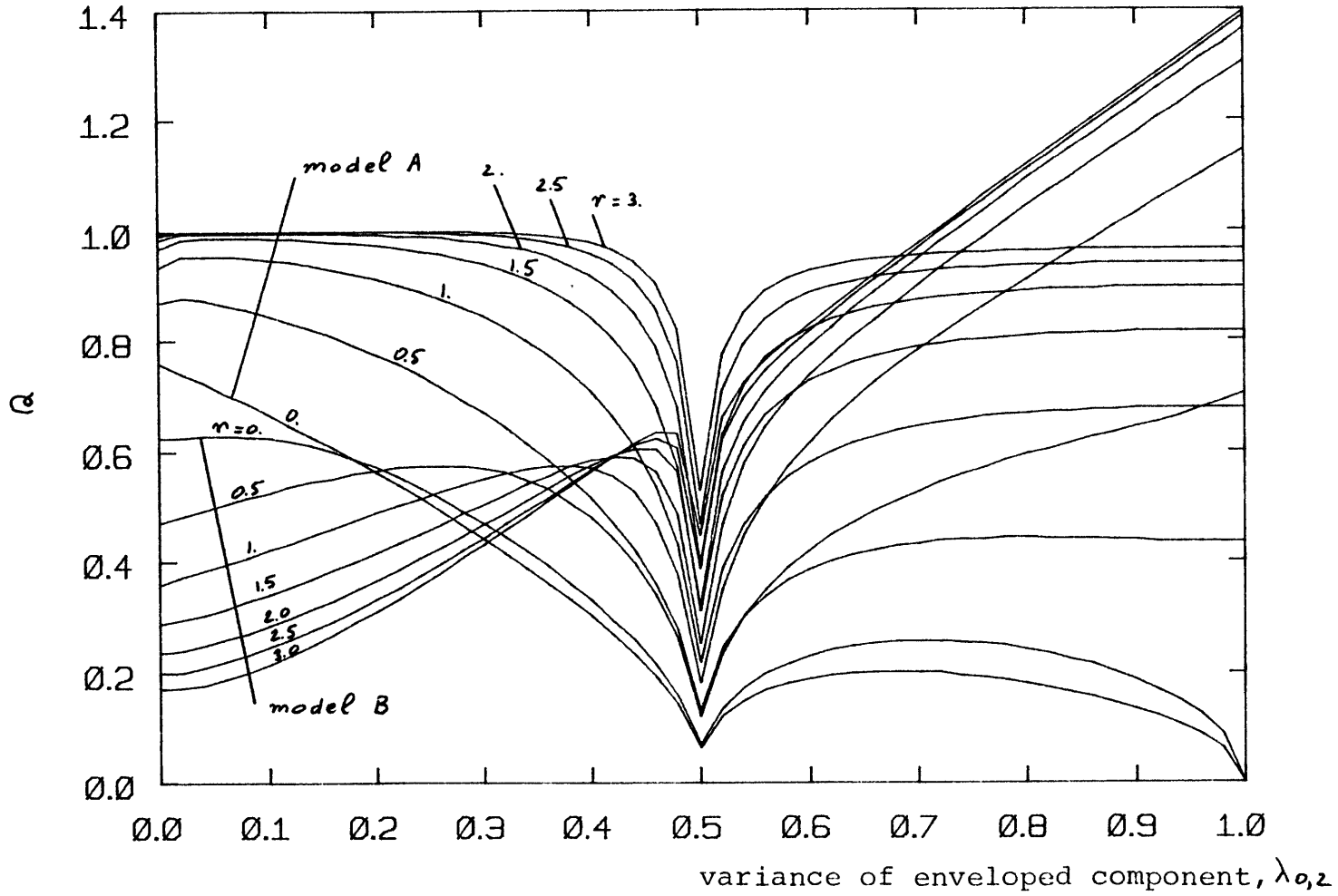

Fig. 74 - Factor Q for discrete spectrum, $\omega_2/\omega_1=10$

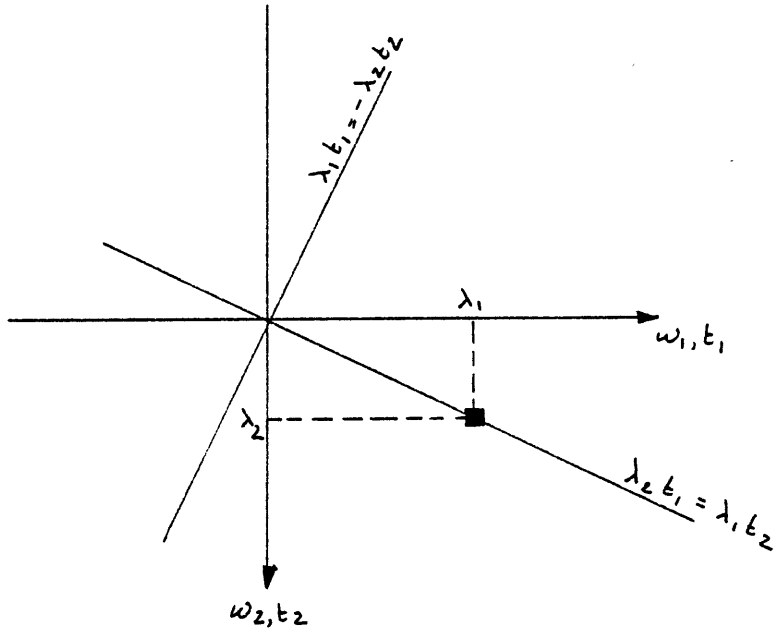

Fig. 75 - One sided spectral density of a discrete spectrum with a single peak

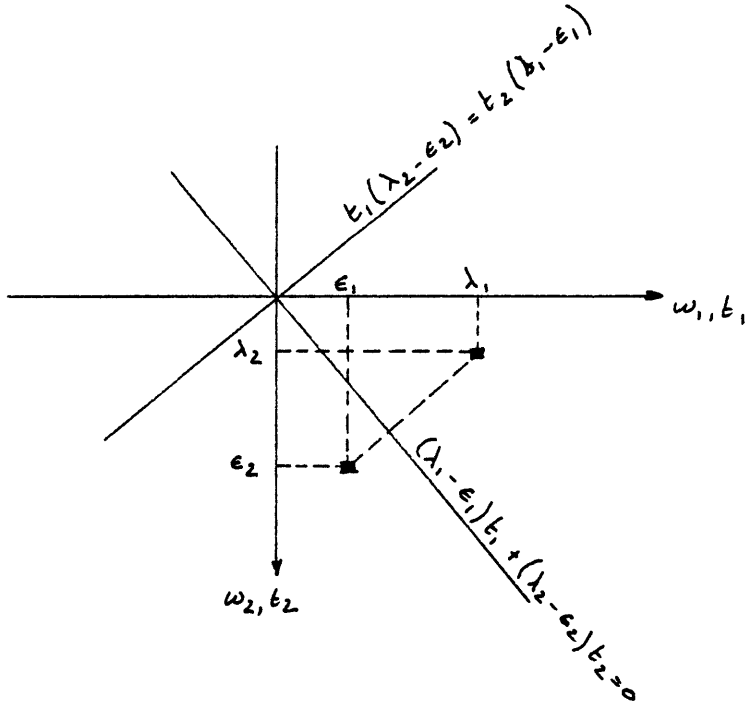

Fig. 76 - One sided spectral density of a discrete spectrum with two peaks

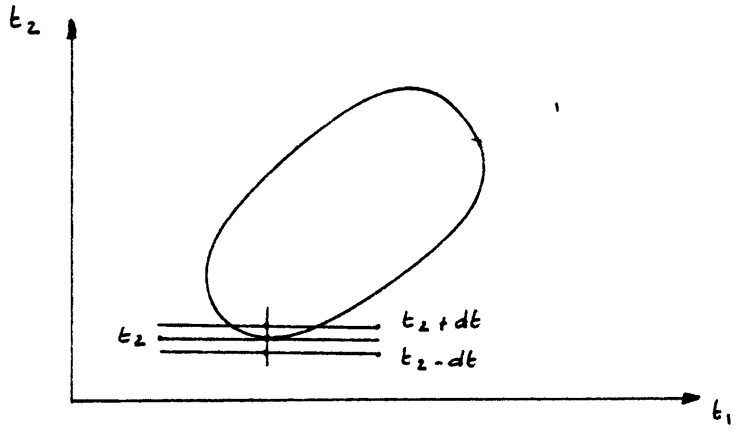

Fig. 77 - Positive critical point along contourline in (t_1,t_2)-section

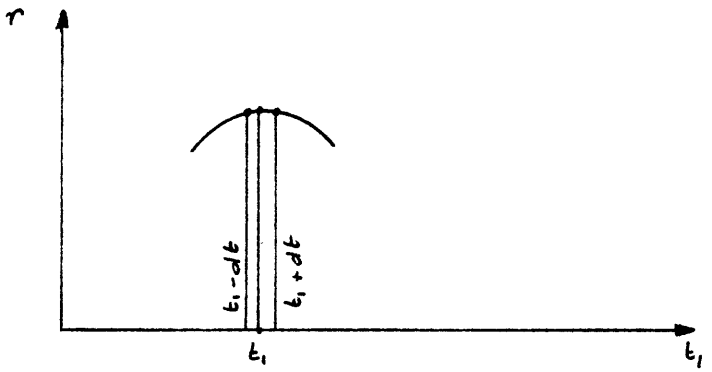

Fig. 78 - Positive critical point in (t_1,r)-section

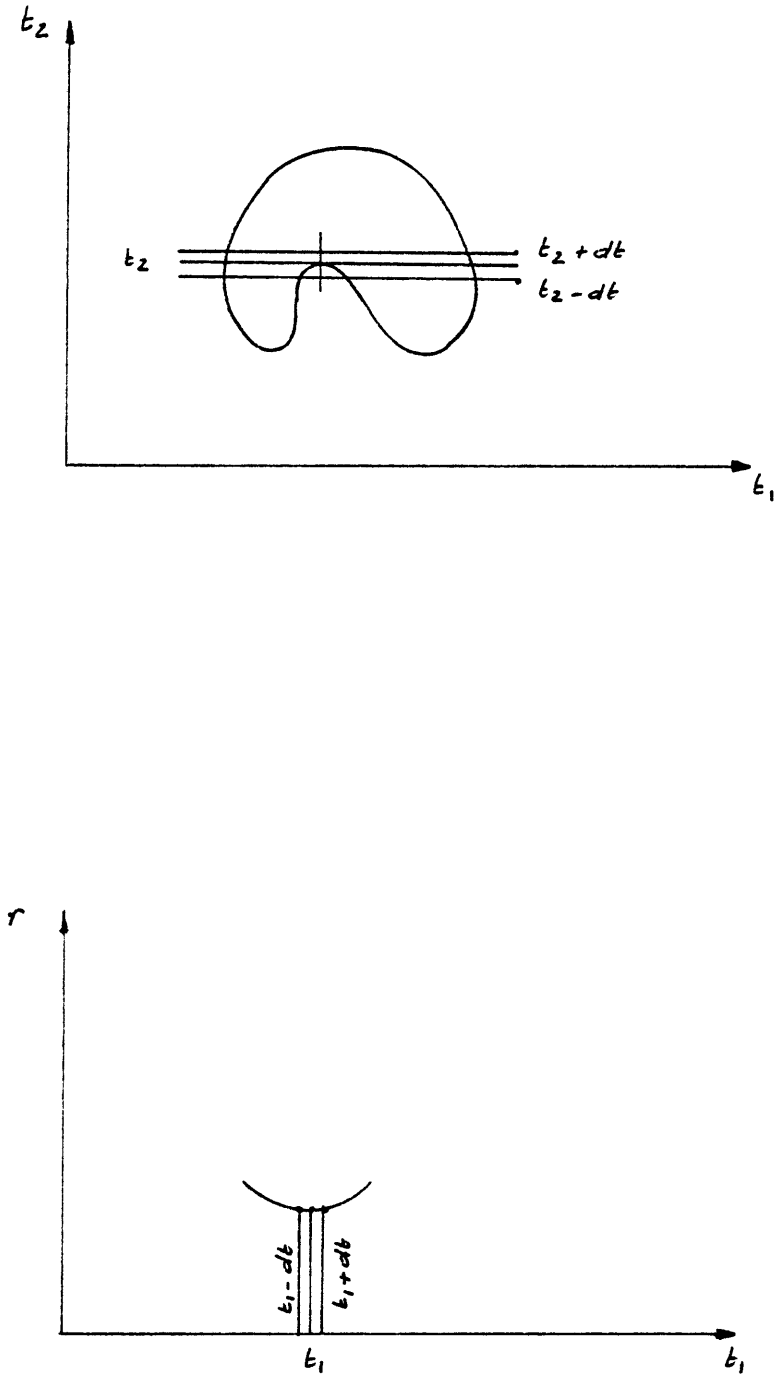

Fig. 79 - Negative critical point in (t_1,t_2)- and (t_1,r)-section

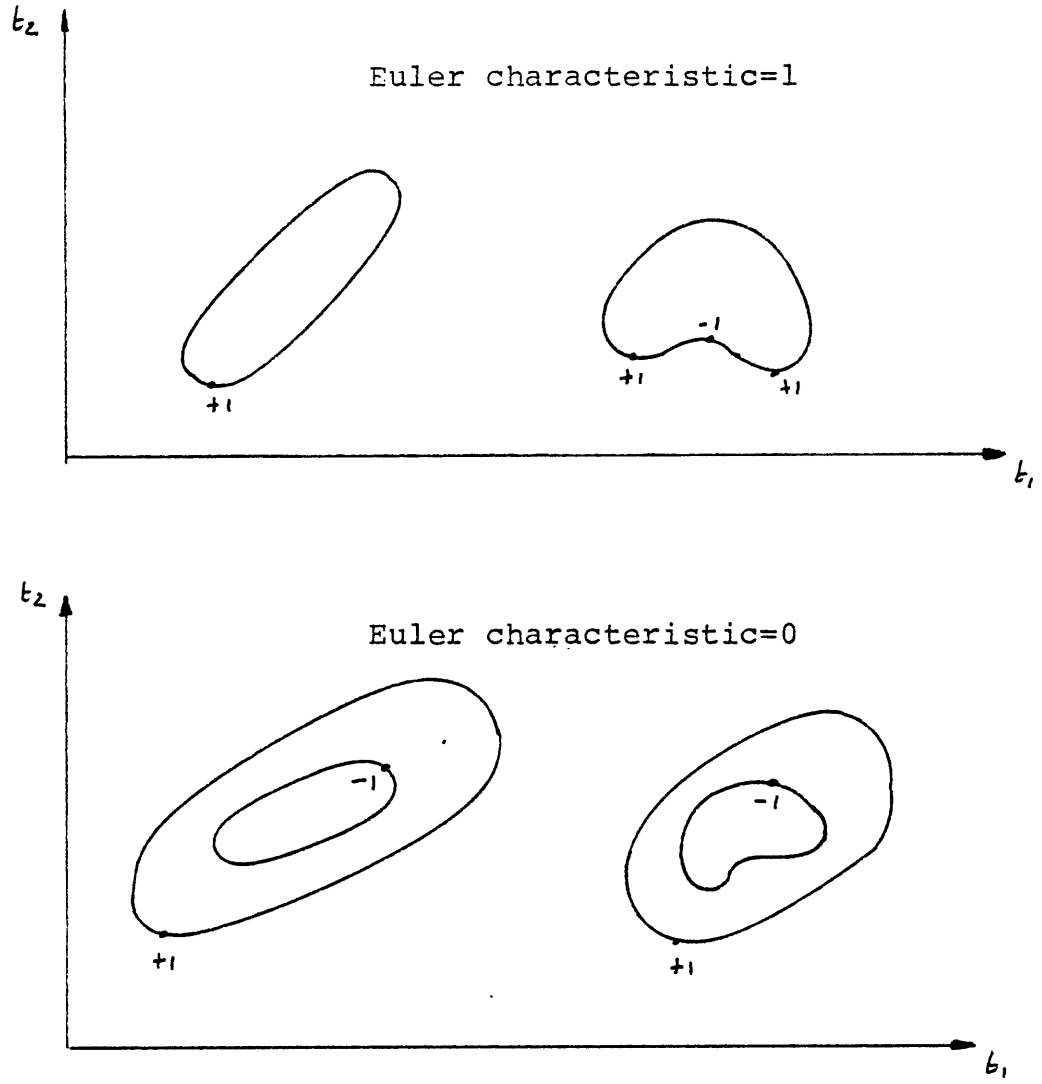

Fig. 80 - Euler characteristic for different excursions

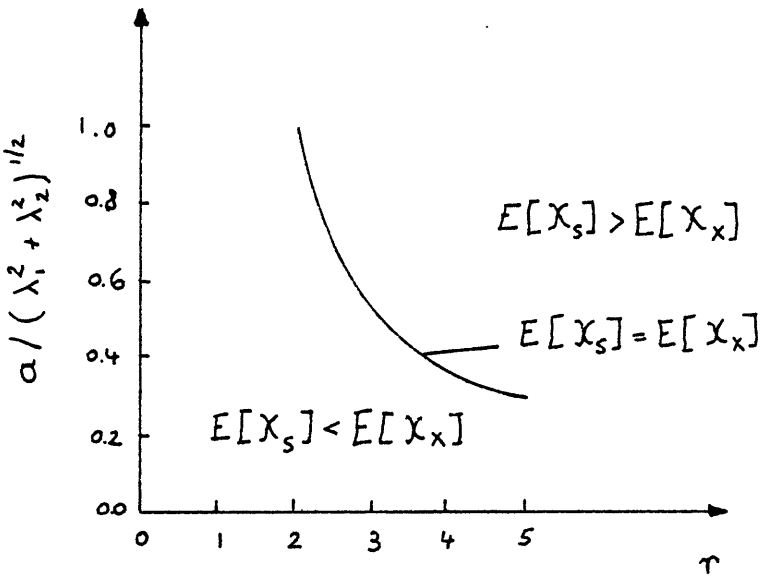

Fig. 81 - Euler characteristic of the random field $X(\underline{t})$ and of the associated envelope $S(\underline{t})$ as a function of the relative bandwidth of a spectrum uniformly distributed over a rectangular area with side a, centered at (λ_1, λ_2), and as a function of the crossing level r

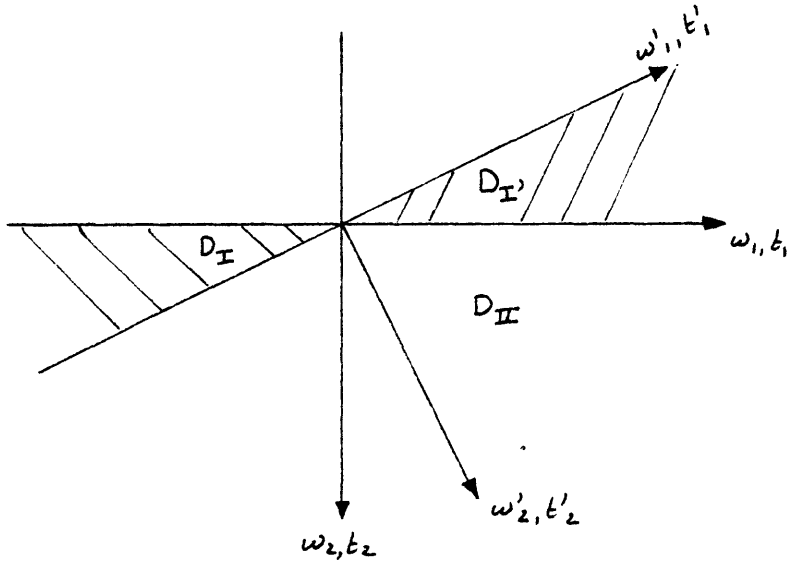

Fig. 82 - Rotated axissystem in the frequency and time-domain

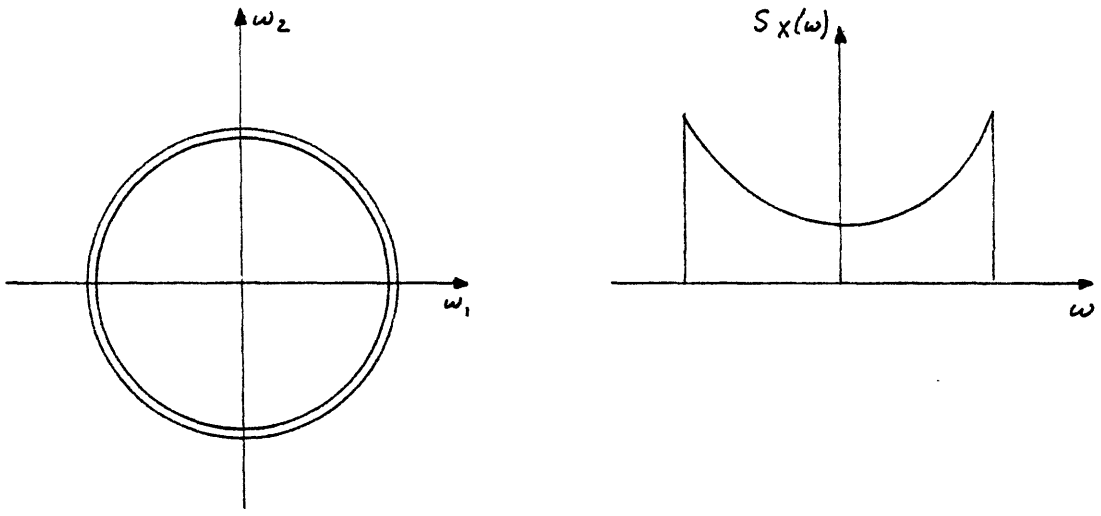

Fig. 83 - Spectral density in the plane and associated spectral density along the line